UGI 46-1

TO: MR. THOMAS WILSON

FROM: MR. KEN DINGWALL
GEOPHYSICAL SERVICES INC.
7800 BANNER DRIVE
DALLAS, TEXAS 75265
(214) 995-7749

THREE DIMENSIONAL SEISMIC INVESTIGATION
IN THE COTTAGE FIELD
WEST VIRGINIA

Prepared for

US ENERGY RESEARCH DEVELOPMENT ADMINISTRATION
AND
CONSOLIDATED GAS SUPPLY CORPORATION

By

GEOPHYSICAL SERVICE INC.
P.O. Box 225621
Dallas, Texas 75265

APPENDIX

Map	Title
1	Base Map
2.A	Green Reflector – Time Contour Map
2.B	Green Reflector – Time Contour Map 5 x 5 Filter Smoothing
2.C	Green Reflector – Time Contour Map 49 x 49 Filter Smoothing
3.A	Blue Reflector – Time Contour Map
3.B	Blue Reflector – Time Contour Map 5 x 5 Filter Smoothing
3.C	Blue Reflector – Time Contour 49 x 49 Filter Smoothing
4.A	Red Reflector – Time Contour Map
4.B	Red Reflector – Time Contour Map 5 x 5 Filter Smoothing
4.C	Red Reflector – Time Contour Map 49 x 49 Filter Smoothing
5.A	Yellow Reflector – Time Contour Map
5.B	Yellow Reflector – Time Contour Map 5 x 5 Filter Smoothing
5.C	Yellow Reflector – Time Contour Map 49 x 49 Filter Smoothing
6.A	Brown Reflector – Time Contour Map
6.B	Brown Reflector – Time Contour Map 5 x 5 Filter Smoothing
6.C	Brown Reflector – Time Contour Map 49 x 49 Filter Smoothing
7.A	Purple (P1) Reflector – Time Contour Map
7.B	Purple (P2) Reflector – Time Contour Map
7.C	Purple (P3) Reflector – Time Contour Map
8	Blue-Green Reflectors – Isochron Map
9	Red-Blue Reflectors – Isochron Map
10	Green Reflector – RMS Velocity Contour Map
11	Blue Reflector – RMS Velocity Contour Map
12	Red Reflector – RMS Velocity Contour Map
13.A	Green Reflector – Velocity Contour Map – 50-foot Interval
13.B	Green Reflector – Interval Velocity Contour Map – 100-foot Interval
14.A	Blue Reflector – Interval Velocity Contour Map – 50-foot Interval
14.B	Blue Reflector – Velocity Contour Map – 100-foot Interval
15.A	Red Reflector – Interval Velocity Contour Map – 50-foot Interval
15.B	Red Reflector – Interval Velocity Contour Map – 100-foot Interval
16.A	Green Reflector – Average Velocity Contour Map – 50-foot Interval
16.B	Green Reflector – Average Velocity Contour Map – 100-foot Interval
17.A	Blue Reflector – Average Velocity Contour Map – 50-foot Interval
17.B	Blue Reflector – Average Velocity Contour Map – 100-foot Interval

APPENDIX (CONTD)

TABLES

ILLUSTRATIONS

ILLUSTRATIONS (CONTD)

ILLUSTRATIONS (CONTD)

ILLUSTRATIONS (CONTD)

SECTION I
INTRODUCTION

The Devonian shale underlies more than 100,000 square miles in the Appalachian basin including Kentucky, Pennsylvania, Ohio, and West Virginia. The Devonian shale in this area has produced gas for many decades and its enormous gas potential is the subject of much interest. Some exceptional wells have initial production of over a million cubic feet per day and ultimate cummulative production may reach a billion cubic feet of gas per day.

The Devonian shale in southwestern West Virginia includes a formation between the Berea sandstone (Mississippian) and the Onondaga Limestone (lower Middle Devonian). Estimated recoverable reserves exceed one trillion cubic feet.

Generally, the shale in this area is not marked by structural deformation traps characteristic of hydrocarbon accumulation. Gas accumulation in Devonian shale results from stratigraphic traps. Although shale generally is very tight and has very low porosity, the Devonian shale has acquired a secondary porosity induced by fracturing. Fractures may have been produced as a result of volume increase, due to erosion of the above formation, or as a result of tectonic movements in the basement. Precambrian and Cambrian fault activities have produced fracturing which probably has propagated upward into the Devonian shale.

The object of this survey is to conduct a detailed three-dimensional seismic survey to reveal any correlation that might exist between basement movements and any characteristics associated with gas in the Devonian shale (e.g., interval velocity and thickness). When integrated with other data the 3-D survey also will show, in detail, structural features of the dominant stratigraphic layers in the area.

SECTION II

SUMMARY

Geophysical Service Inc. conducted a three-dimensional seismic survey for Consolidated Gas Supply Corp. under Energy Research Development Administration (ERDA) prime contract No. E (46-1)-8047 in Cottage Field in southwestern West Virginia. The SEISLOOP* method of 3-D seismic data aquisition was employed. It consisted of nine loops covering approximately 12 square miles.

Data was processed and 3-D migrated and 77 northeast-southwest cross-sections were produced, each with 169 CDPs. Horizontal time slices (SEISCROP** maps) were generated at 8-millisecond intervals from 0.456 to 1.368 seconds reflection time.

Eight horizons were selected on the seismic sections and were identified using available geological information. The eight horizons included three horizons thought to be Precambrian. The upper three horizons, including the Devonian shale, were digitized and input to a data base constructed for that purpose. Reflection times were merged with coordinates and the velocity field corresponding to each CDP.

The data base was manipulated to compute other attributes such as interval reflection time, interval velocity, average velocity, interval thickness, and depth. All attributes were then automatically contoured and checked for quality control purposes.

It was demonstrated that the SEISCROP map could be efficiently used to produce a workable contour map. This was done by producing contours for a reflector from different levels of SEISCROP maps and comparing these contours to those generated by the computer.

---

*Service mark of Geophysical Service Incorporated; U.S. Patent No. 3,867.713

**Trademark of Geophysical Service Incorporated

The reflection times of the three "Precambrian" horizons were hand-posted and hand-contoured.

All maps produced for the "Precambrian" horizons and the associated fault patterns are discussed.

The "Precambrian" tectonic activity apparently affected the shallower horizons and especially the Devonian zone to a great extent. It is noted that the fault orientation in the "Precambrian" horizon is predominantly in a NE-SW direction. This correlates with the structural trend of the above horizons. Moreover, studies of fracture orientation in the area reveal a NE-SW direction which could be related to the "Precambrian" fault system. The fault pattern is correlated with the average velocity-to-base and the interval velocity of the Devonian. Both correlations of low velocity, which may be indicative of a gas zone or high-pressured zone, show an association with the upward propagation of the "Precambrian" faults.

SECTION III

SEISMIC DATA ACQUISITION

Figure 3.1 shows the area surveyed in Jackson and Mason counties of West Virginia. Figure 3.2 depicts the surface layout utilizing the SEISLOOP method for 3-D seismic data acquisition. Geophone groups and seismic sources were placed along the roads for expediency. A total of 9 loops were surveyed in this area, covering approximately 12 square miles. The surface coverage obtained is shown by the computer printout map on Figure 3.3 for Loop I. Similar coverage is obtained for other loops.

Field parameters used in the survey were as follows:

Seismic source: VIBROSEIS* Seismic Source – with shot array in line, generates 10-15 sweeps per pattern. Each sweep was 60-20 Hz, duration was 10 seconds, and listening time was 14 seconds. In-line offset was 440 feet and shot interval was 220 feet.

Seismic receiver: 48 groups, each consisting of 24 L21A geophones spaced at 5-ft intervals; group interval was 440 feet.

Seismic recorder: The DFS** IV recording instrument was used. Filter setting was 8-62 Hz, the sampling interval was 4 milliseconds, and record length was 4 seconds. Instantaneous Floating Point (IFP) gain control was used.

*Trademark of Continental Oil Co.

**Trademark of Texas Instruments Incorporated

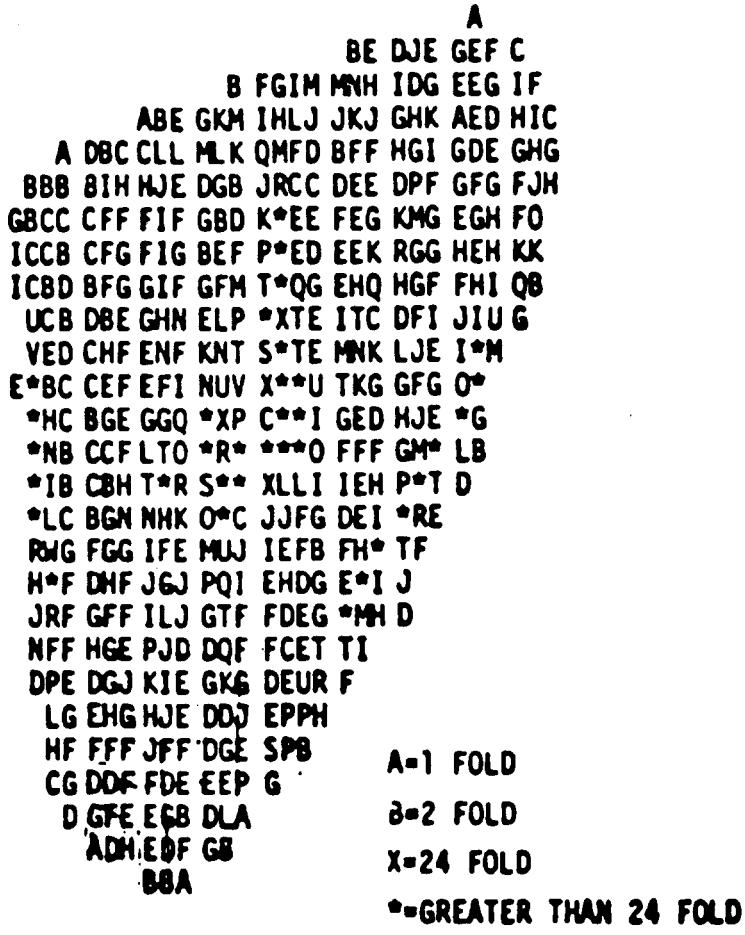

SUBSURFACE COVERAGE IN LOOP 1

SECTION IV

SEISMIC DATA PROCESSING

Figure 4.1 depicts the processing sequence applied to the data. Once the field work was completed, the data was prepared for quality control checks and initial processing (i.e., data initialization). In order to develop Common Depth Point (CDP) stack tables for subsequent processing, the area was divided into 220-foot square bins. Each CDP trace will be assigned an x-y identification determined at the center of gravity of the bin; the x-y coordinates identify each CDP trace uniquely and is used later as means of retrieving it from the 3-D seismic data base. Since each CDP trace was associated with an individual set of x-y coordinates, it became unnecessary to retrieve a trace by shot number or line number as in 2-D seismic processing.

Preprocessing includes True Amplitude Recovery (TAR), consisting of gain removal, spherical divergence, and inelastic attenuation correction. A 4.5 db/second correction factor was used. Time-varying deconvolution (TVD) followed where two 200-millisecond whitening filters were applied but not normalized. The data were then subjected to time-varying scaling (TVS) utilizing unity scaling. At this stage the traces from the same bin CDP were gathered and datum statics were applied. Seismic traces were corrected to a datum plane 800 feet above sea level using a velocity of 9000 feet/second.

Brute stack sections were then produced to conduct processing analysis in order to determine optimum processing parameters. Processing analysis encompassed velocity analysis, ramp analysis, autostatic estimation, migration aperature evaluation, and digital filter analysis.

The determined velocity field was stored in a 3-D velocity file which was used subsequently. Ramp analysis resulted in the following optimum muting parameters:

75 milliseconds	at	0 feet
310 milliseconds	at	1925 feet
575 milliseconds	at	5750 feet
1200 milliseconds	at	9000 feet

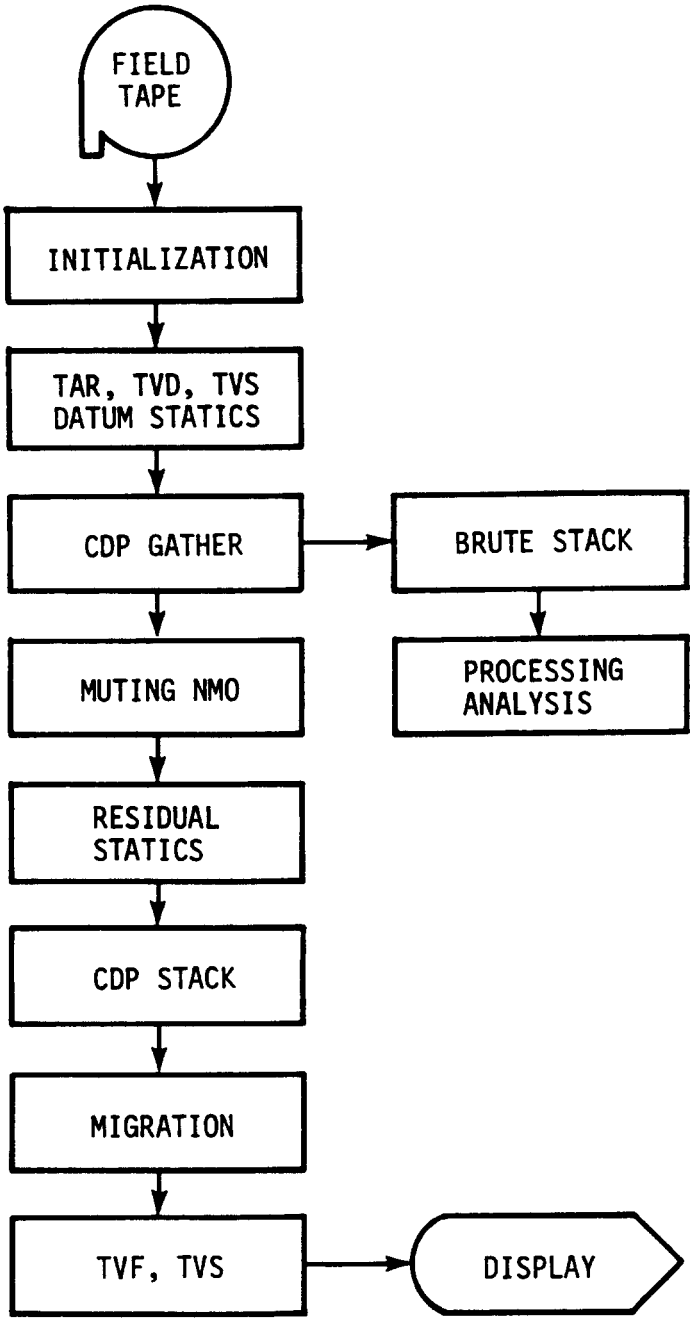

Figure 4.1. Processing Sequence of Seismic Data

This was followed by normal moveout correction (NMO) using the velocity field stored in the 3-D velocity file. The automatic residual static file computed in the residual static analysis was applied to the seismic traces; this was followed by CDP stacking in which the corrected traces of the same bin were stacked to produce one trace. The 3-D migration process was applied at this stage. Frequency digital filter processing was then performed in a time-varying fashion with 50% overlap; filters were normalized. The optimum filter parameters were:

20 - 55 Hz at 0.0 seconds
20 - 50 Hz at 1.0 seconds
20 - 40 Hz at 3.0 seconds

TVS was then performed.

The seismic data were displayed in seismic sections (vertical slices) and SEISCROP (horizontal) slices.

Displays of seismic sections were made at 12 traces per inch and 5 inches per second. Sections were displayed in VAR format with normal polarity and 15 percent bias. Seventy-seven northeast vertical slices (lines) were selected from the data base and displayed. Each line constituted 169 CDPs.

SEISCROP maps were displayed from 0.456 seconds to 1.368 seconds at 8-millisecond intervals. The scale used was: 1 inch equals 2640 feet, or twelve traces per inch.

SECTION V

SEISMIC DATA INTERPRETATION

5.1 SELECTION AND IDENTIFICATION OF REFLECTORS.

Figure 5.1 shows an interpreted seismic section with color codes of the selected major reflectors.

Although deep-well information is not available, concentration is made on associating the "typing" of only the shallow reflector to the available well data and literature. Table 5.1 summarizes the association of seismic reflectors to the geologic horizons in the area. Figure 5.2 shows the geologic column of western West Virginia (1). Table 5.2 gives the reflection times and depths of the reflectors used.

Table 5.1

Association of Seismic Reflectors to Geologic Horizons in Cottage Field Area

Reflector	Period and Epoch	Age	Comments and References
Green	Miss., Middle	Greenbrier (Big Lime)	Consolidated Gas Corp. (No date) and Bargnall and Rayan (1976)
Blue	Dev., Upper	Ballier (Brownshale II)	Consolidated Gas Corp. (No date) Halliburton Services (1975), Martin and Nuckols (1976), Bargnall and Rayan (1976)
Red	Dev., Lower	Delaware limestone	Only possibility based on depth estimate [West Virginia (map)]
Yellow	Silurian, Upper	Tonoloway Dolomite	Only possibility based on depth estimate [West Virginia (map)]
Brown	Ordovician, Lower	Beekmantown Dolomite?	Only possibility based on depth estimate [West Virginia (map)]
Purple 1 Purple 2 Purple 3	Proterozoic (Pre-Cambrian)?		Only possibility-based on depth estimate [West Virginia (map)]

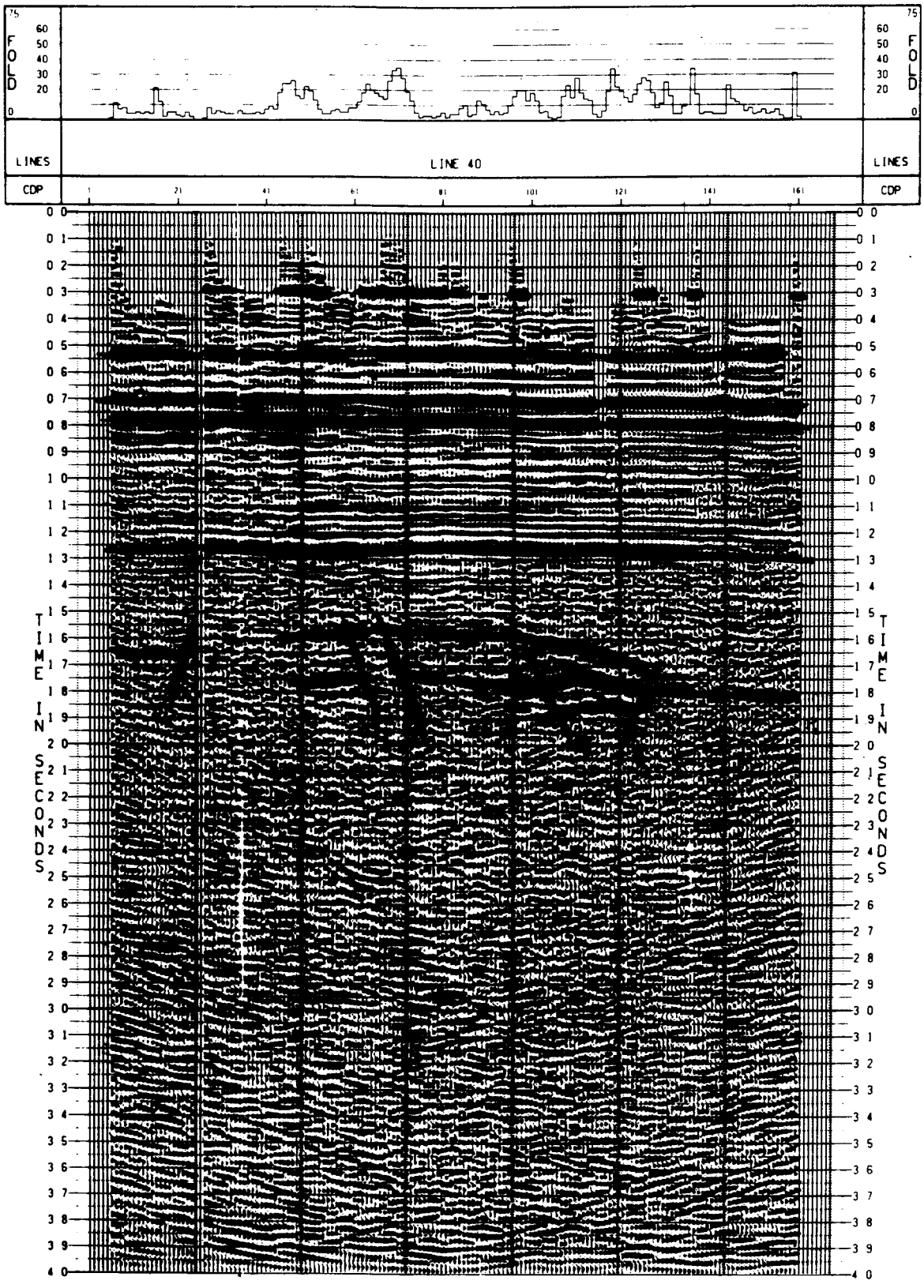

Figure 5.1. Example of Interpreted Seismic Section

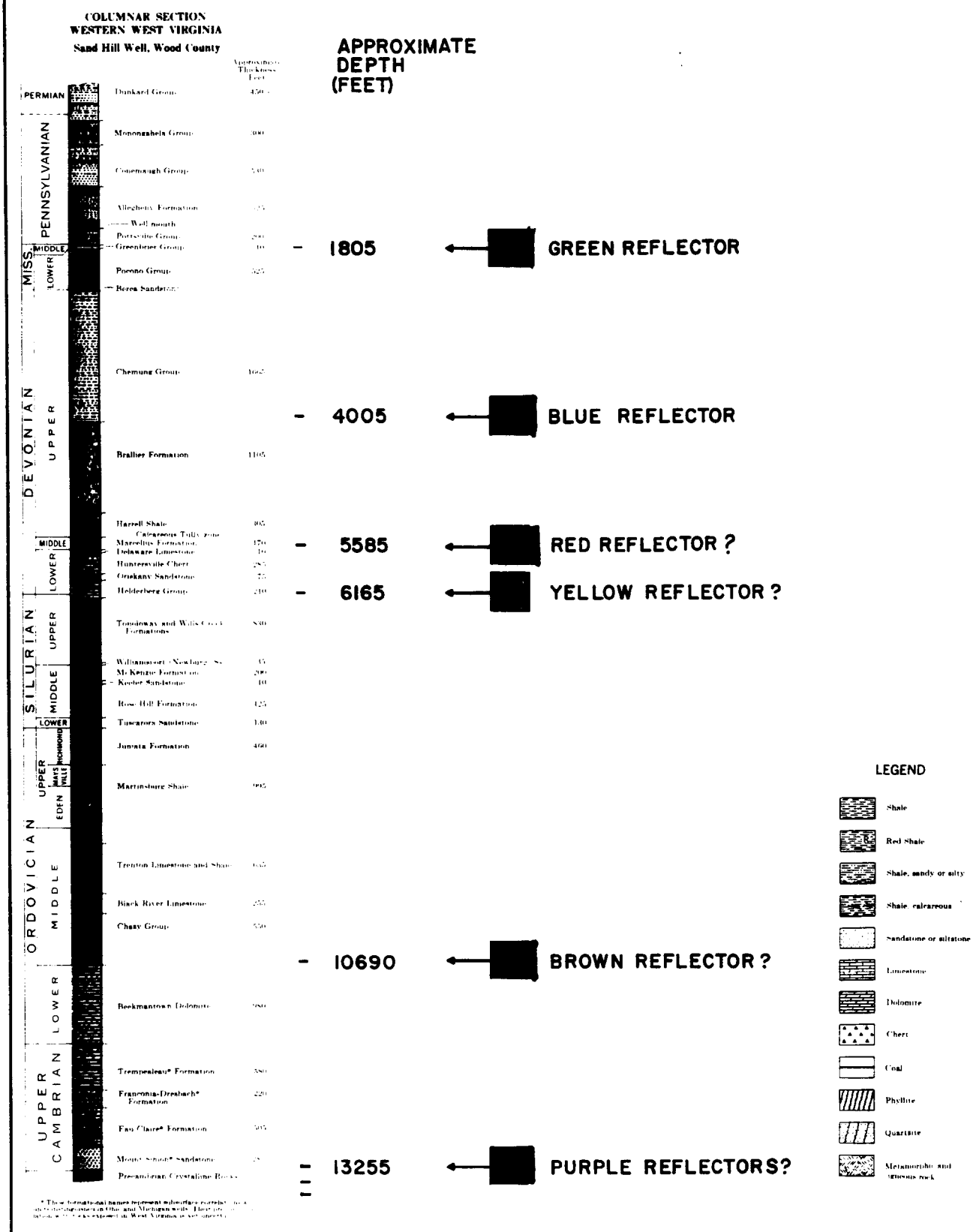

GEOLOGIC COLUMN OF WESTERN WEST VIRGINIA

Table 5.2

Reflection Times and Depths of Reflectors

Reflector	Tmx.	Tmn.	Tav.	St. Dev.	Dmx.	Dmn.	Dav.	St. Dev.
Green	325.9	269.2	293.4	10.4	2042.0	1629.3	1830.2	82.404
Blue	567.2	478.4	531.4	15.3	3801.1	3165.9	3498.2	121.28
Red	752.8	661.6	703.9	20.7	5155.4	4449.2	4808.2	129.24
Yellow	819.8	730.9	778.9	24.4	–	–	5434	–
Brown	1305	1209.8	1248.3	32.	–	–	9721	–
Purple 1	1731	1451	1591	28.3	–	–	13200	–
Purple 2	1828	1688	1758	29.8	–	–	14973	–
Purple 3	2000	1820	1910	30.8	–	–	17132	–

5.2 DIGITIZATION AND PRODUCTION OF MAPS

A schematic representation of the map production sequence described in this subsection is demonstrated by Figure 5.3. A data base consisting of approximately 14,000 data points was constructed for ease of storage and updates and retreival of horizon times, coordinates, RMS velocities, and elevations.

Once the horizons were selected, the sections were digitized and converted from digitization units to times with associated CDPs. Reflection time is referenced to the datum elevation which is 800 feet above sea level. The data were retrieved from the data base and overlays were produced which defined the horizons. The sections and overlays were then compared and the proper corrections made to erroneous data stored in the data base. The corrected horizon time data were then merged with the proper x, y, and CDP coordinates. Time and CDP information was retrieved from the data base and passed through the mapping package, which produces a grid of times to be machine contoured and filtered. The maps were checked for quality control purposes and necessary corrections were made.

The next step was to input the gridded RMS velocity file into the data base and merge the velocity and CDP information with the x, y, and CDP coordinate information.

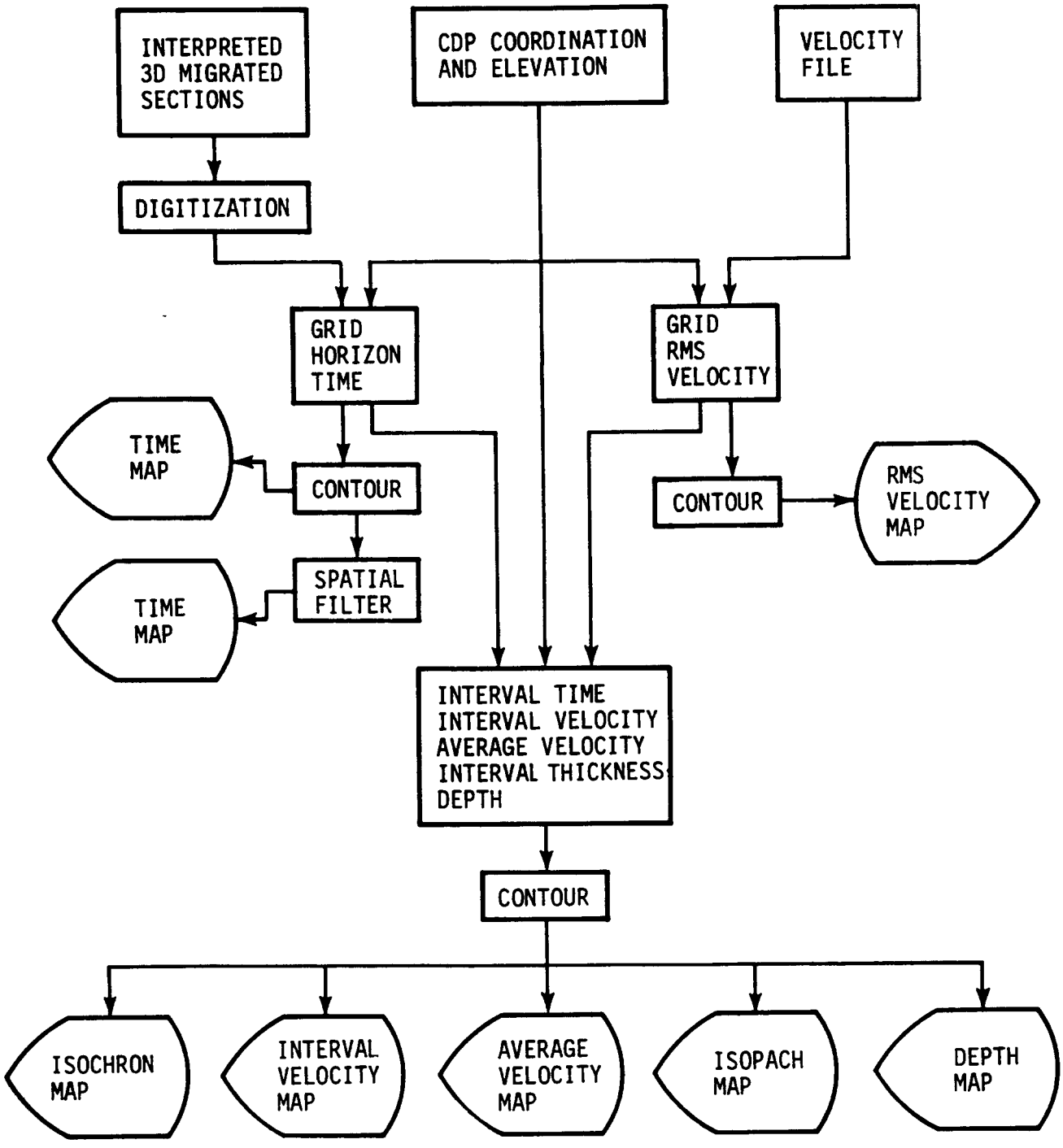

Figure 5.3. Map Production Sequence

GSI-709

The velocities were retrieved from the data base and gridded and mapped. The maps were checked and any corrections and updates made.

A near-surface grid of elevations, to be used to produce the datum statics, was then produced. Since the velocities were surface-referenced, the datum statics were added back into the datum-corrected horizon times. The standard formula utilized was:

$$DSC = \frac{SE - DE}{V_{rpl}}$$

DSC = Datum Static Correction
SE = Surface elevation
DE = Datum elevation, 800 feet above sea level
V_{rpl} = Replacement velocity, 9000 feet/second.

Surface-referenced time (T_n) and velocity grids (V_n) were then input into a program which produces isochron, interval velocity, isopach, average velocity, and depth (Z_n) grids. Depths were then referenced to the 800-foot datum.

The equations used in these calculations are as follows:

Interval Time: $\Delta T_n = T_n - T_{(n-1)}$

Interval Velocity: $V_{in} = \frac{V_n^2 T_n - V_{(n-1)}^2 T_{(n-1)}}{T_n}$

Interval Thickness: $\Delta Z_n = \frac{V_{in}\ \Delta Tn}{2}$

Depth: $Z_n = Z_{(n-1)} + \Delta Z_n - (SE - DE)$

Average velocity: $\bar{V} = Z_n/T_n$

Two spatial filters were designed and applied to the five time horizons. The filter characteristics were as follows:

- 5 x 5 (25-point, spatial, low-pass, 440-foot grid); passed wave lengths in excess of 2750 feet.
- 49 x 49 (2,401-point, spatial, low-pass, 440-foot grid); passed wave lengths in excess of 3500 feet.

These filters were considered smoothing filters to remove various high-frequency anomolies. The methodologies used for design of spatial filters is found in a paper by Fuller (1968).

Table 5.3 is a summary of the average values for reflection times, depth (referenced to datum elevation), RMS velocity, average velocity (surface-referenced), and interval velocity associated with each reflector.

Figure 5.4 displays a composite of time depth and velocity depth curves for the area.

Table 5.3

Time, Depth, and Velocities of Reflectors

	TIME	DEPTH	V_{RMS}	V_{INT}	$\bar{V}$
GREEN	293.4	1830.2	12475	12475	12475
BLUE	531.4	3498.2	13183	14007	13161
RED	703.9	4808.2	13698	15169	13654
YELLOW	778.9	5434.0	13928	14915	14169
BROWN	1248.3	9721.0	15560	17861	15591
PURPLE 1	1591	13200	16799	20771	16688
PURPLE 2	1758	14973	17317	21702	17157
PURPLE 3	1910	17132	18117	24731	17846

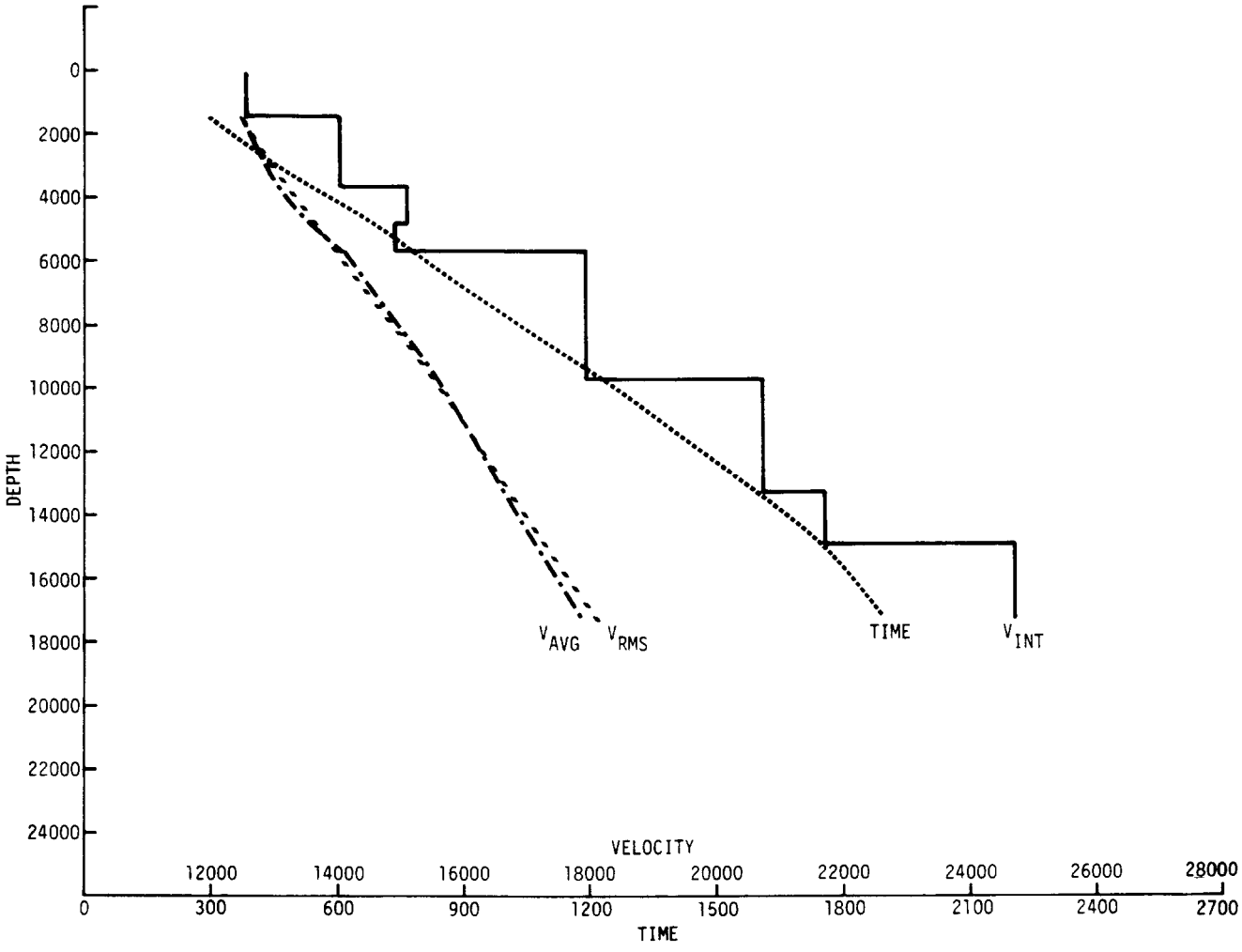

Figure 5.4. Reflection Time and Velocities Versus Depth Reflectors

5.3 DISCUSSION OF MAPS

All maps were produced at 1:24000 scale and are enclosed in the appendix. Reduced versions of the maps (35% of original size) are incorporated in the text, and are referenced to the corresponding appendix maps. The base map is shown as Figure 5.5.

5.3.1 REFLECTION TIME CONTOUR MAPS. Three reflection-time contour maps were generated for the green, blue and red reflectors. For each horizon one map is unfiltered and the two others are smoothed (two-dimensionally filtered using 5 x 5 and 49 x 49 operators). The contours are at 5-millisecond intervals.

5.3.1.1 Green Reflector Time Contour Maps. (See figures 5.6, 5.7, and 5.8.) The reflection times of the green reflector ranged from 269 to 326 milliseconds with an average of 293 milliseconds. Generally, there is a slight tendency of low dip towards the east and an even lower dip towards the northeast. The trend of the structure is approximately northeast to southwest.

5.3.1.2 Blue Reflector Time Contour Maps. (See figures 5.9, 5.10, and 5.11.) The blue horizon reflector times in the surveyed area were between 478 and 568 milliseconds with an average reflection time of 531 milliseconds. Again there is a slight eastward dip with a general trend in the northeast direction. A few high anomalies are concentrated on the southwest half of the surveyed area.

5.3.1.3 Contour Maps From SEISCROP Time Slices. (Blue). SEISCROP time slices may be utilized to construct work contour maps in a very short time. Trough contours shown in figures 5.12 through 5.15 are composited into a contour map shown in Figure 5.16. This map is considered a "work" map which can be refined. Such a map is very valuable in areas where dip is steep and geology is more complex. The SEISCROP map compares very well with the corresponding map (Figure 5.17) produced by digitizing, posting, and computer-contouring and could save time and effort in some areas.

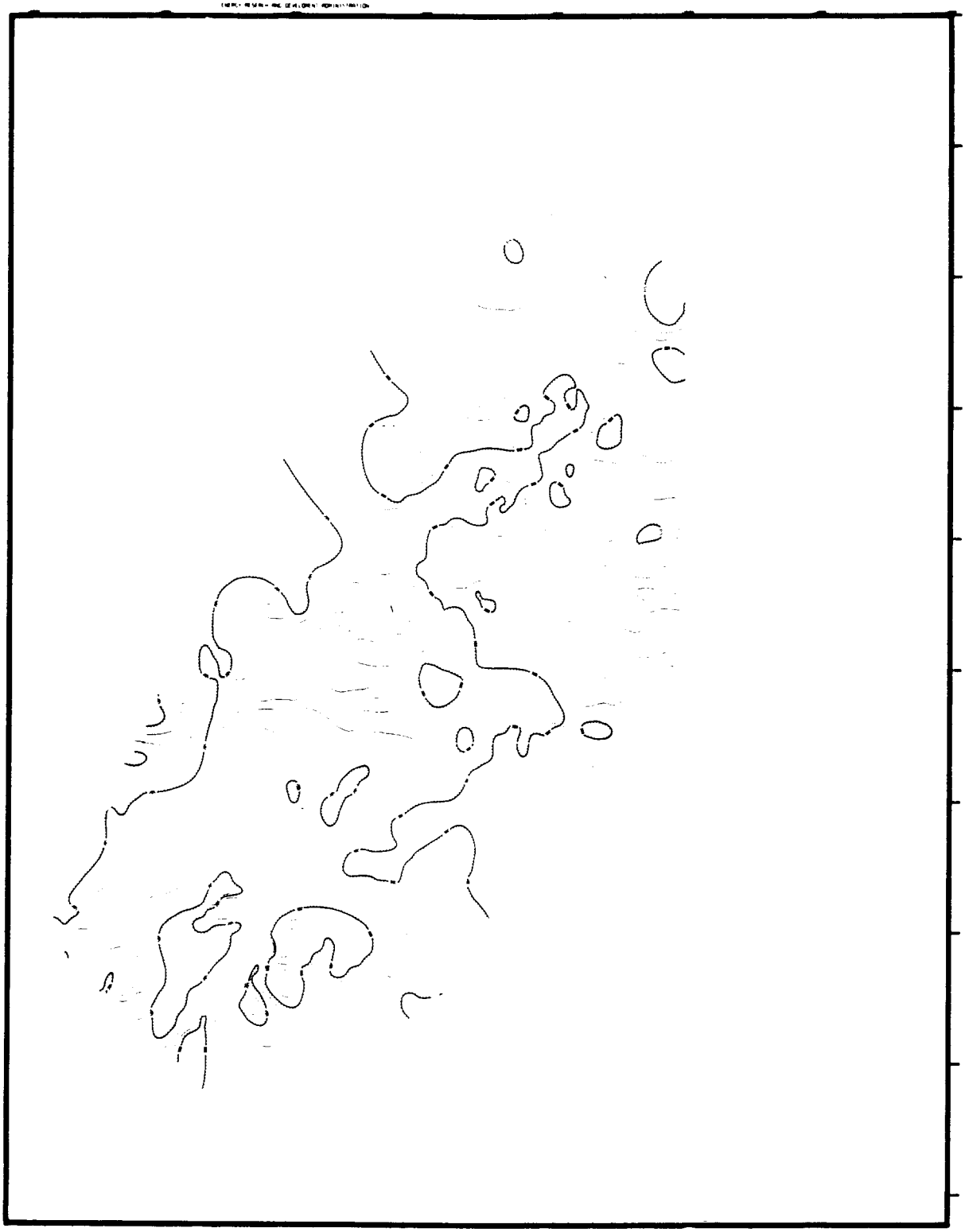

Figure 5.6 (Map 2.A). Time Contour Map, Green Reflector

Figure 5.7 (Map 2.B). Time Contour Map, Green Reflector — 5 x 5 Filter Smoothing

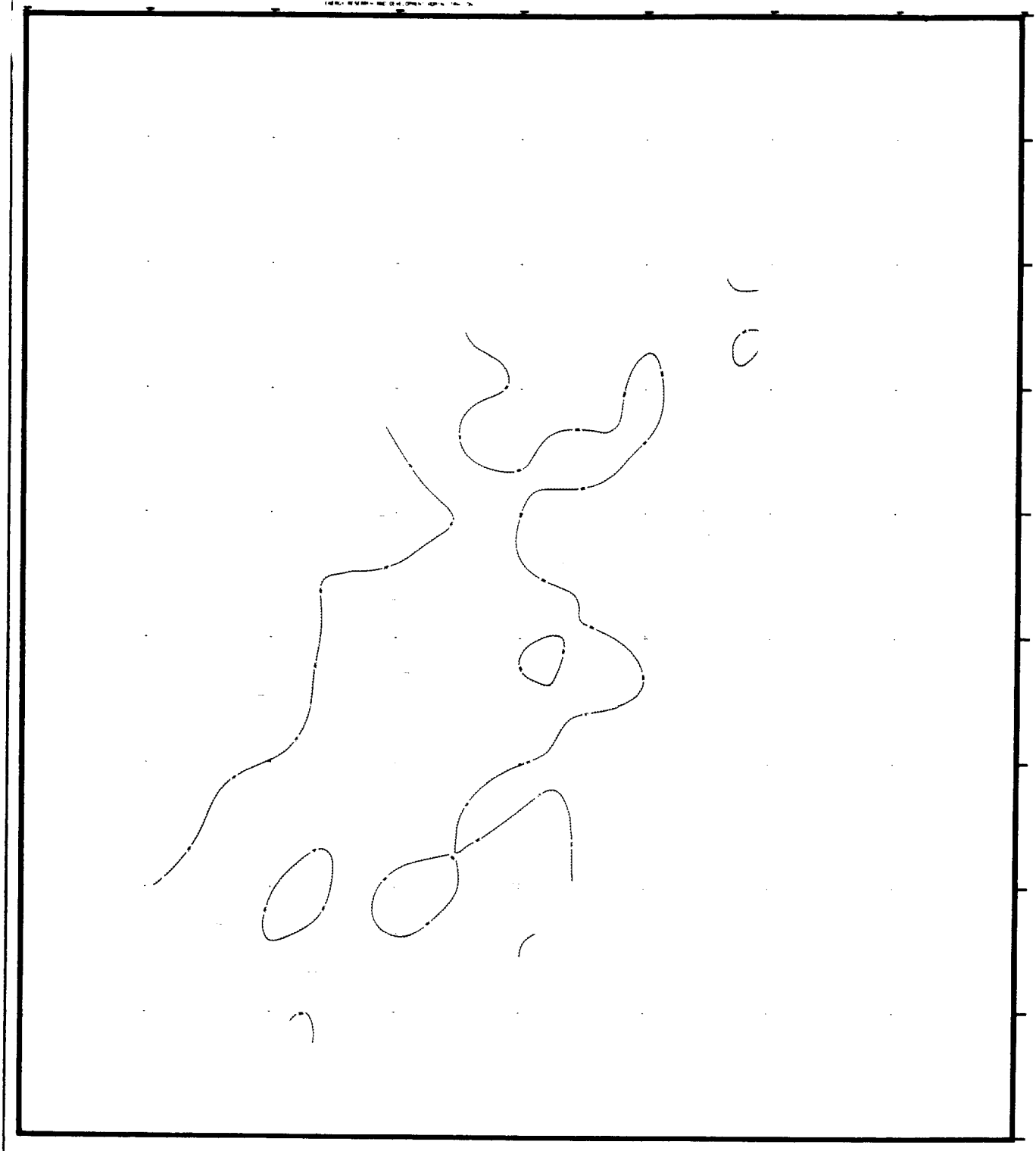

Figure 5.8 (Map 2.C). Time Contour Map, Green Reflector — 49 x 49 Filter Smoothing

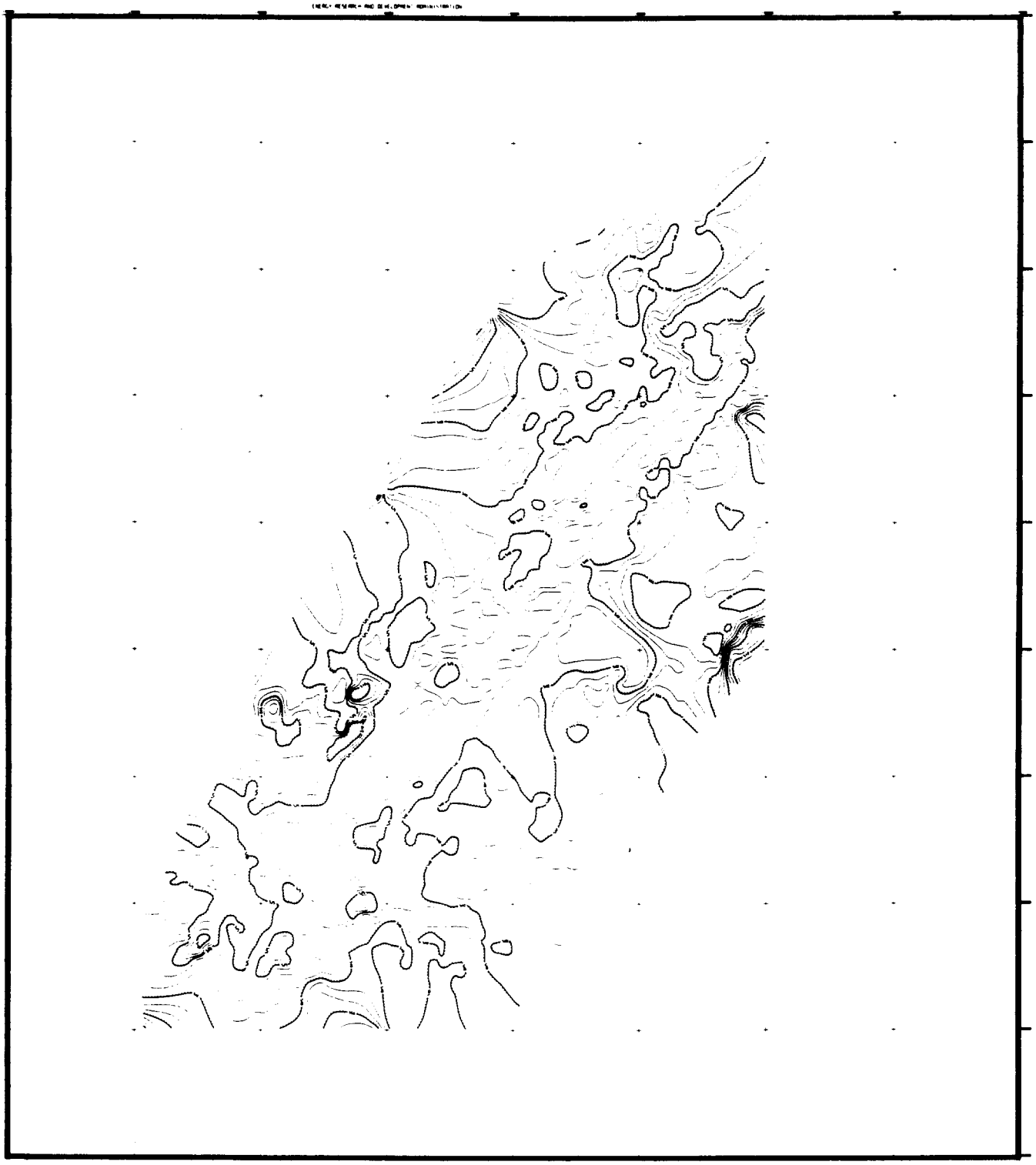

Figure 5.9 (Map 3.A). Time Contour Map, Blue Reflector

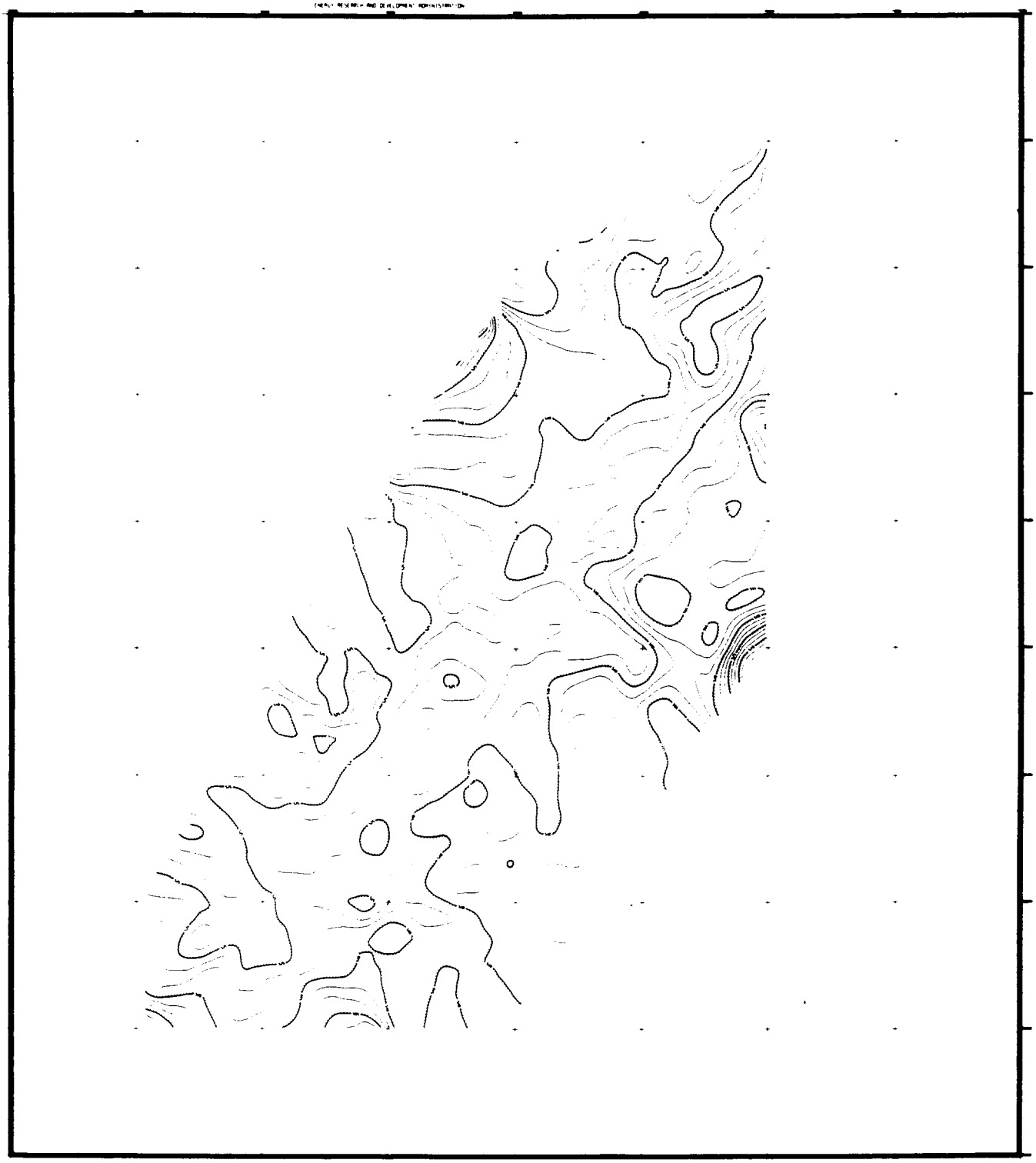

Figure 5.10 (Map 3.B). Time Contour Map, Blue Reflector — 5 x 5 Filter Smoothing

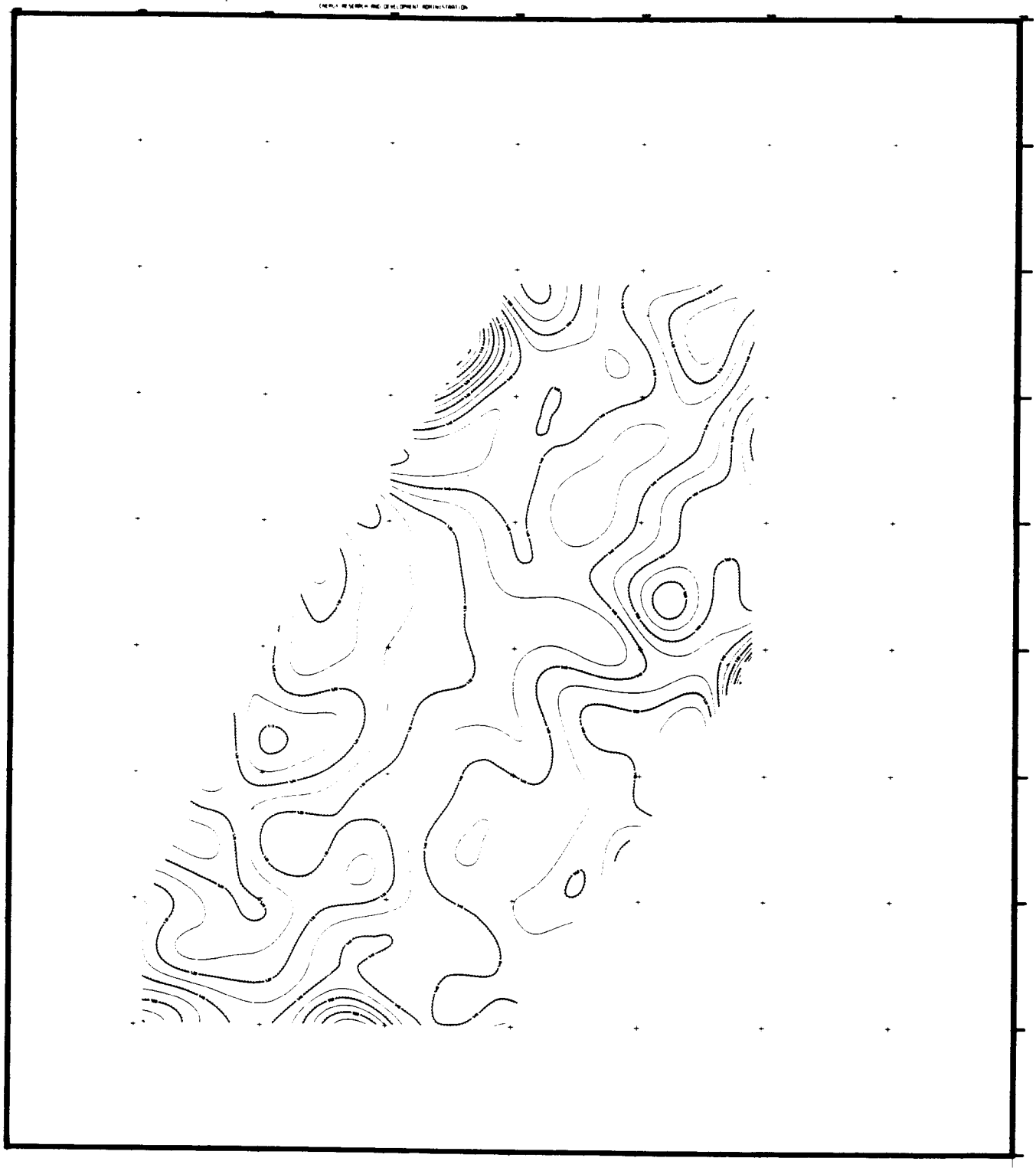

Figure 5.11 (Map 3.C). Time Contour Map, Blue Reflector — 49 x 49 Filter Smoothing

Figure 5.12. SEISCROP Map at 0.520 Second

Figure 5.13. SEISCROP Map at 0.528 Second

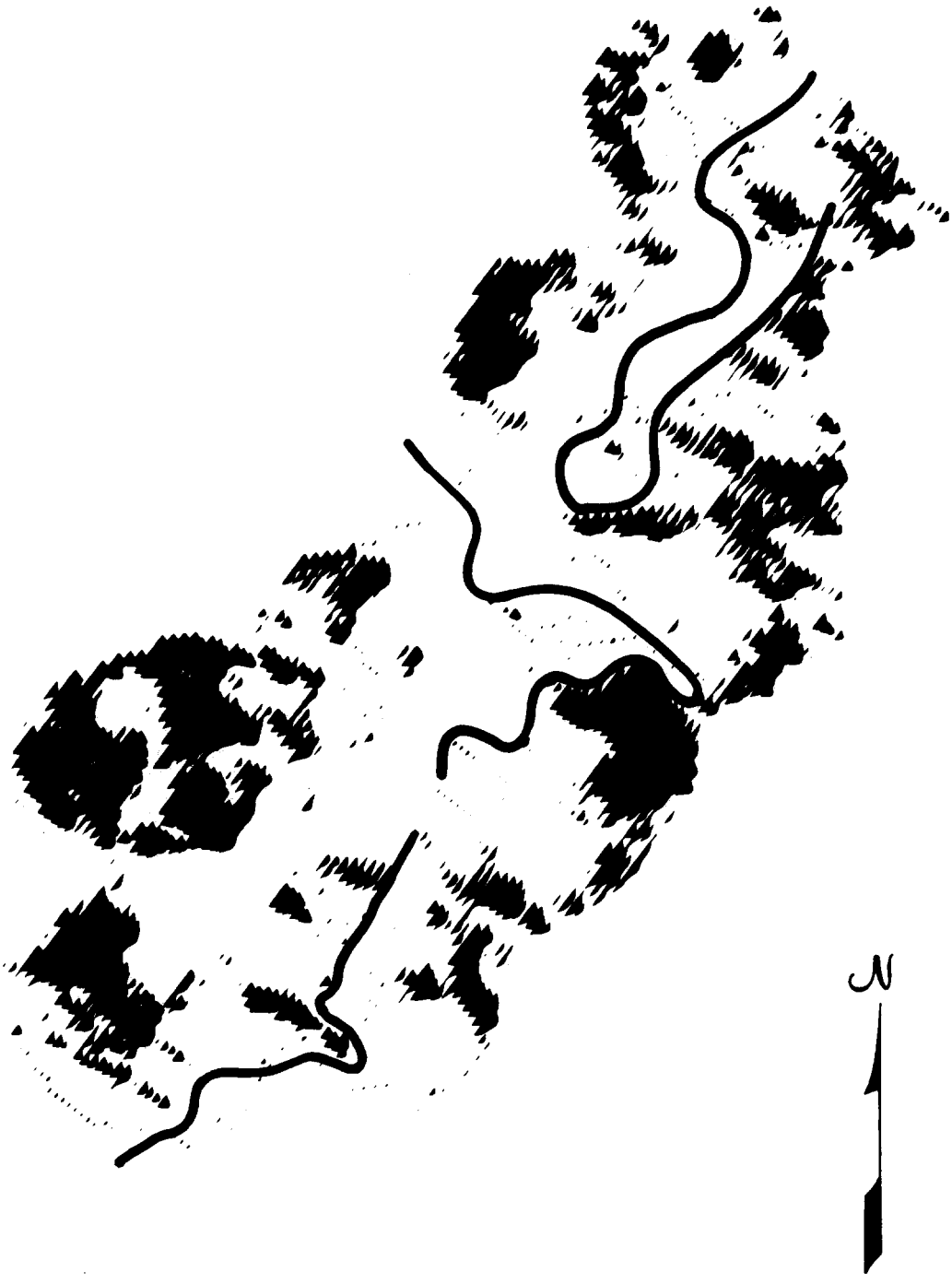

Figure 5.14. SEISCROP Map at 0.536 Second

Figure 5.15. SEISCROP Map at 0.544 Second

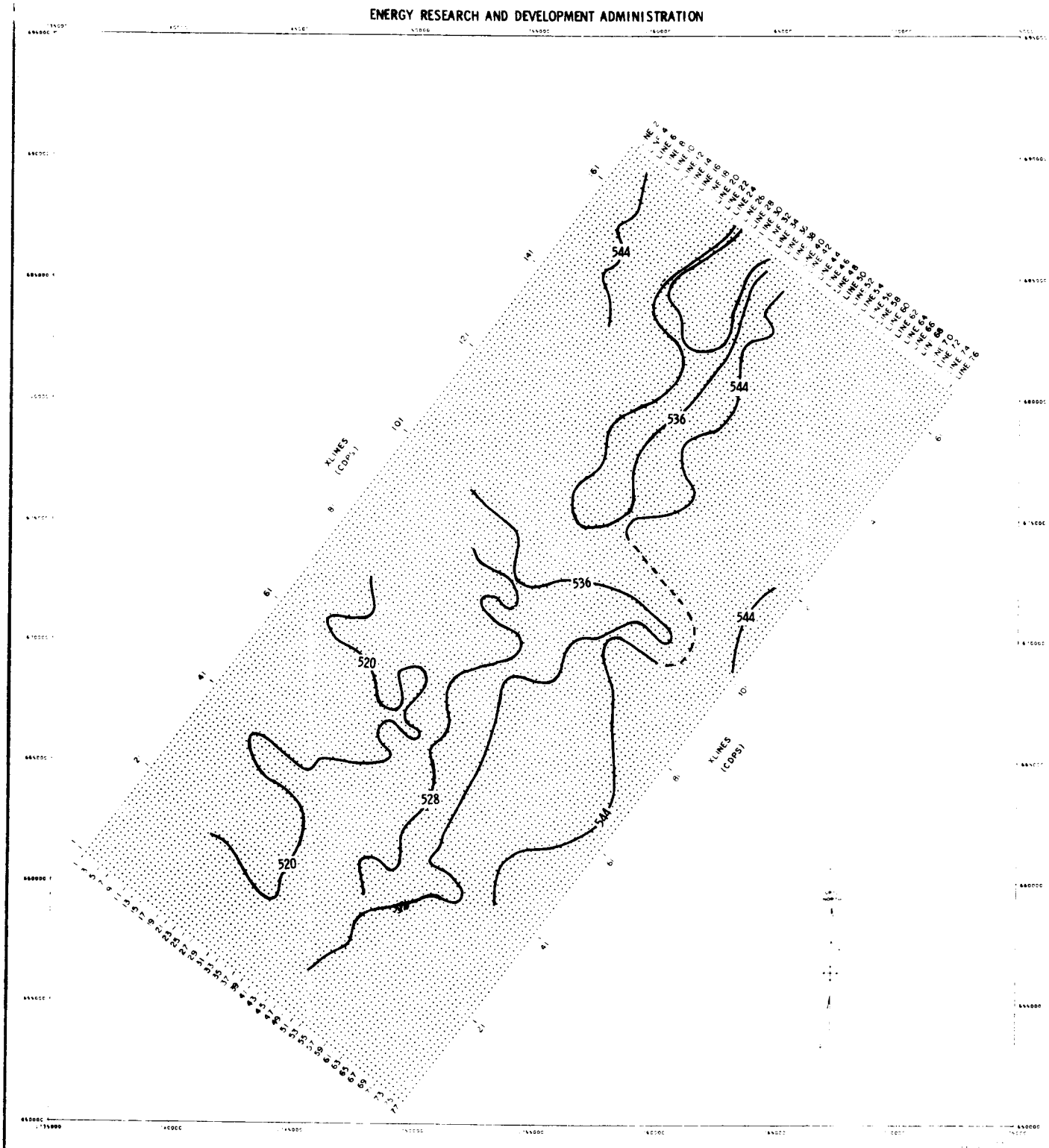

Figure 5.16. Time Contour Map from SEISCROP Maps, Red Reflector

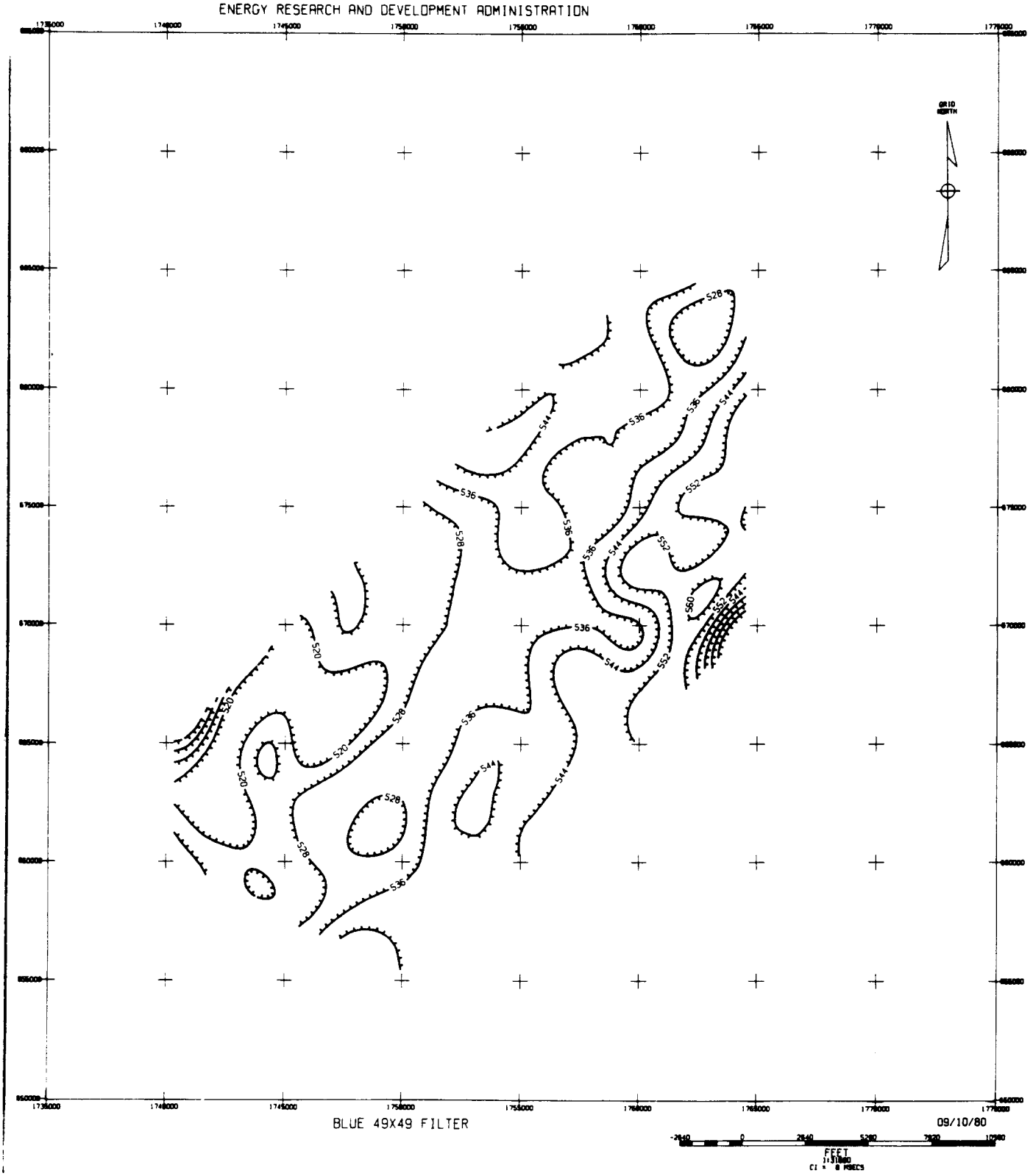

Figure 5.17. Time Contour Map from Computer, Blue Reflector

5.3.1.4 Red Reflection Time Contour Maps. (See figures 5.18, 5.19, and 5.20.) Reflection times of the red reflector ranged from 662 to 753 milliseconds and averaged 704 milliseconds. The contour map exhibits a similar pattern as the blue reflector for which a general northeast trend is observed and eastward dipping is dominant.

5.3.1.5 Yellow Reflector Time Contour Maps. (Figures 5.21, 5.22, and 5.23) The yellow reflection times ranged from 731 to 820 milliseconds and the average reflection time was 779 milliseconds. The contour lines indicate a northeast dip, with maximum dip in the eastern part of the prospect. High-amplitude anomalies are shown in the southwest corner of the area.

5.3.1.6 Brown Reflector Time Contour Maps. (Figures 5.24, 5.25, and 5.26) Reflection times to the brown reflector ranged from 1210 to 1305 milliseconds and averaged 1248 milliseconds. Here the trend changes direction when compared to the above horizons. The trend of the brown horizon shifted eastward while the above reflectors showed a northeastern trend; the brown reflector exhibits east-northeast strike and south-southeast dip rather than the predominant east dip for the upper reflectors. This observation may be emphasized by simply connecting the highs together and the lows together on any of the contour maps. This could be interpreted as a possible unconformity between the brown and yellow reflectors.

5.3.1.7 Purple Reflector Contour Maps. (Figures 5.27, 5.28, and 5.29). The levels of the purple reflector were selected and hand contoured. They are labeled P1, P2, and P3, with P1 the shallowest and P3 the deepest. The purple reflectors are believed to be Precambrian and are the most structurally complicated with faults as dominant features.

Purple Reflector P1, Contour Map (Figure 5.27). The P1 reflection is the shallowest of the "Precambrian" reflections that could be traced on the seismic sections and contoured. Reflection times ranged from 1.451 to 1.731 seconds, averaging 1.591 seconds. The dominant structural trend is northeast and the dip, in the southwest region, is predominately southeast. As with P2, it is broken by a fault system trending in northeast and southwest

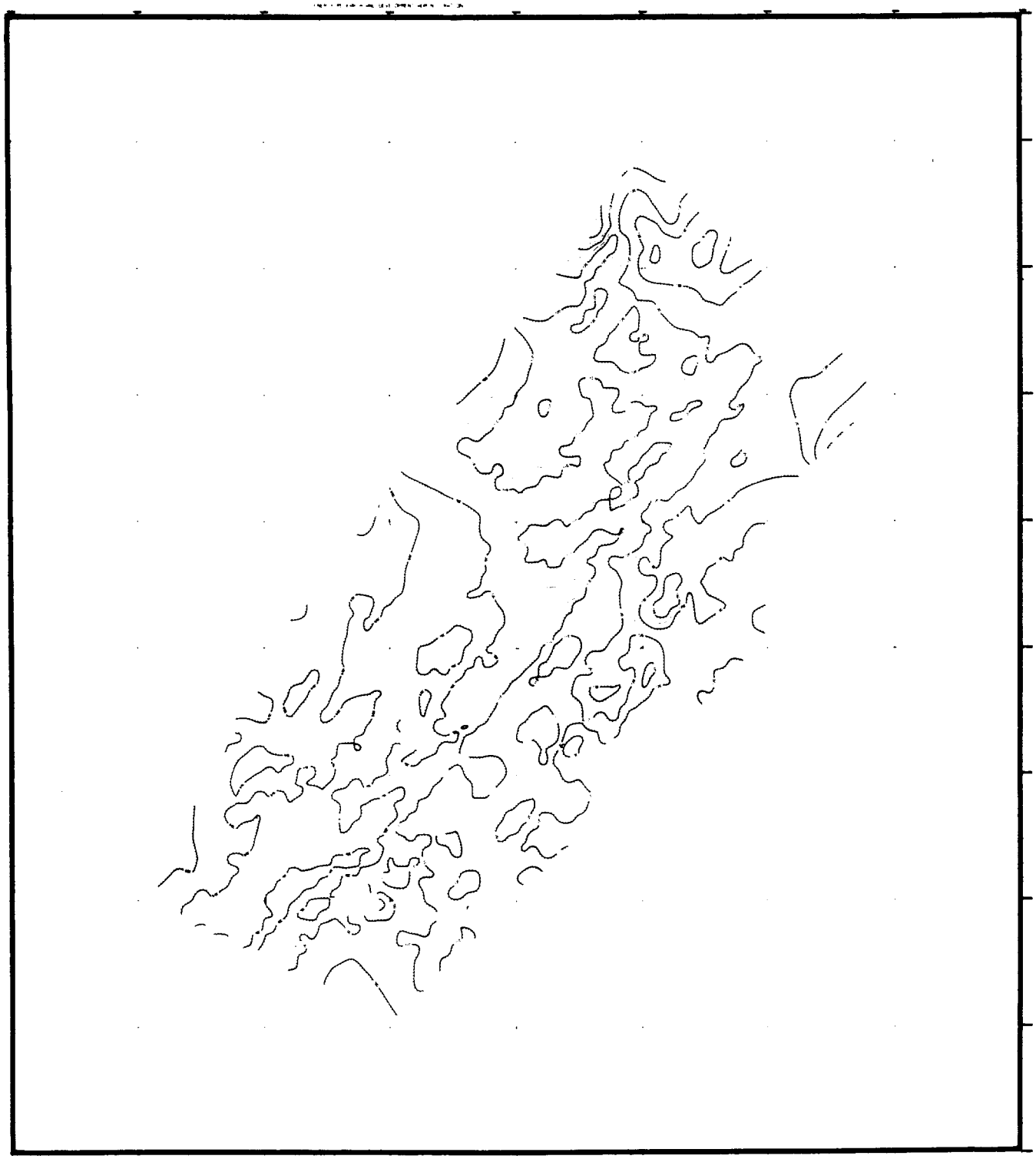

Figure 5.18 (Map 4.A). Time Contour Map, Red Reflector

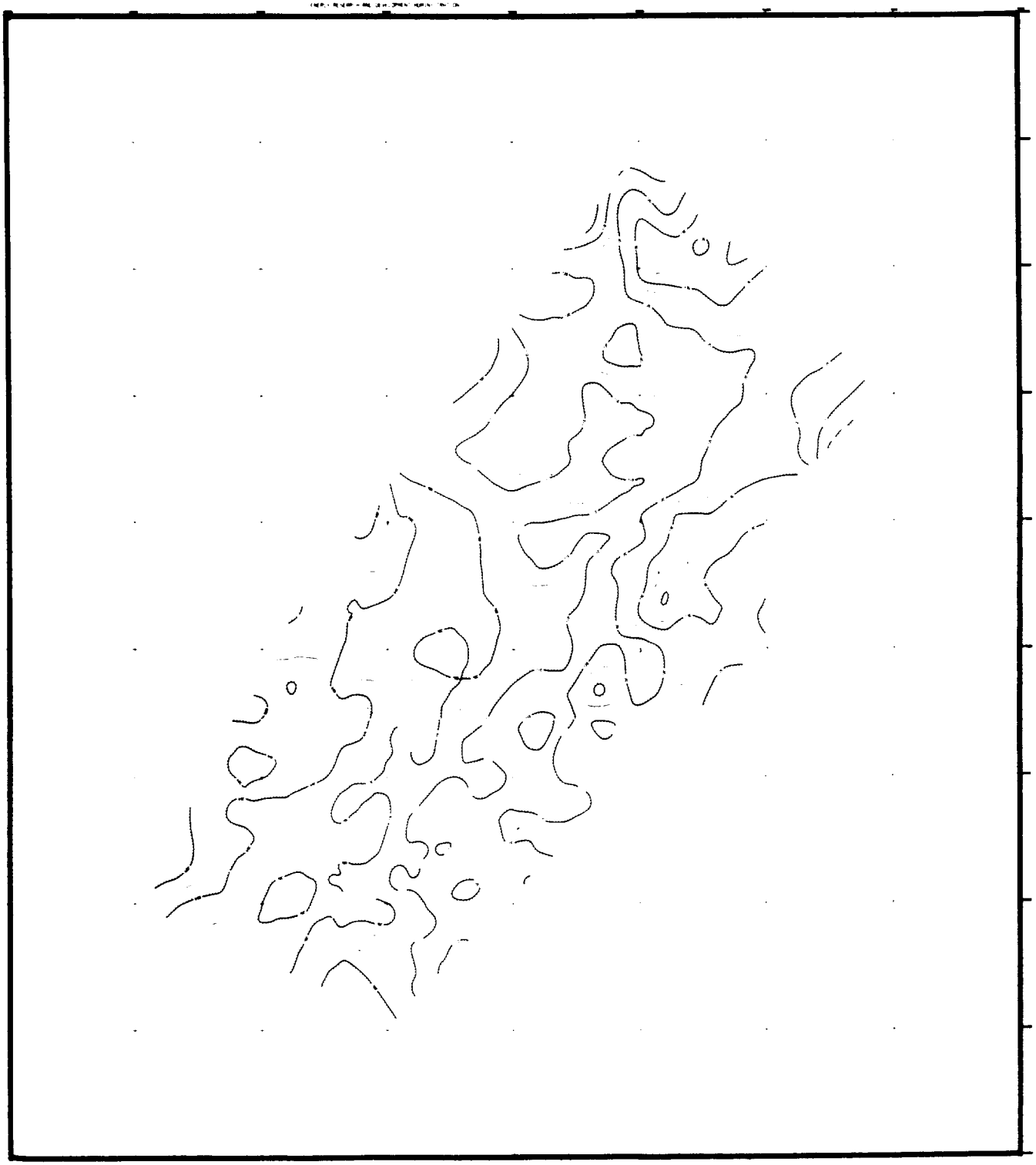

Figure 5.19 (Map 4.B). Time Contour Map, Red Reflector — 5 x 5 Filter Smoothing

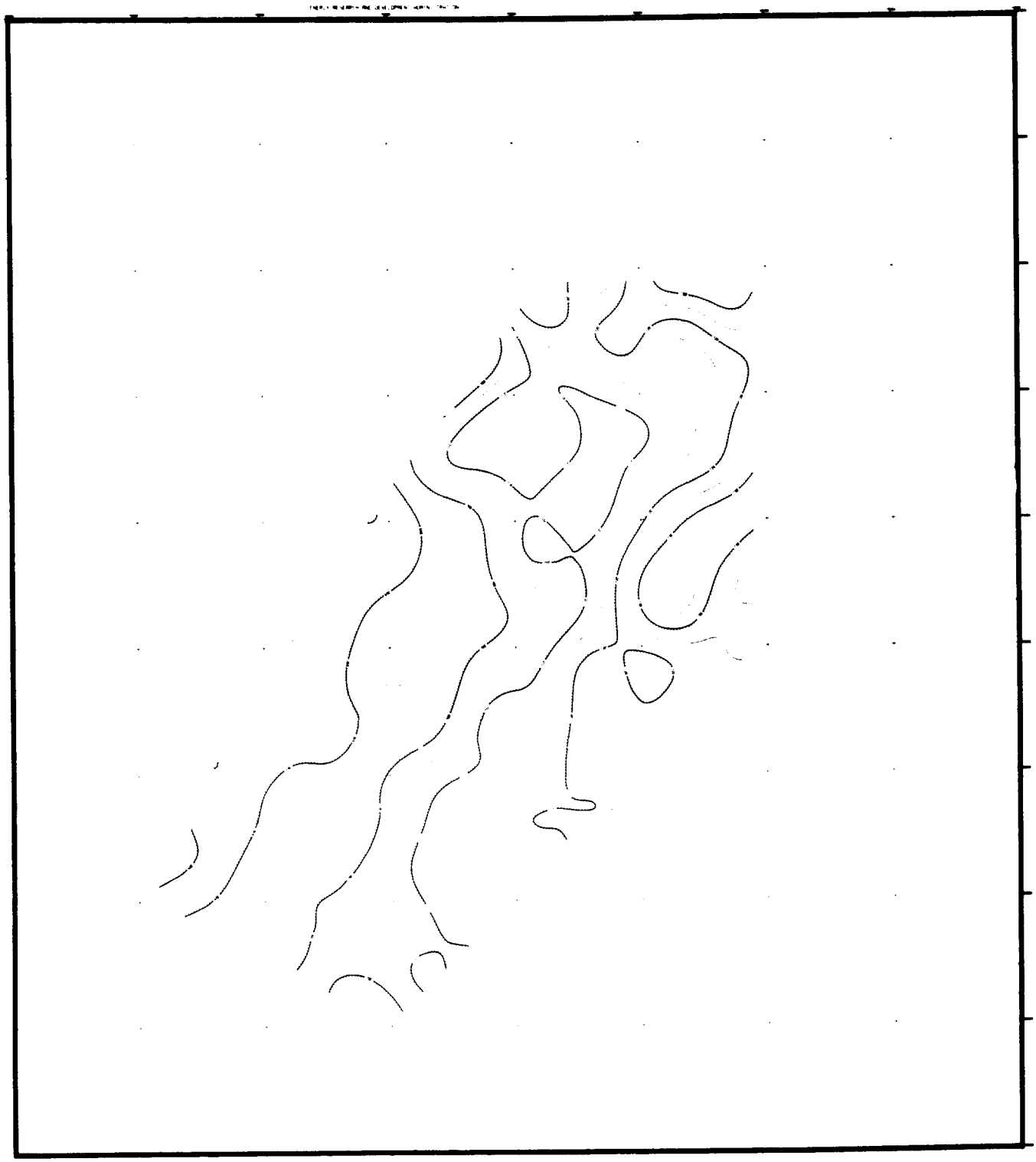

Figure 5.20 (Map 4.C). Time Contour Map, Red Reflector — 49 x 49 Filter Smoothing

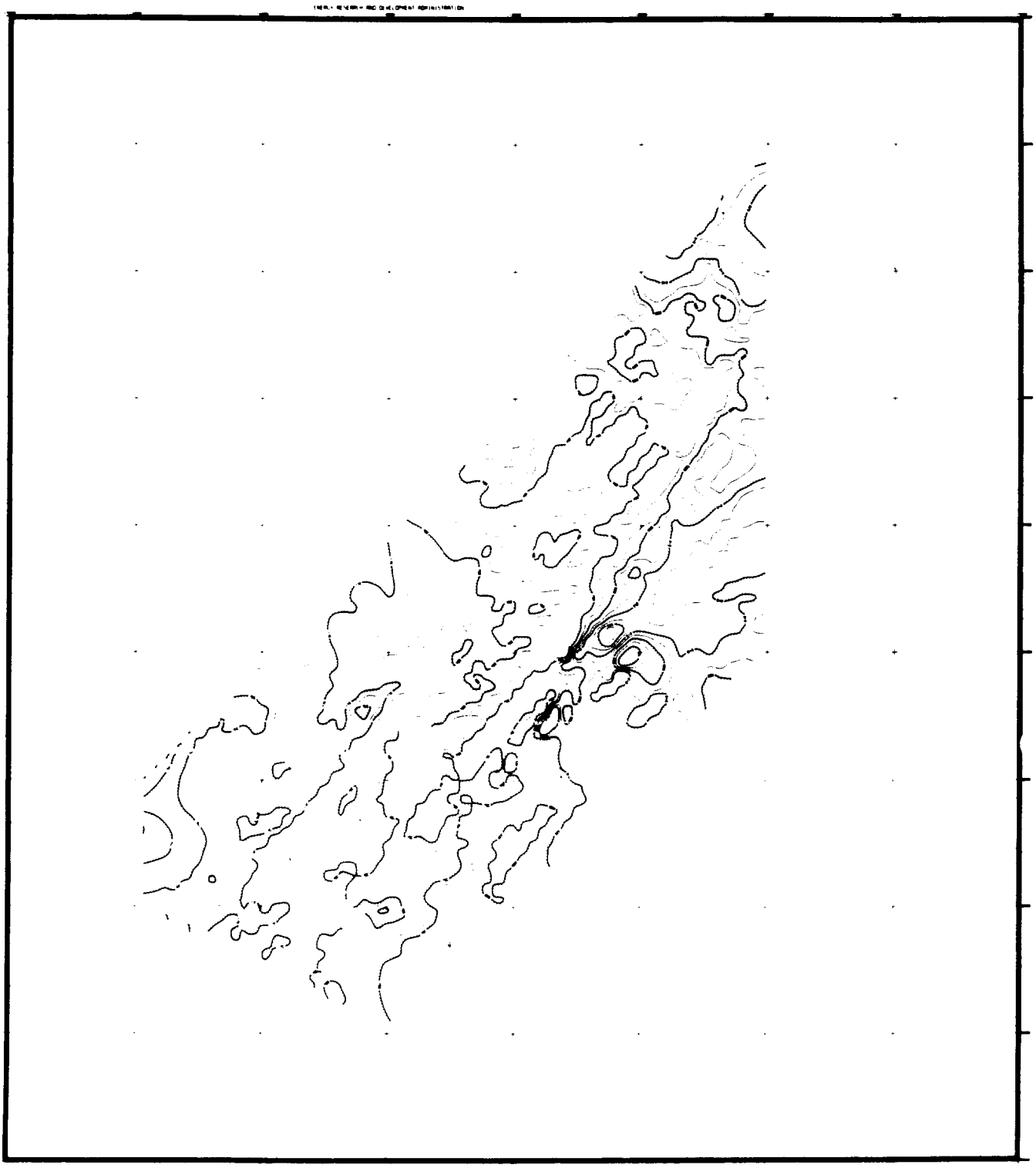

Figure 5.21 (Map 5.A). Time Contour Map, Yellow Reflector

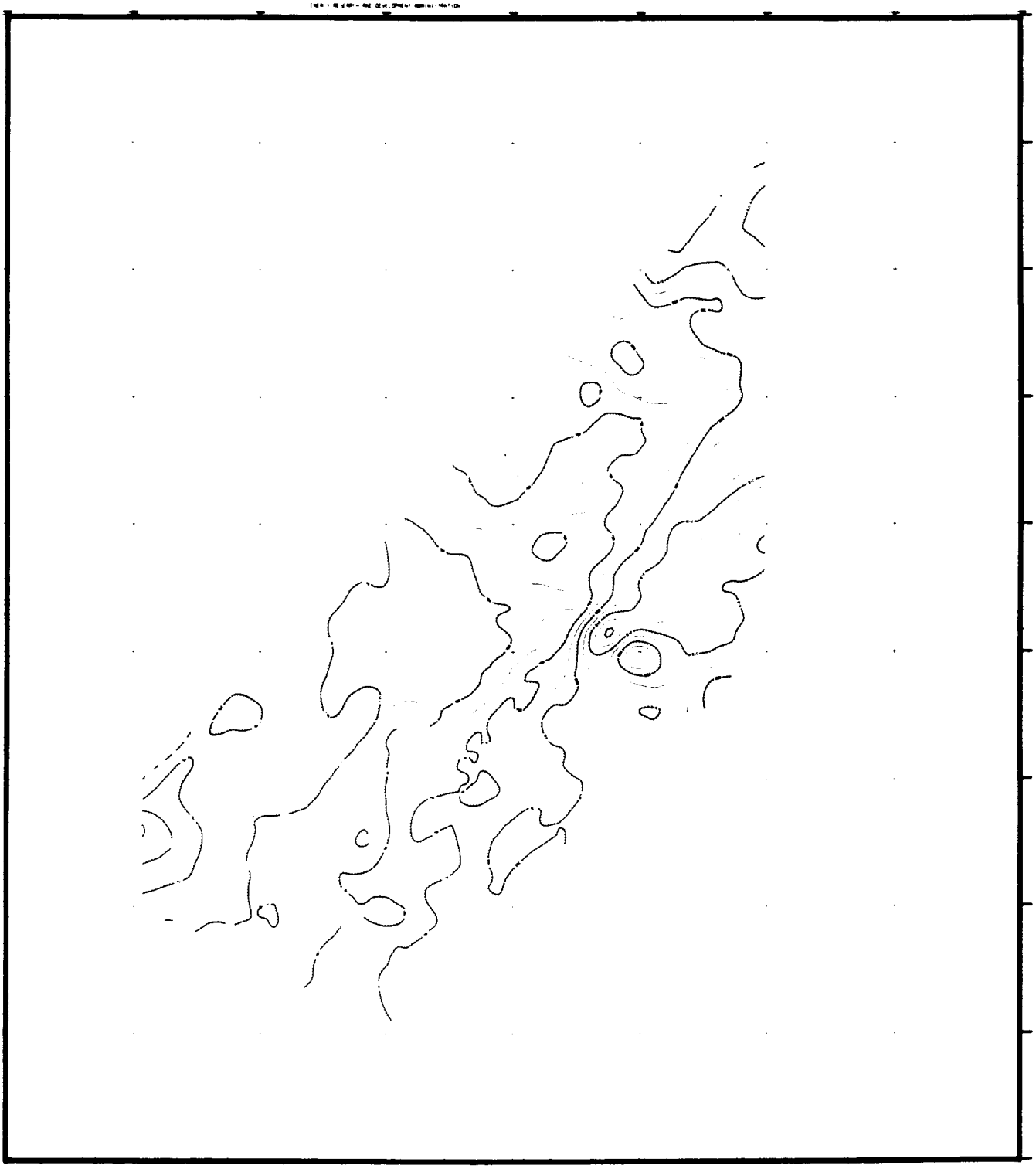

Figure 5.22 (Map 5.B). Time Contour Map, Yellow Reflector — 5 x 5 Filter Smoothing

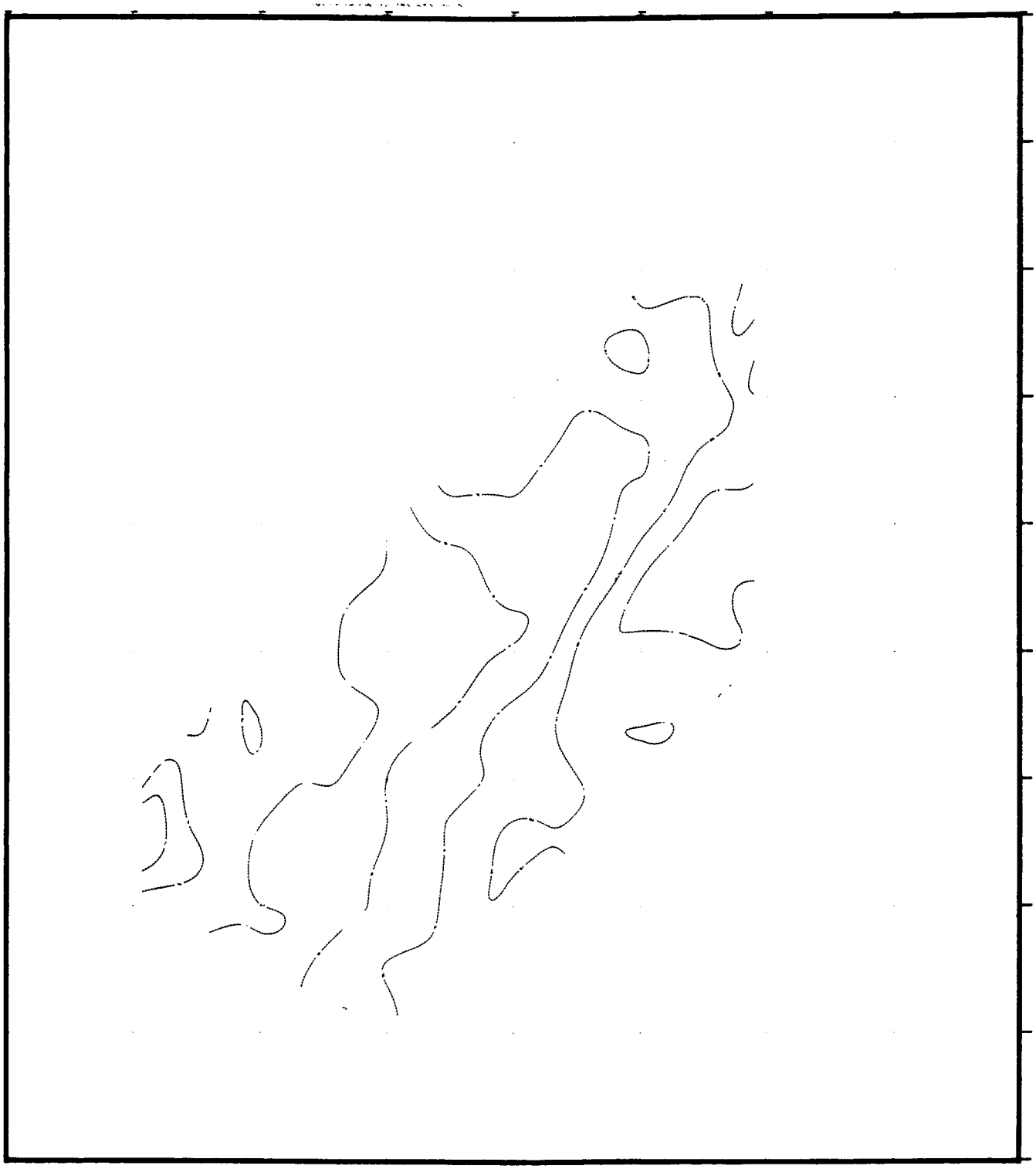

Figure 5.23 (Map 5.C). Time Contour Map, Yellow Reflector — 49 x 49 Filter Smoothing

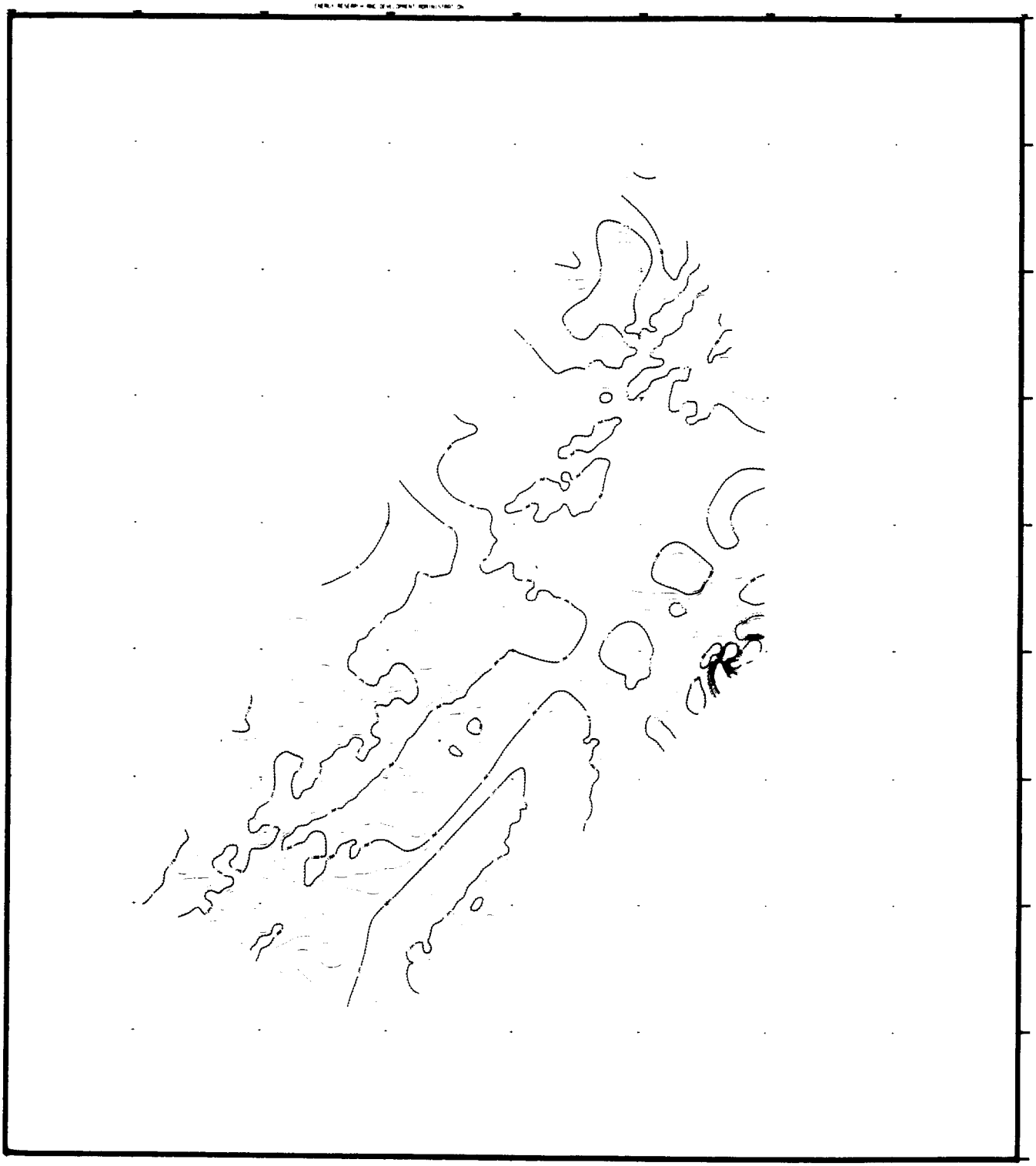

Figure 5.24 (Map 6.A). Time Contour Map, Brown Reflector

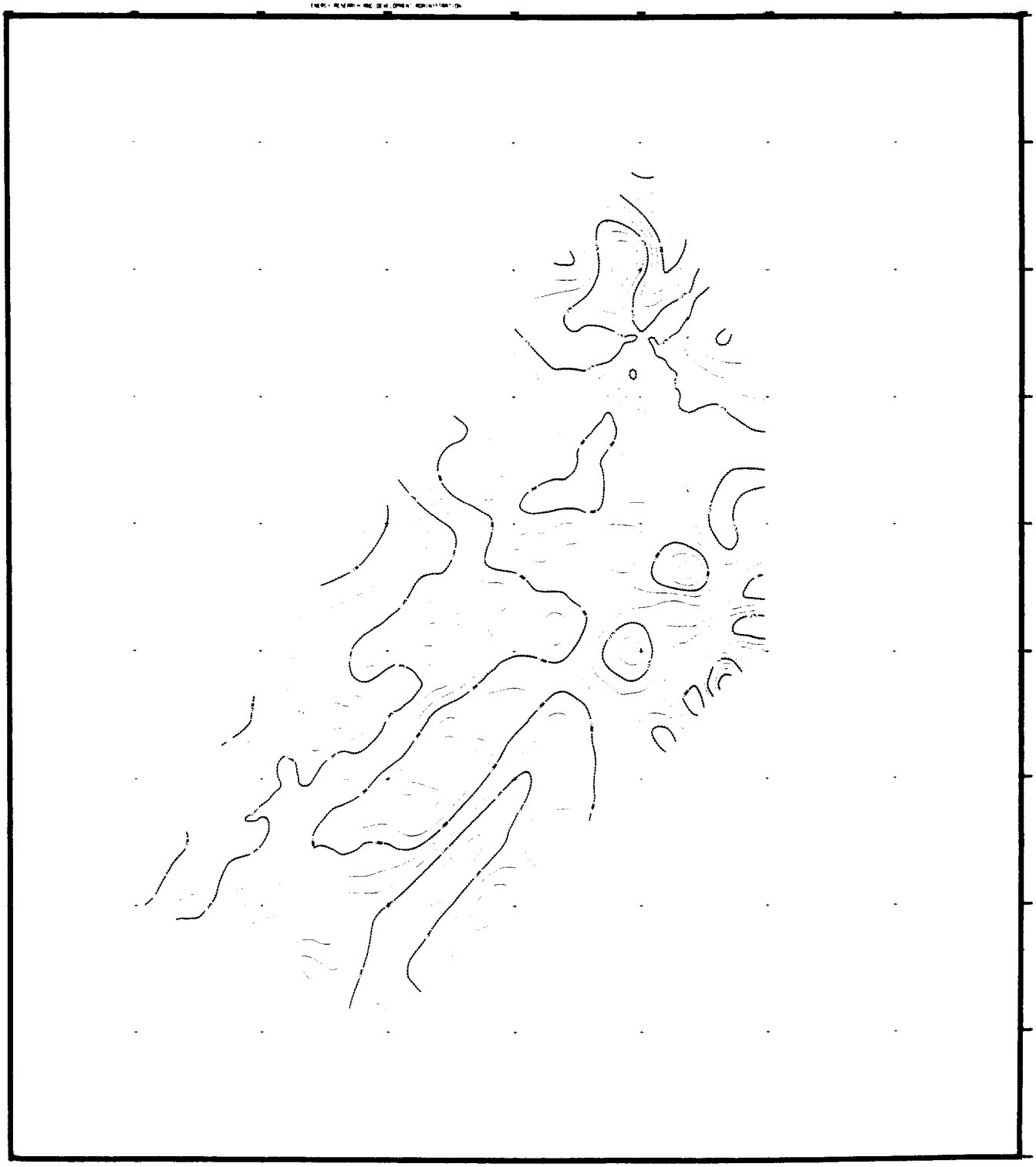

Figure 5.25 (Map 6.B). Time Contour Map, Brown Reflector — 5 x 5 Filter Smoothing

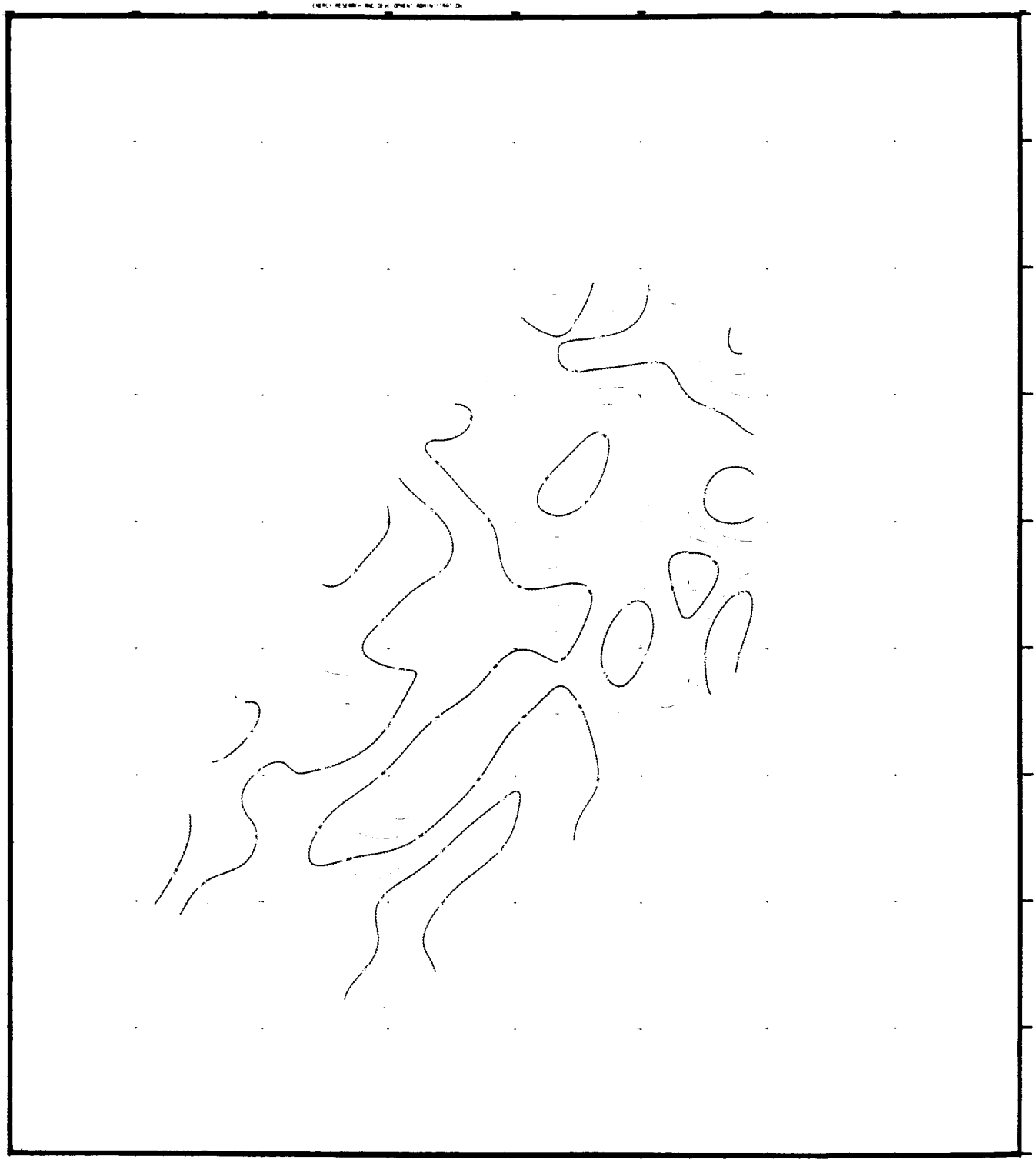

Figure 5.26 (Map 6.C). Time Contour Map, Brown Reflector — 49 x 49 Filter Smoothing

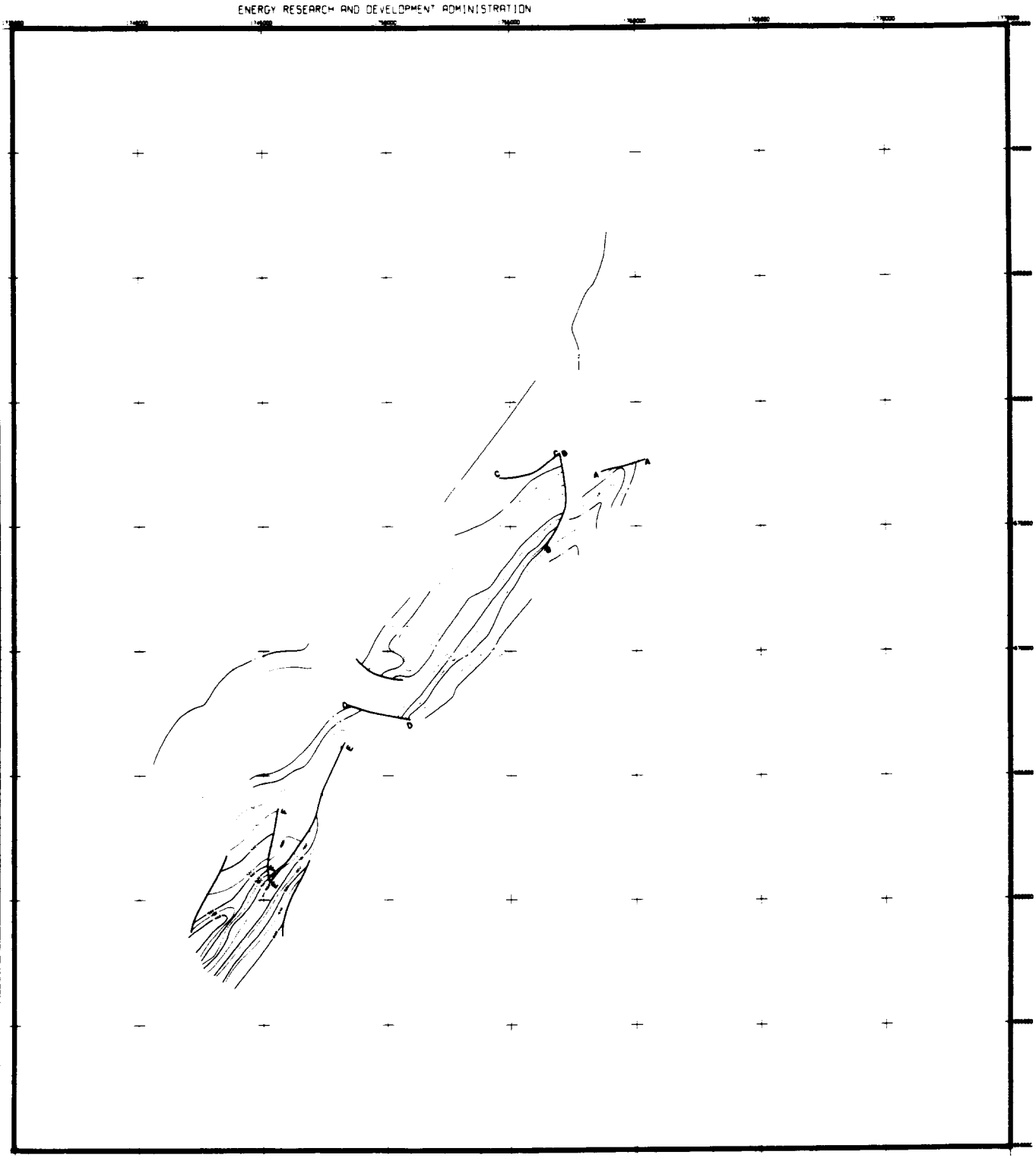

Figure 5.27 (Map 7.A). Time Contour Map, Purple (P1) Reflector

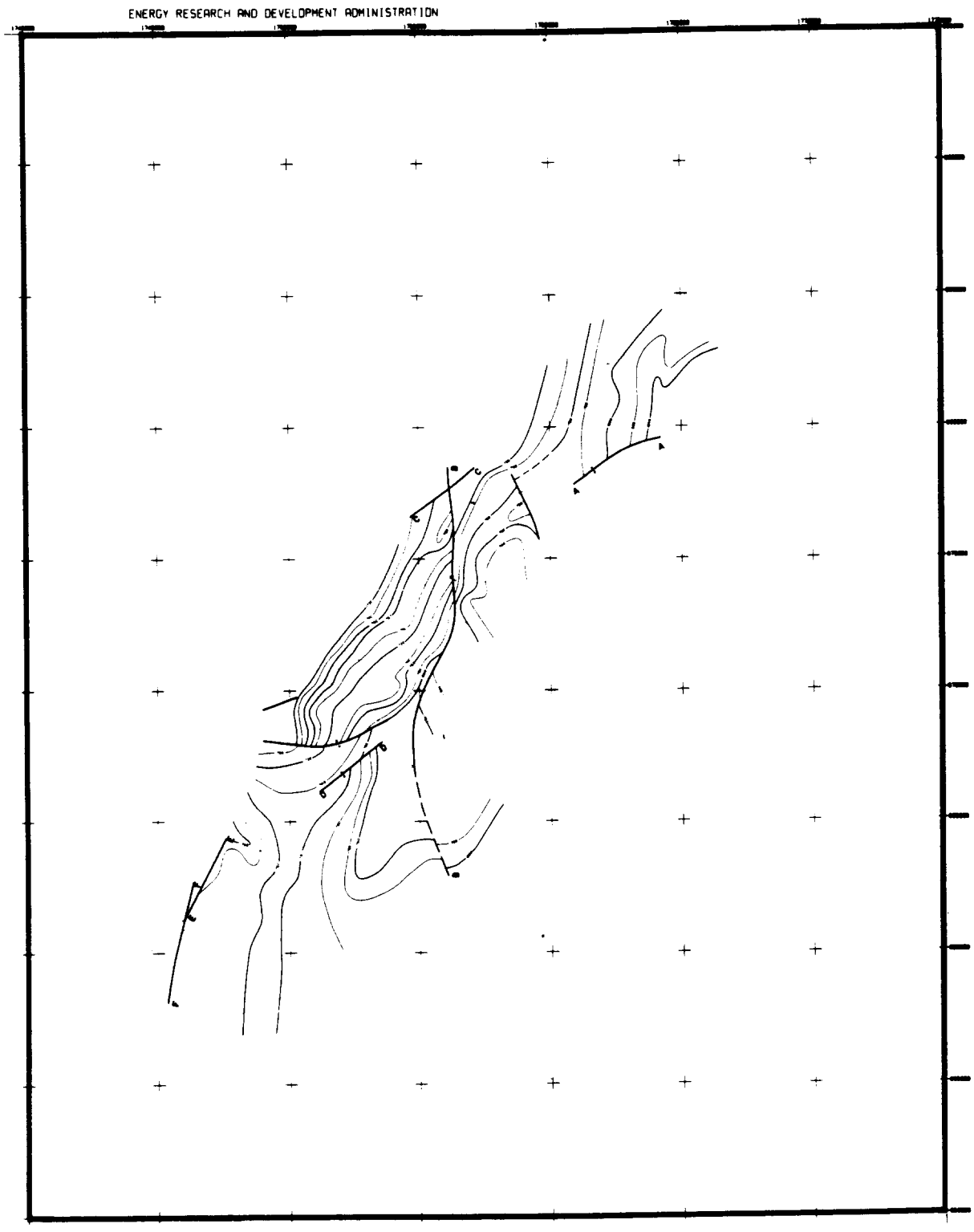

Figure 5.28 (Map 7.B). Time Contour Map, Purple (P2) Reflector

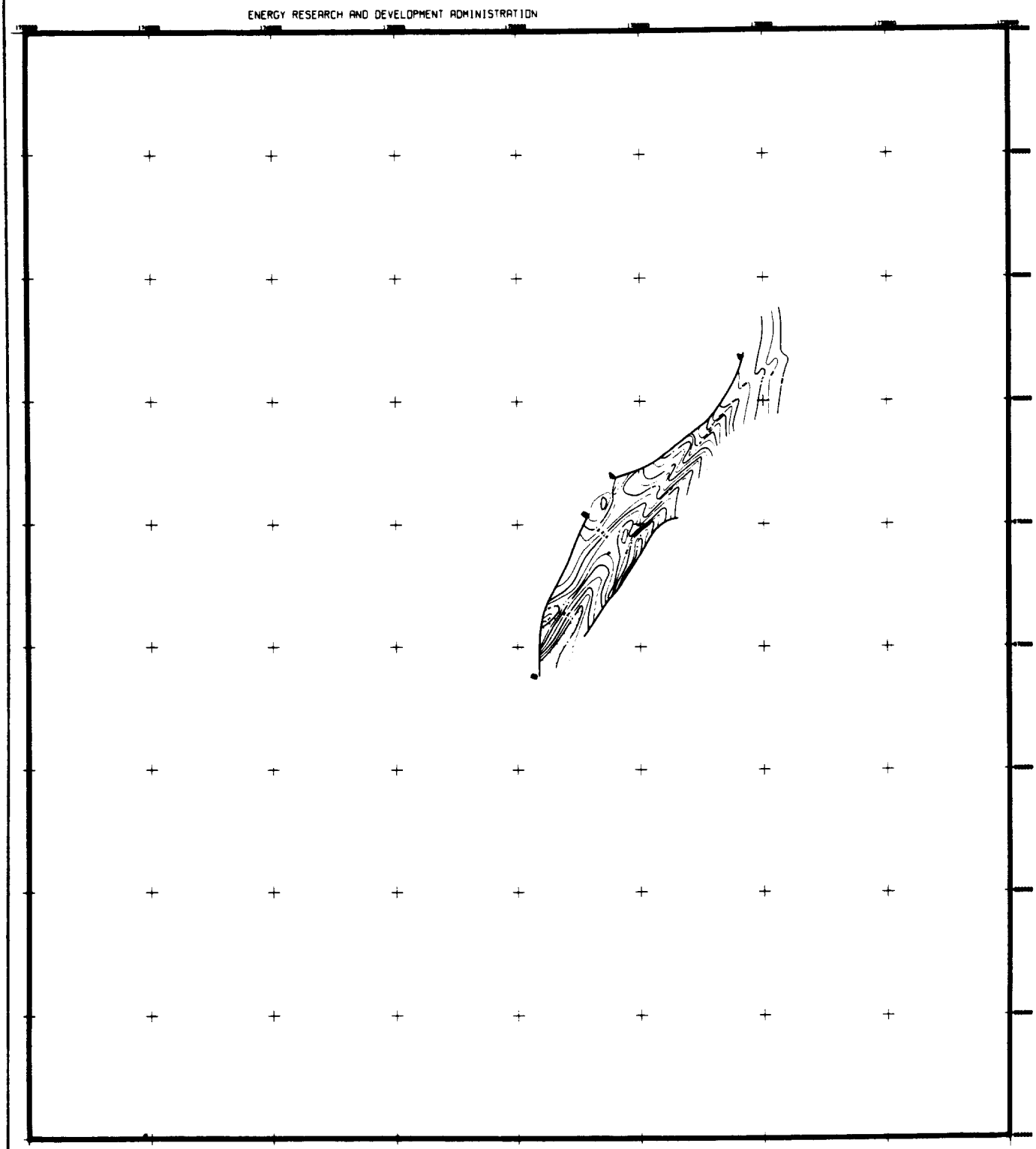

Figure 5.29 (Map 7.C). Time Contour Map, Purple (P3) Reflector

directions. P1 Fault B, which extends upward from P3 to P2 is also shown at the P1 level. A block is bounded by Fault B and Fault D in the central zone of the survey with a syncline elongated in a NE-SW direction. Faults B and C enclose a wedge-shaped block as do faults E and F. Tectonic activity is dramatized by the numerous faults in the southwest part of the P1 contour map.

Purple Reflector P2 Contour Map (Figure 5.28). The P2 reflector extends to a larger area than does the P3 reflector. Reflection time ranged from 1.688 to 1.828 seconds and averaged 1.758 seconds. The reflector was broken into many blocks by a fault system. Most faults are NE-SW oriented; however, faults at right angles do exist – namely, Fault B which is extended upward and in a western direction from P1 level. The major block of P2 is bounded by faults B and D and is thought to be a graben block. A horst block is shown SW of the graben block. Additionally, there exist two wedge-shaped blocks bounded by faults F and E on the southwest boundary and by faults B and C on the northeast boundary.

Purple Reflector P3 Contour Map (Figure 5.29). The reflection time ranged between 1.820 to 2.000 seconds with an average of 1.82 seconds. The reflector could only be picked from line 39, depth points 112-120, and line 51, depth points 80-120. The P3 reflector is bounded by three major faults striking in approximately a NE-SW direction. The faults are believed to be thrust type but no concrete evidence exists outside the fault boundaries. The trend of the horizon is NE-SW and dip is in a NW-SE direction. Features of "squeezed" highs and lows are shown on the figure.

5.3.1.8 Isochron Contour Maps. The isochron maps were produced from the unfiltered reflection times. The isochron contour interval is 5 milliseconds. The green isochron contour map is the same as the corresponding reflection time contour map (Figure 5.6).

Blue Layer Isochron Map (Figure 5.30). The interval time of the blue-green layer ranged from 99 to 133 milliseconds with average of 119 milliseconds. One may observe the consistency of time intervals throughout the surveyed

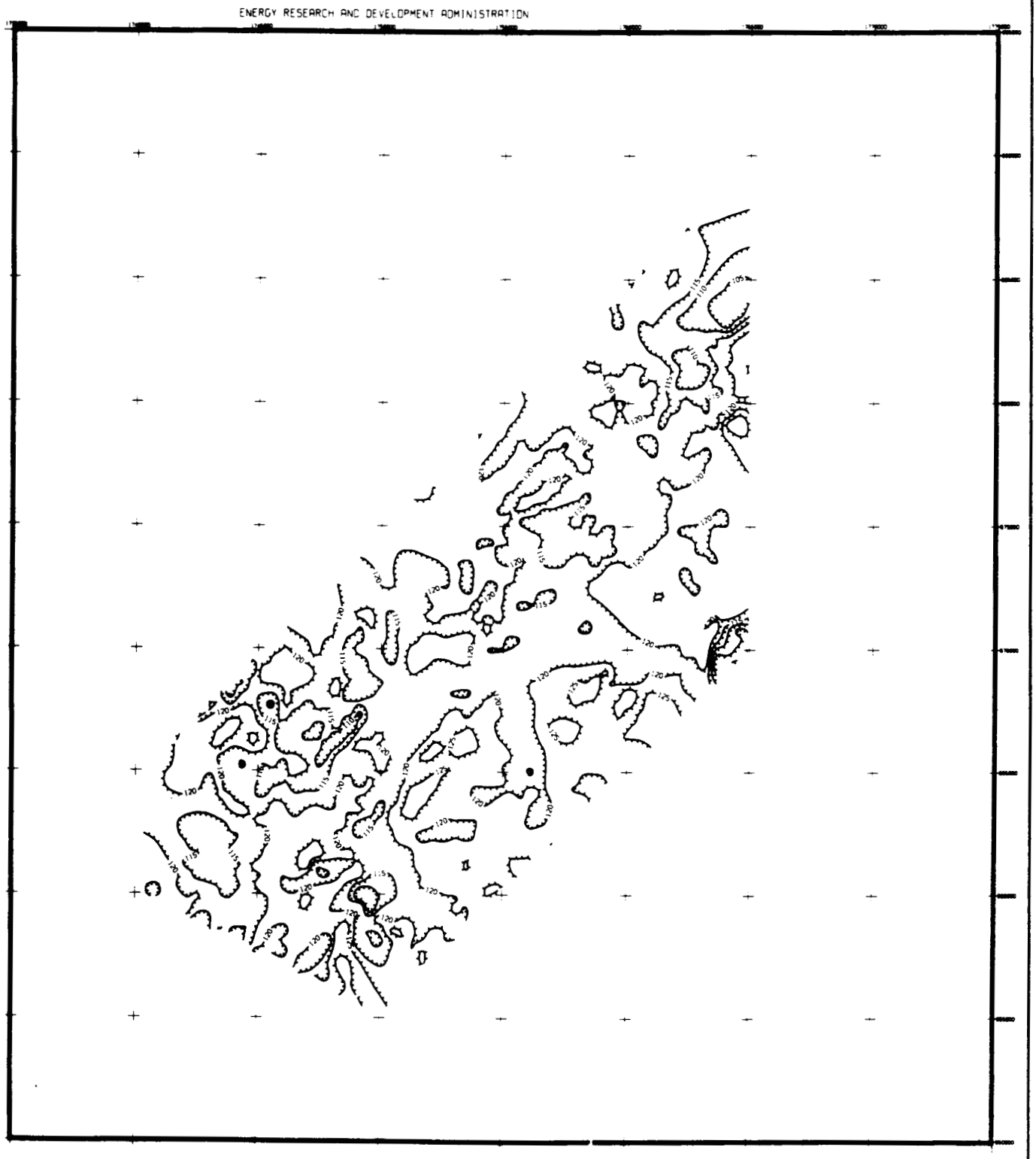

Figure 5.30 (Map 8). Isochron Map, Blue-Green Reflectors

GSI-709

area, with the possible exception of thinning toward the extreme northeast corner. Also of note is the thickening of the blue layer in the central region of the southeast edge of the prospect.

Red Layer Isochron Maps (Figure 5.31). The isochron contours of the red layer varied from 70 to 110 milliseconds. The average time interval was 86 milliseconds. There is an indication of thinning in the southwest corner and thickening in the northeast corner.

5.3.2 VELOCITY MAPS. The root mean square (RMS) velocity field is used in conjunction with travel times to calculate the interval velocities of a layer at each depth point.

$$V_{in} = \sqrt{\frac{\hat{V}_n^2 \; T_n - \hat{V}_{n-1}^2 \; T_{n-1}}{T_n - T_{n-1}}}$$

where

V_{in} = interval velocity of the layer

$\hat{V}_n, \hat{V}_{n-1}$ = The RMS velocity at the lower and the upper boundaries of the layer, respectively

T_n, T_{n-1} = The reflection time at the lower and upper boundaries, respectively.

Once the interval velocity is computed, the average velocity to a boundary $\bar{V}$ is computed as

$$\bar{V}_n = \frac{\sum_{i=1}^{n} V_{in} \; \Delta T_n}{\sum_{i=1}^{n} \Delta T_n}$$

where

$\bar{V}_n$ = average velocity to a boundary

V_i = internal velocity in layer n

ΔT_n = internal time in layer n

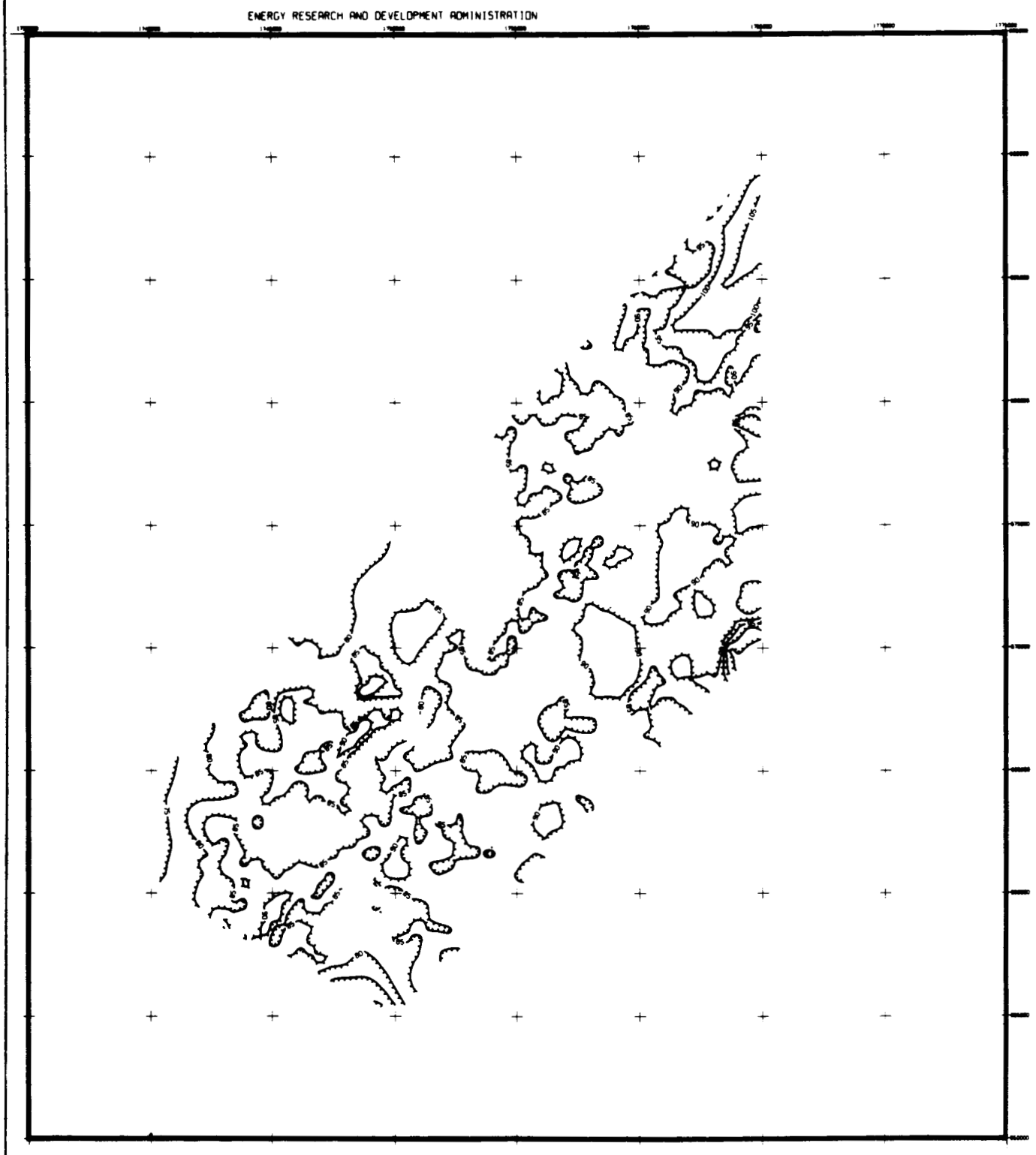

Figure 5.31 (Map 9). Isochron Map, Red-Blue Reflectors

5.3.2.1 RMS Velocity Contour Maps. The RMS velocity contour maps are shown on figures 5.32, 5.33, and 5.34 for the green, blue and red horizons, respectively. Interval contours are 50 feet/second.

The general trend is a decrease towards the northeast and east directions. One may also divide the prospect into three zones: the northeast zone is characterized by lower RMS velocity, and the southwest zone also exhibits lower velocity if compared to the central zone of the surveyed area. This division is more pronounced in the red horizon contour map. Here we see that the two lower velocity zones are distinct and tend to shift more toward the northwest edge of the area.

5.3.2.2 Interval Velocity Contour Maps. Two sets of interval velocity contour maps were produced for the green, blue, and red layers: one set with 50-foot/second intervals and the other with 100-foot/second intervals. The 100-foot/second interval is used for detecting trends, whereas the other set is for more detailed analysis.

Maps are exhibited in figures 5.35 to 5.40. The general trend for the three layers is NE-SE. A high-velocity anomaly is shown on the northeast-central part for the red interval. One observes the low anomaly at the eastern edge of the same interval.

5.3.2.3 Average Velocity Contour Maps. Two sets of average velocity contour maps were generated for the green, blue, and red horizons: one with 50-foot/second and the other with 100-foot/second contour intervals. The sequence of maps are displayed on figures 5.41 to 5.46.

The trend axis is approximately NE-SW with low-velocity anomalies shown to concentrate in the northeast and southwest zones of the surveyed area.

5.3.3 THICKNESS MAPS

5.3.3.1 Isopach Maps. The thickness of a layer is computed from the interval velocity of the layer and the one-way reflection time in the layer.

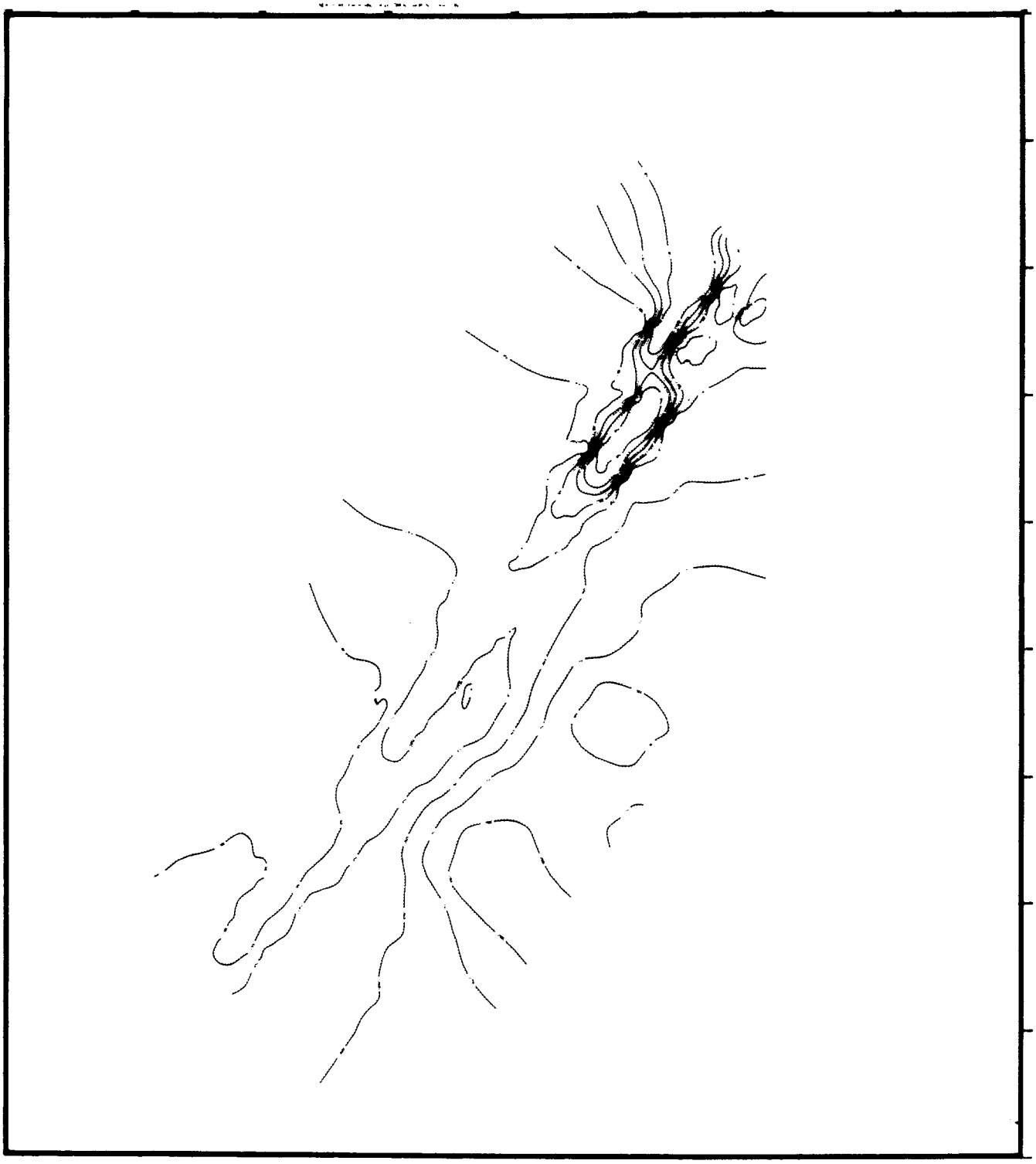

Figure 5.32 (Map 10). RMS Velocity Contour Map, Green Reflector

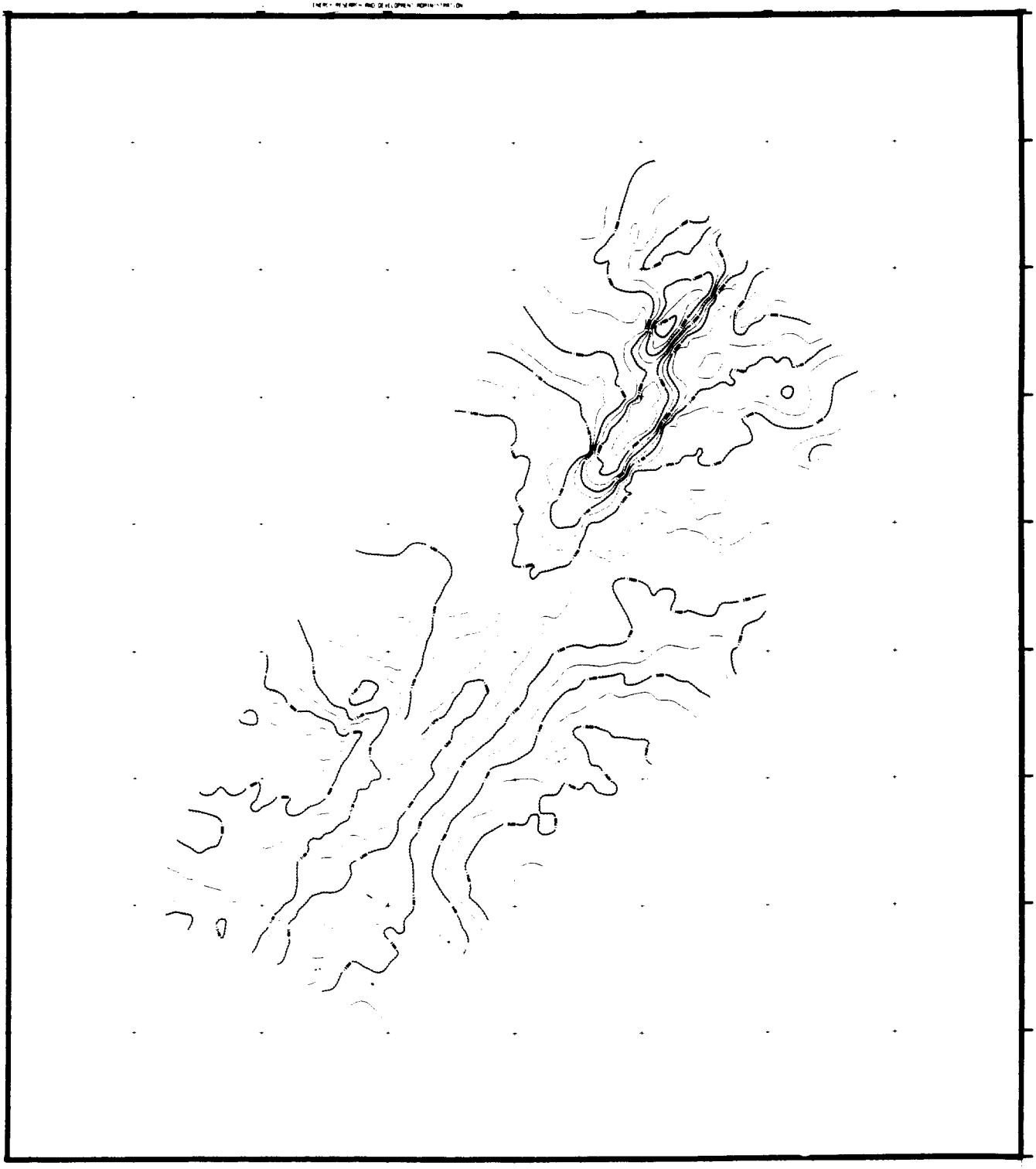

Figure 5.33 (Map 11). RMS Velocity Contour Map, Blue Reflector

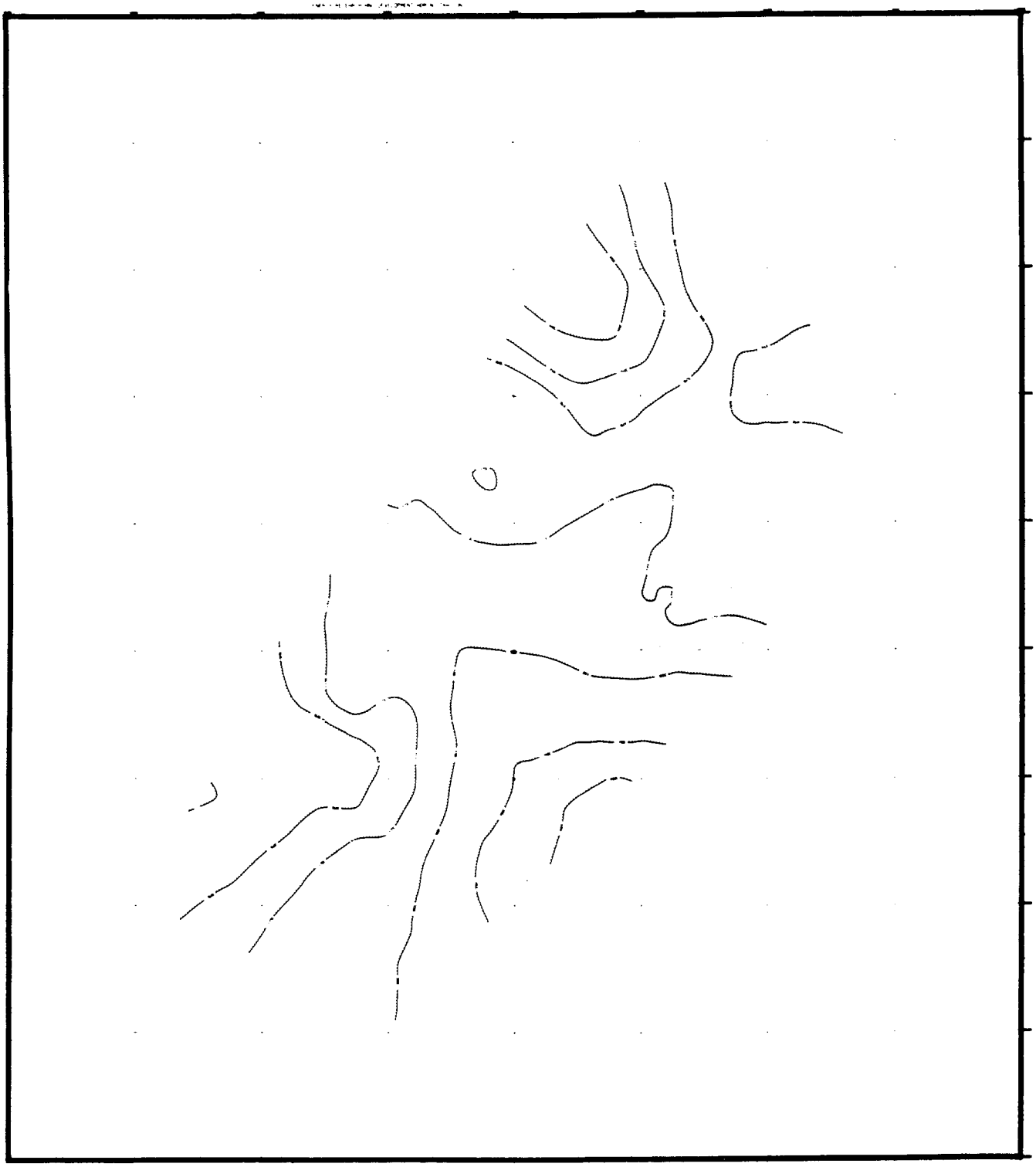

Figure 5-34 (Map 12). RMS Velocity Contour Map, Red Reflector

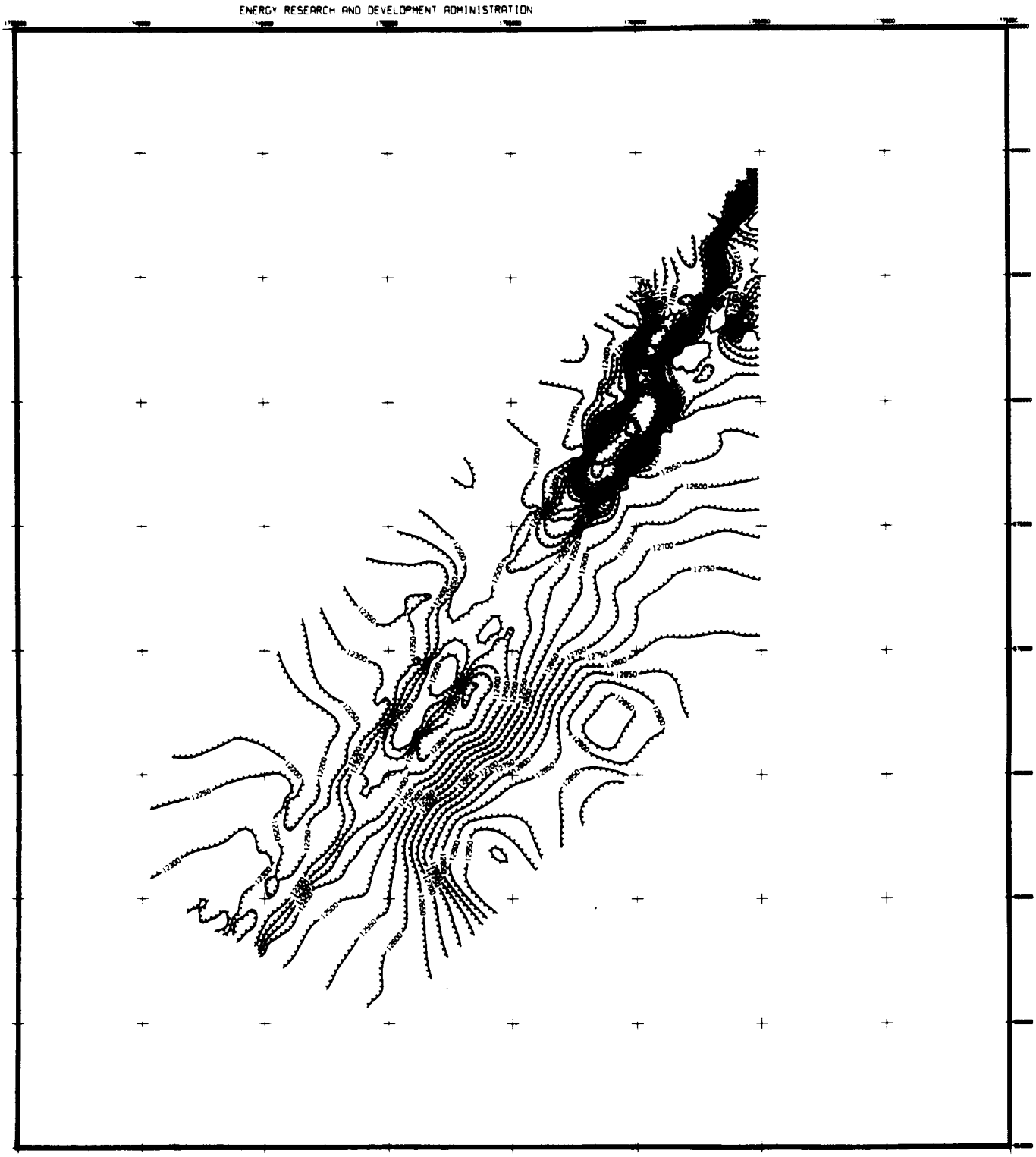

Figure 5.35 (Map 13.A). Interval Velocity Contour Map, Green Reflector — 50-Foot Interval

GSI-709

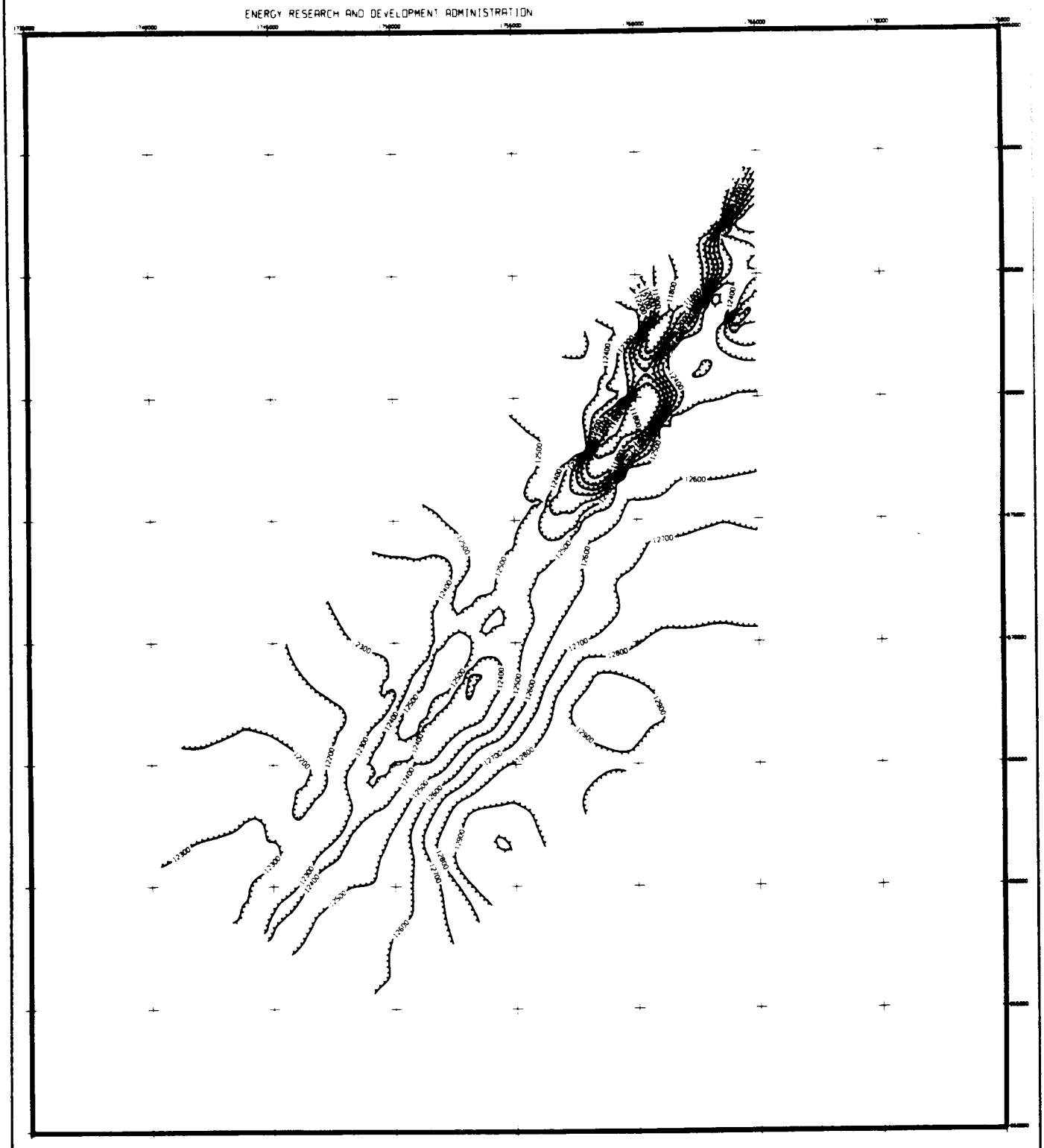

Figure 5.36 (Map 13.B). Interval Velocity Contour Map, Green Reflector — 100-Foot Interval

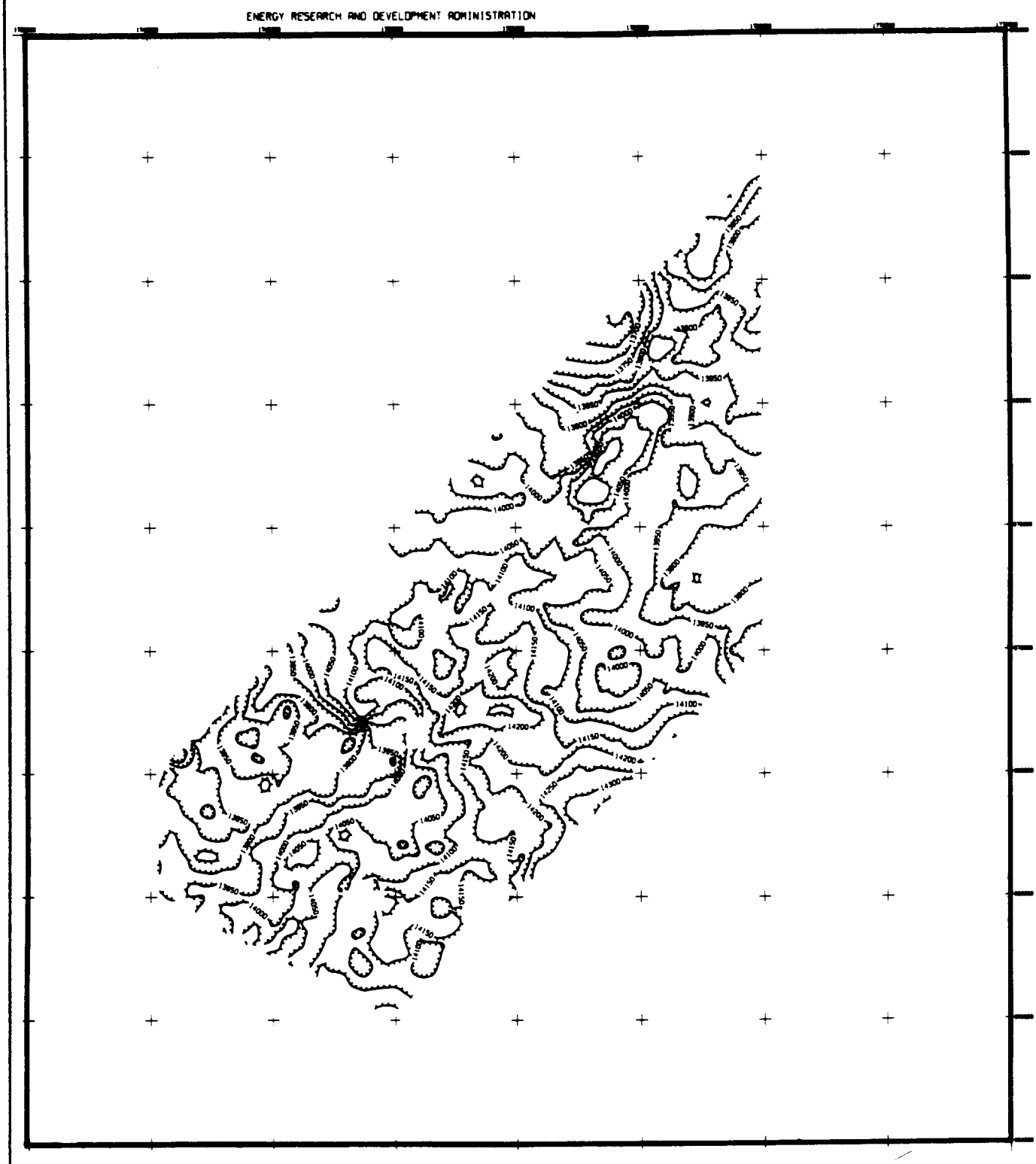

Figure 5.37 (Map 14.A). Interval Velocity Contour Map, Blue Reflector — 50-Foot Interval

GSI-709

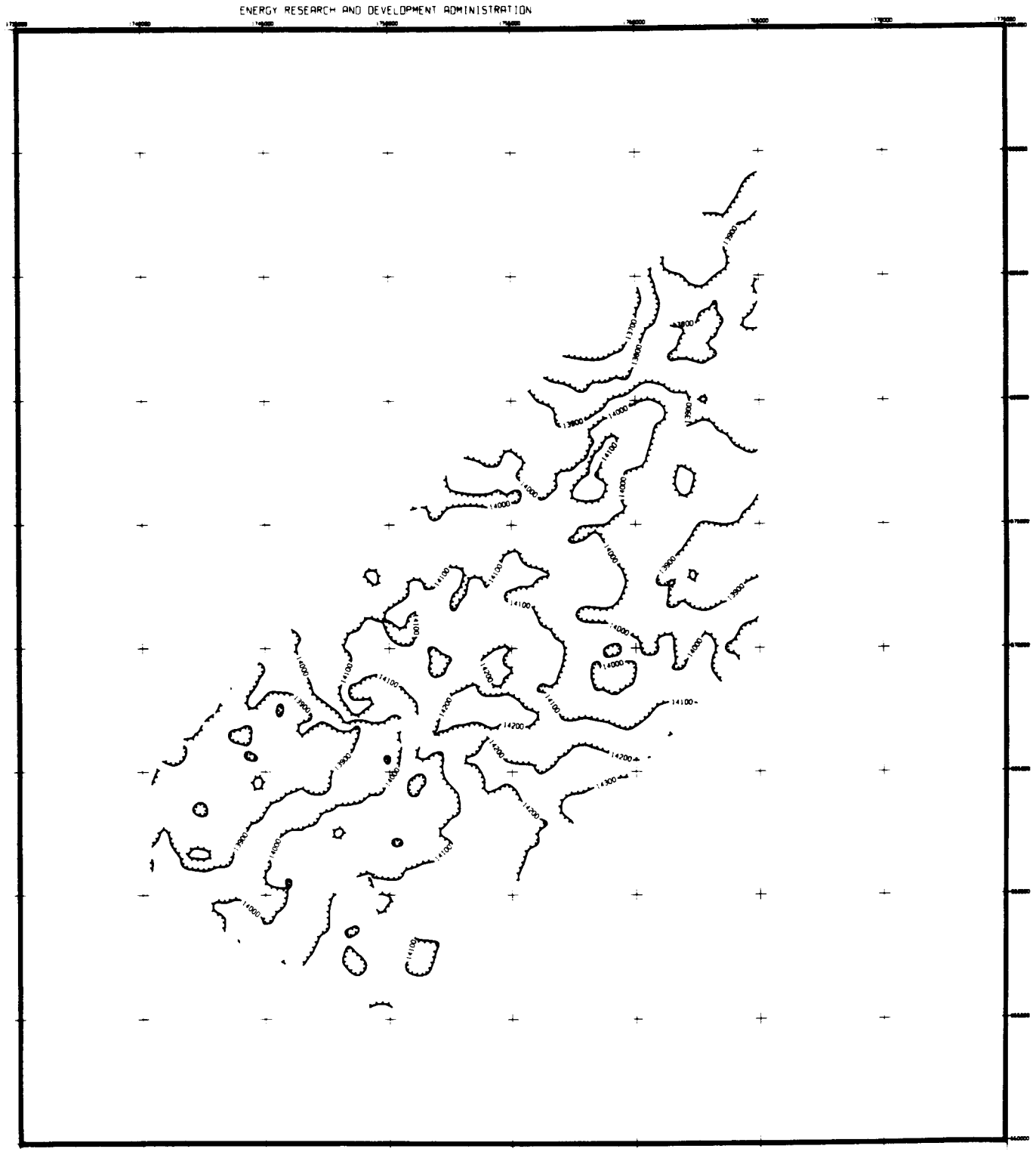

Figure 5.38 (Map 14.B). Interval Velocity Contour Map, Blue Reflector — 100-Foot Interval

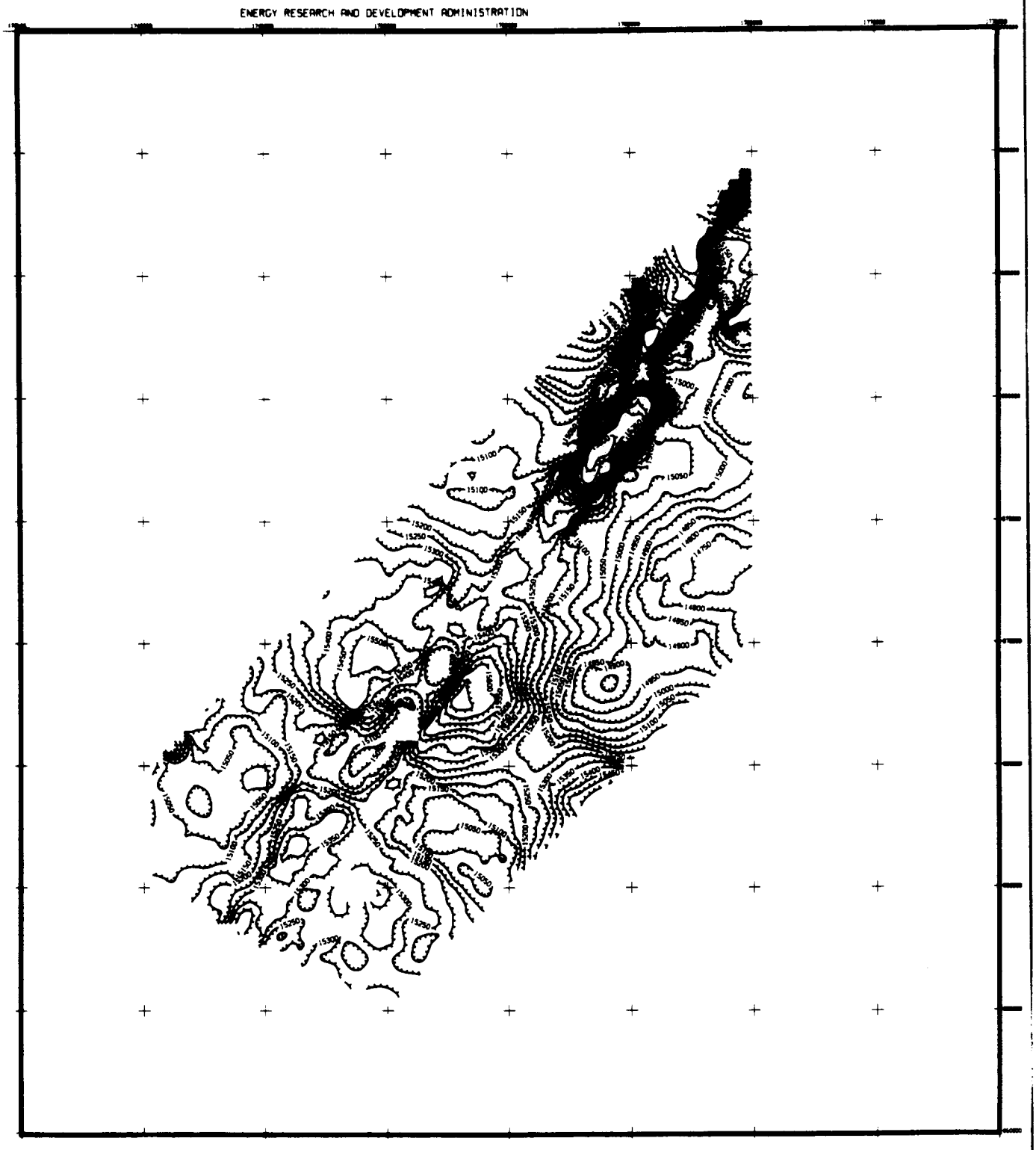

Figure 5.39 (Map 15.A). Interval Velocity Contour Map, Red Reflector — 50-Foot Interval

GSI-709

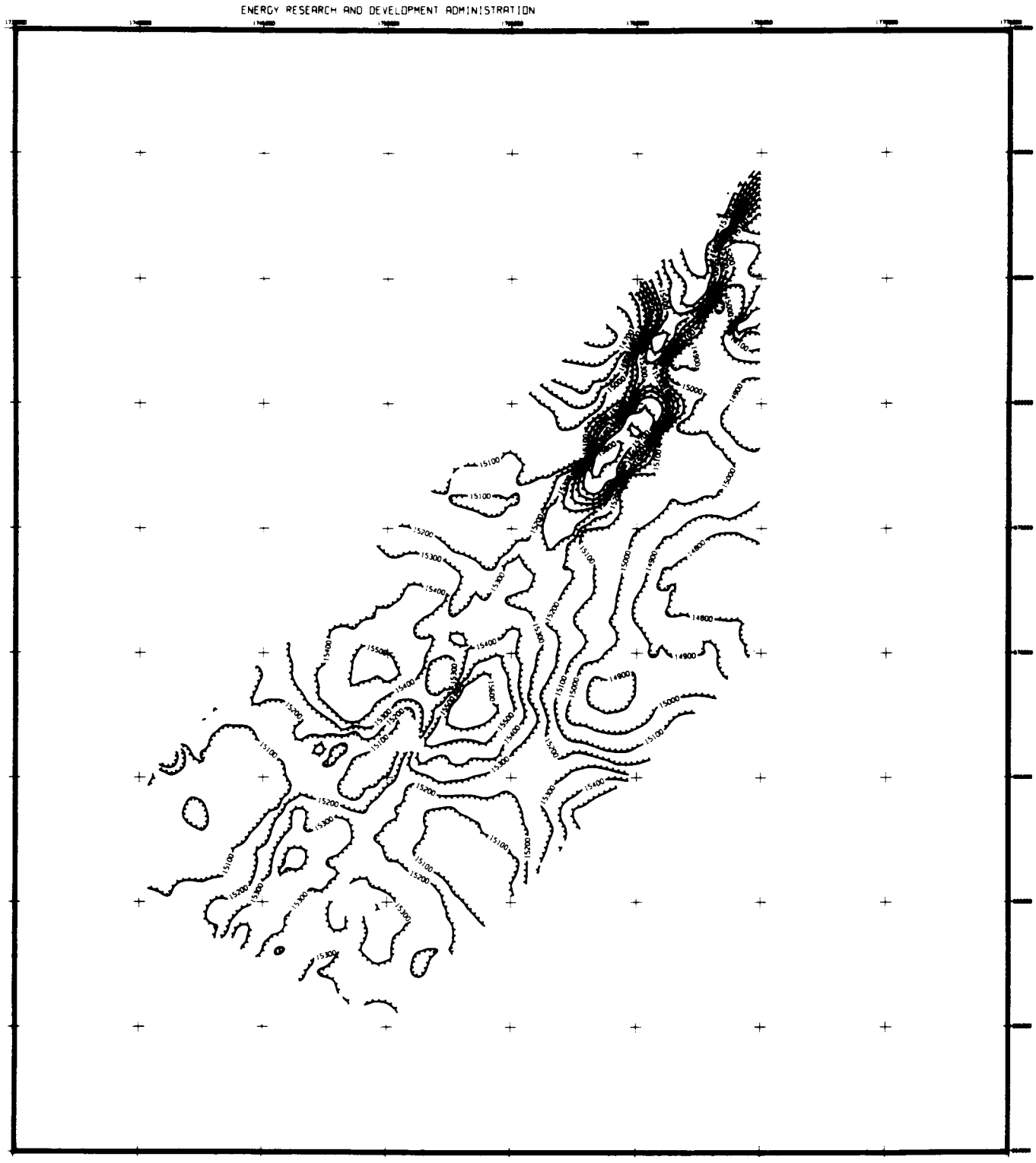

Figure 5.40 (Map 15.B). Interval Velocity Contour Map, Red Reflector — 100-Foot Interval

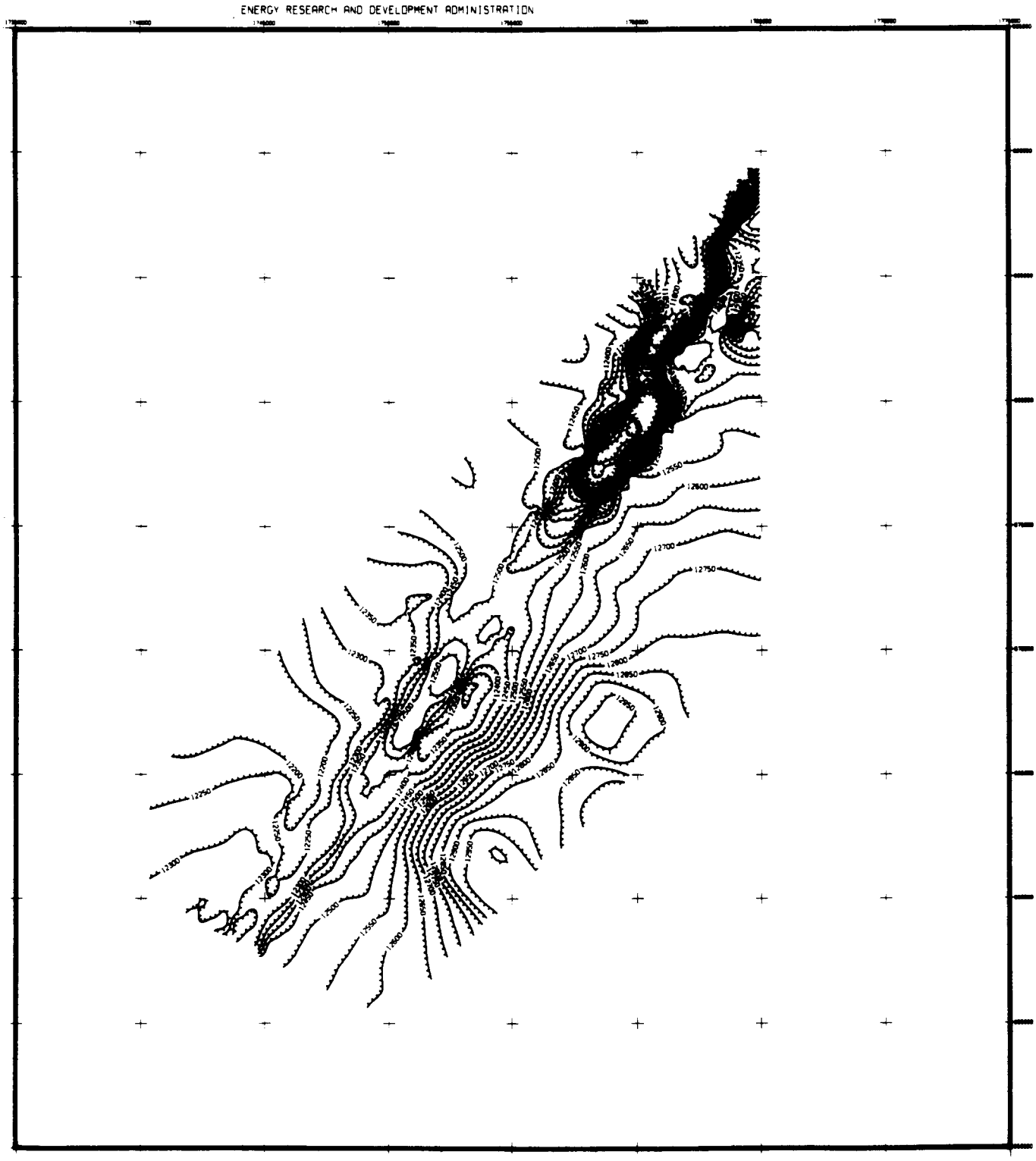

Figure 5.41 (Map 16.A). Average Velocity Contour Map, Green Reflector — 50-Foot Interval

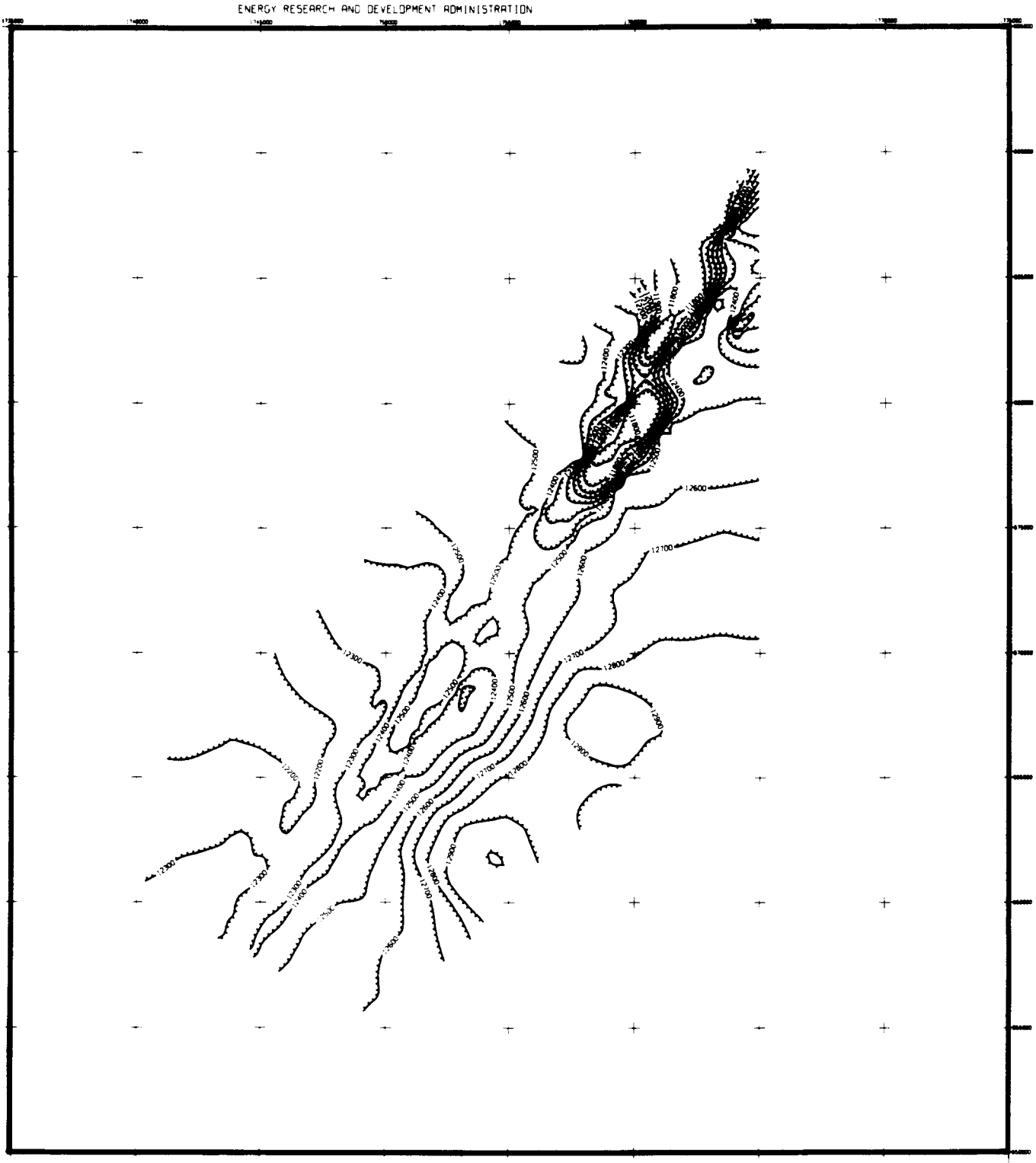

Figure 5.42 (Map 16.B). Average Velocity Contour Map, Green Reflector — 100-Foot Interval

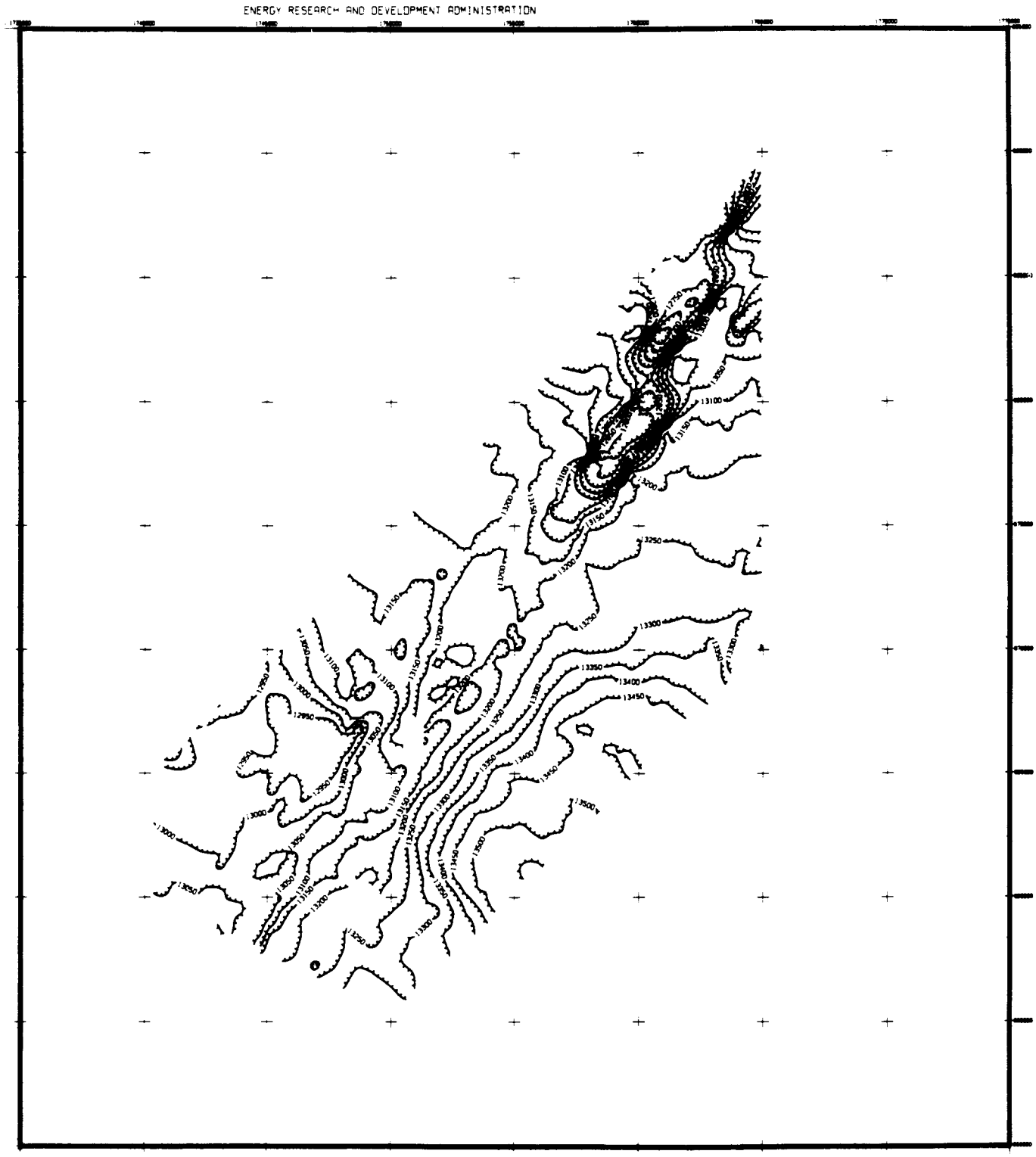

Figure 5.43 (Map 17.A). Average Velocity Contour Map, Blue Reflector — 50-Foot Interval

GSI-709

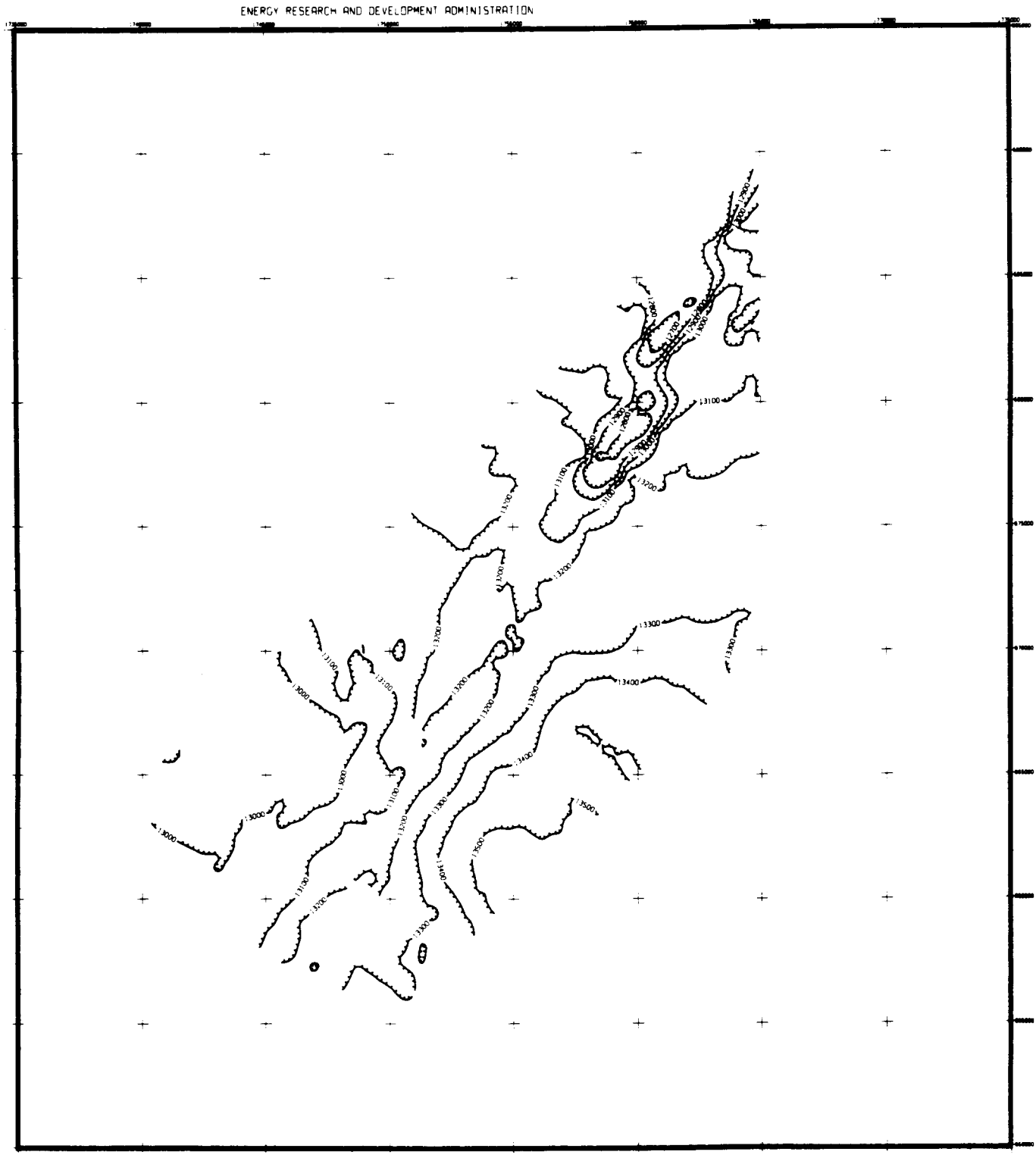

Figure 5.44 (Map 17.B). Average Velocity Contour Map, Blue Reflector — 100-Foot Interval

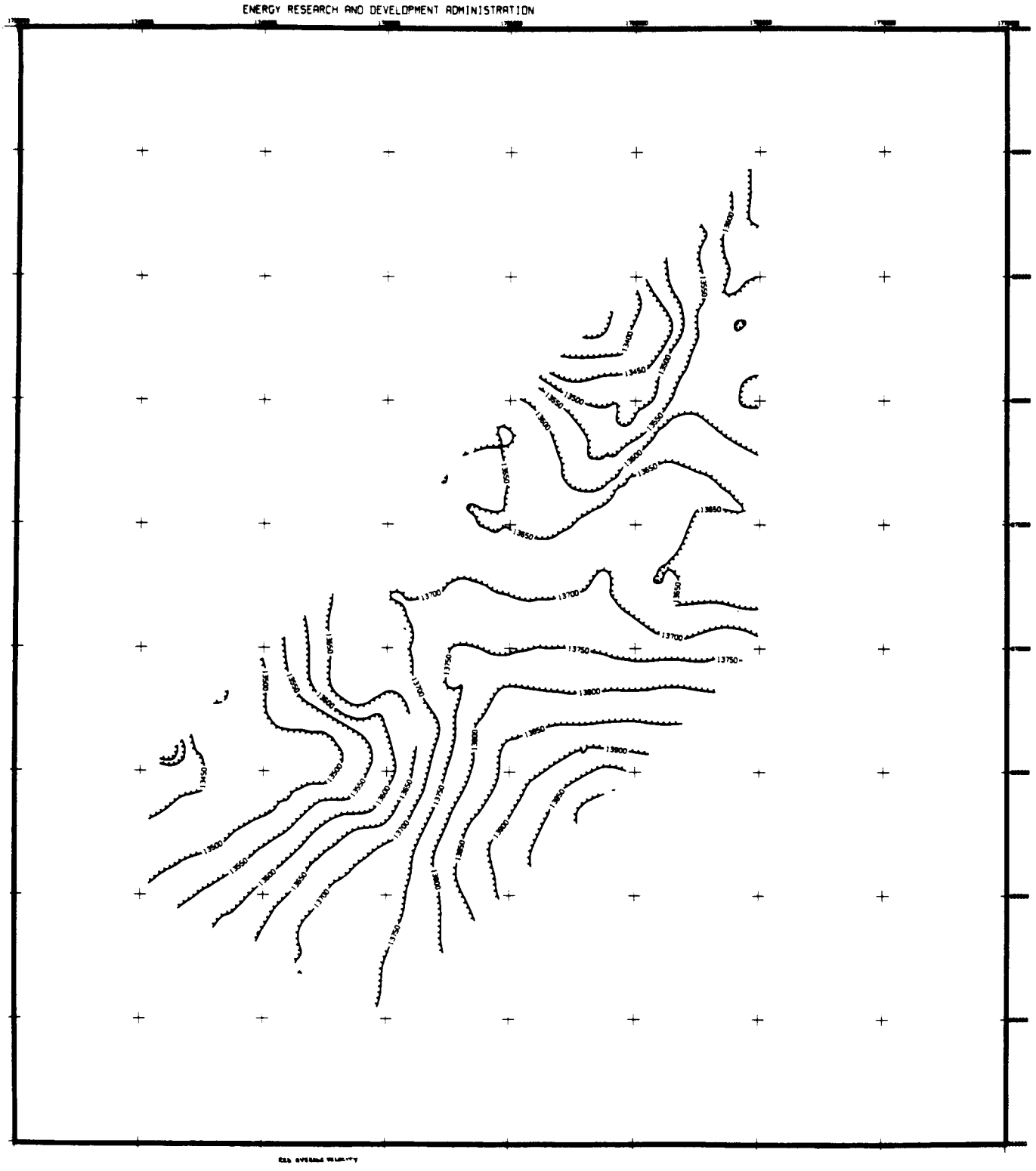

Figure 5.45 (Map 18.A). Average Velocity Contour Map, Red Reflector — 50-Foot Interval

GSI-709

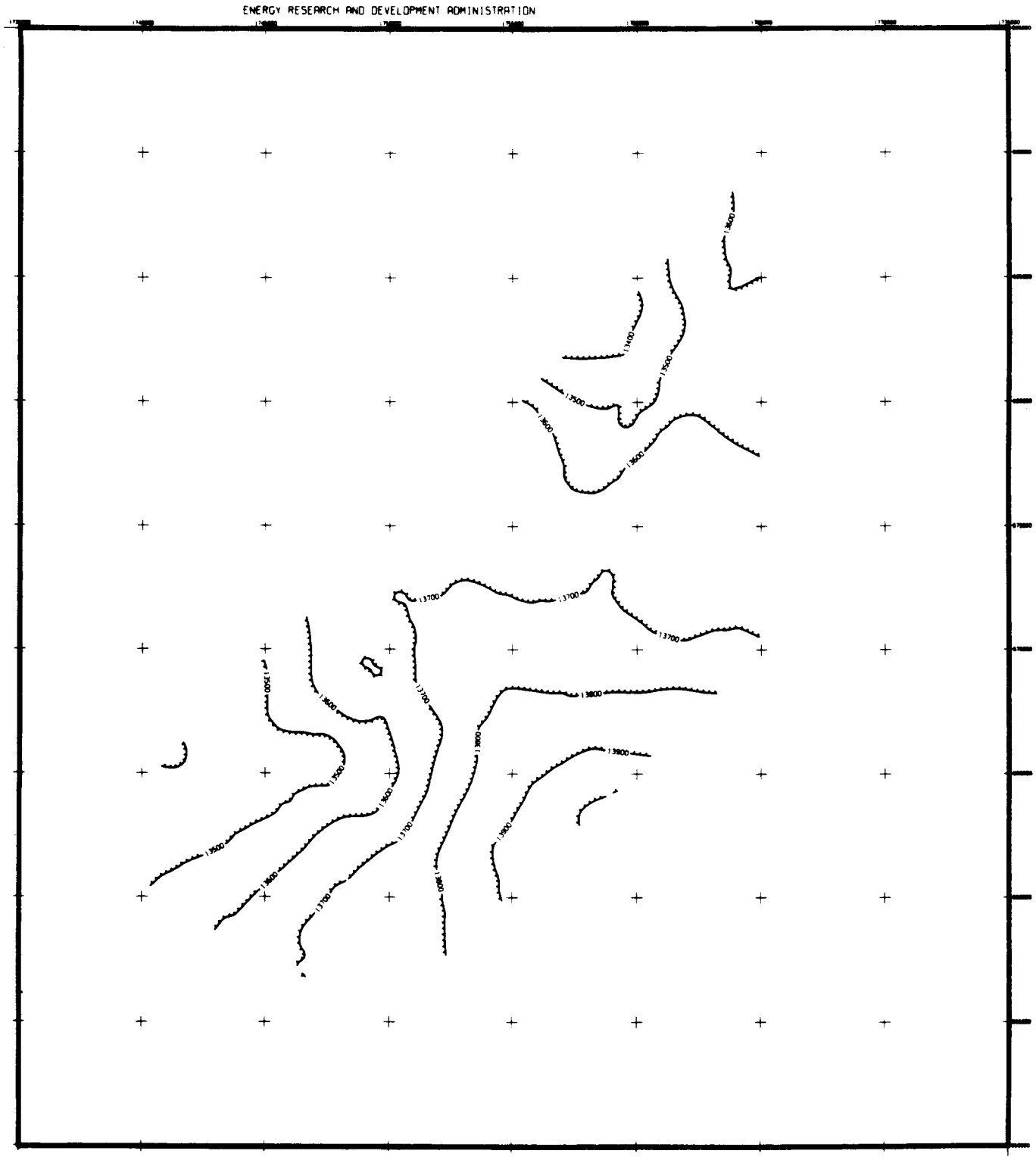

Figure 5.46 (Map 18.B). Average Velocity Contour Map, Red Reflector — 100-Foot Interval

Thus,

$$\Delta Z_n = \frac{V_{in}\,\Delta T_n}{2}$$

where Z_n, V_{in}, and T_n are thickness, interval velocity, and the two-way reflection time in layer n, respectively.

The isopach maps for the green, blue and red are shown on figures 5.47, 5.48, and 5.49. The contour interval was chosen at 50 feet.

Green Isopach Contour Map (Figure 5.47). The thickness of the green layer ranged from 1637 to 2072 feet with an average of 1865 feet. Generally, thickness increased towards the east as well as towards northeast. A thin zone anomaly is shown at the center and also about one-third down from the top of the area. Thin zones are more dominant at the southwest edge of the area.

Blue Isopach Map (Figure 5.48). The thickness of blue layer ranged from 1377 to 1856 feet. The average thickness was 1668 feet. The thin zone anomaly in the extreme northeast corner corresponds to the anomaly shown on the isochron map.

Red Isopach Map (Figure 5.49). The thickness of the red layer ranged from 1061 to 1627 feet. The average thickness was 1310 feet. Close inspection reveals a slight tendency for the red layer to thicken toward the northeast and to exhibit a low gradient. There is a thick zone anomaly at the northeast edge and a thin zone anomaly at the southwest edge of the prospect.

5.3.3.2 Depth Maps. The depth to a reflector was computed by summing thicknesses of layers above it.

$$Z_n = \sum_{i=1}^{n} \Delta Z_n$$

$$Z_n = \sum_{i=1}^{n} \frac{V_{in}\,\Delta T_n}{2}$$

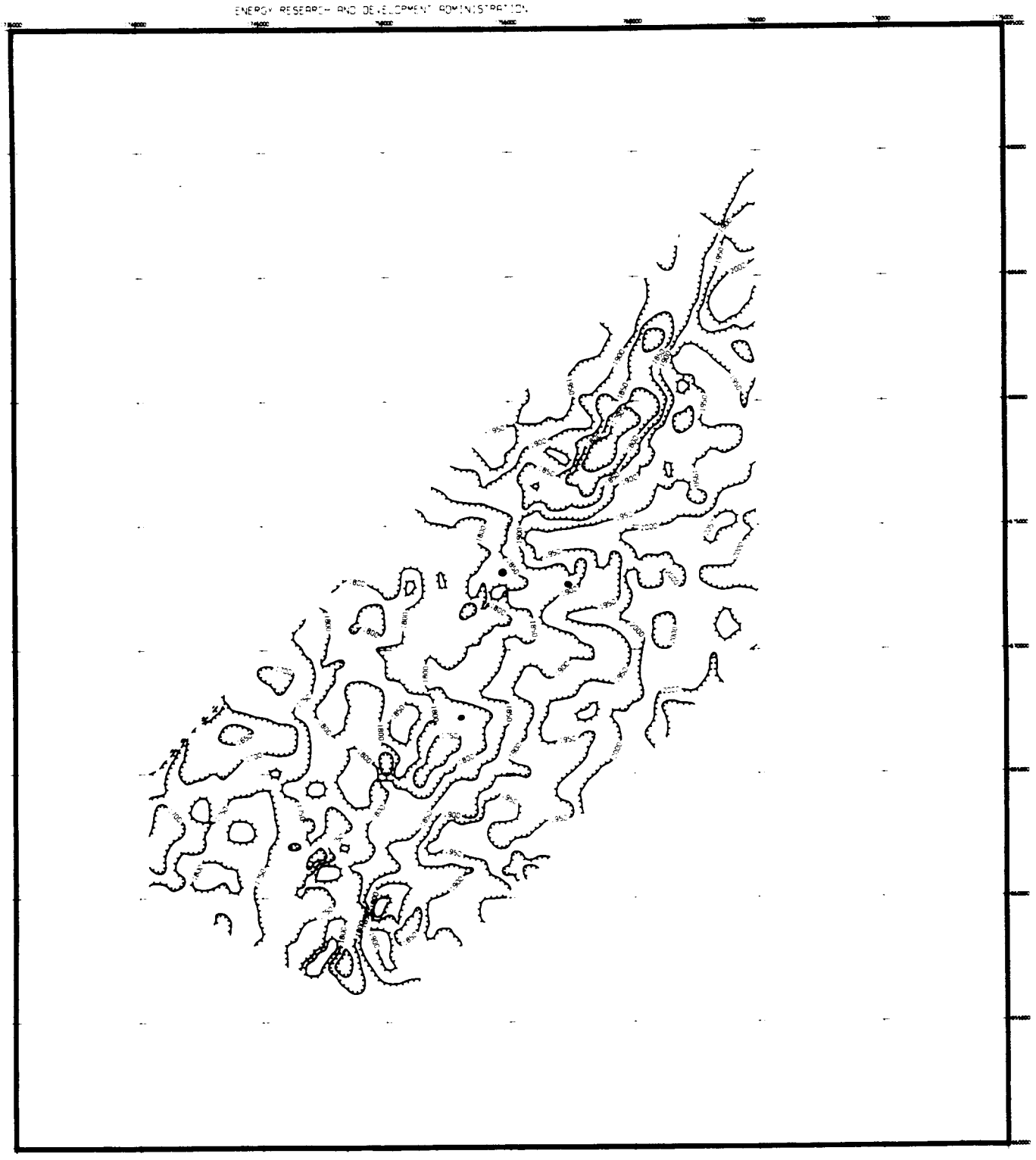

Figure 5.47 (Map 19). Datum Isopach Contour Map, Green Reflector

GSI-709

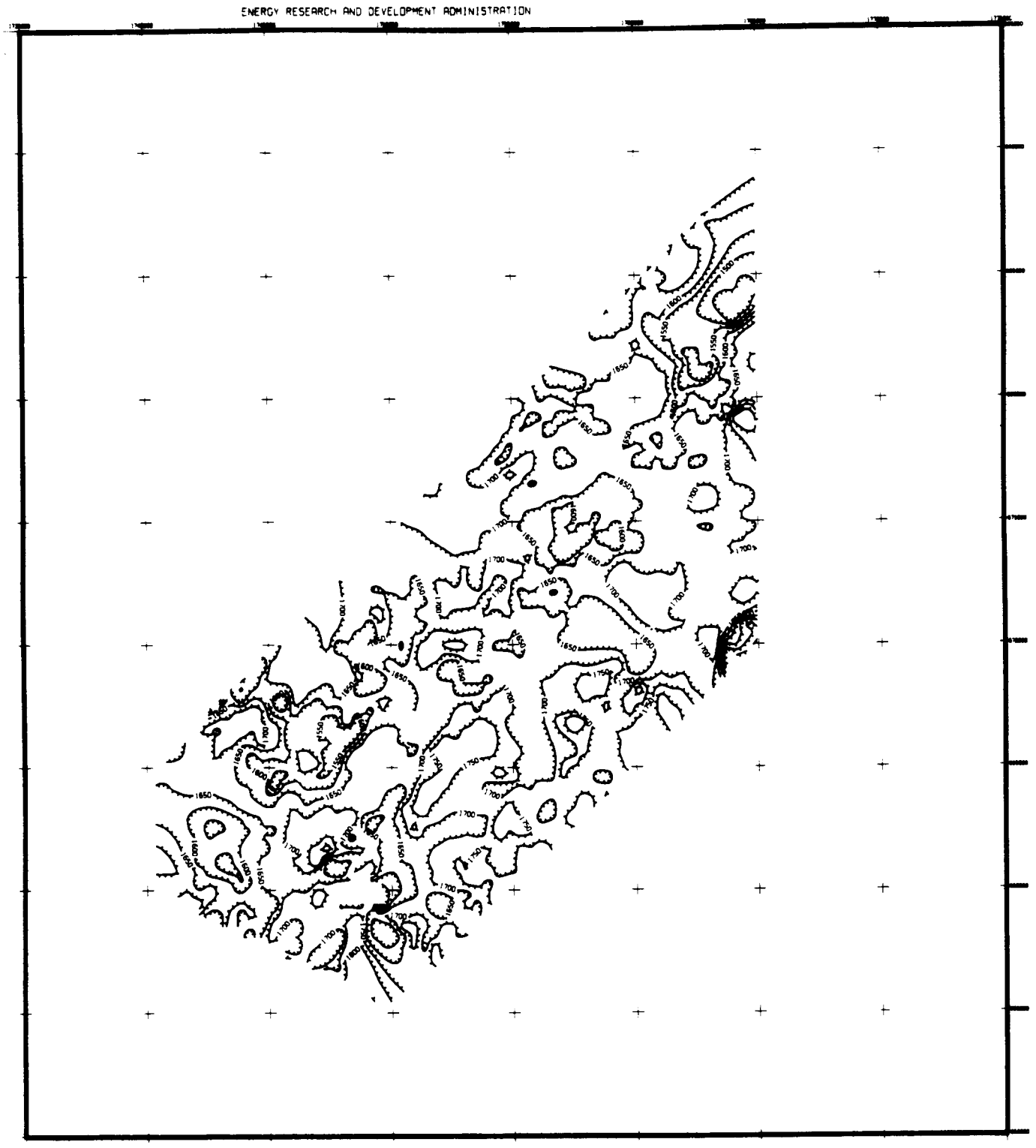

Figure 5.48 (Map 20). Isopach Contour Map, Blue-Green Reflectors

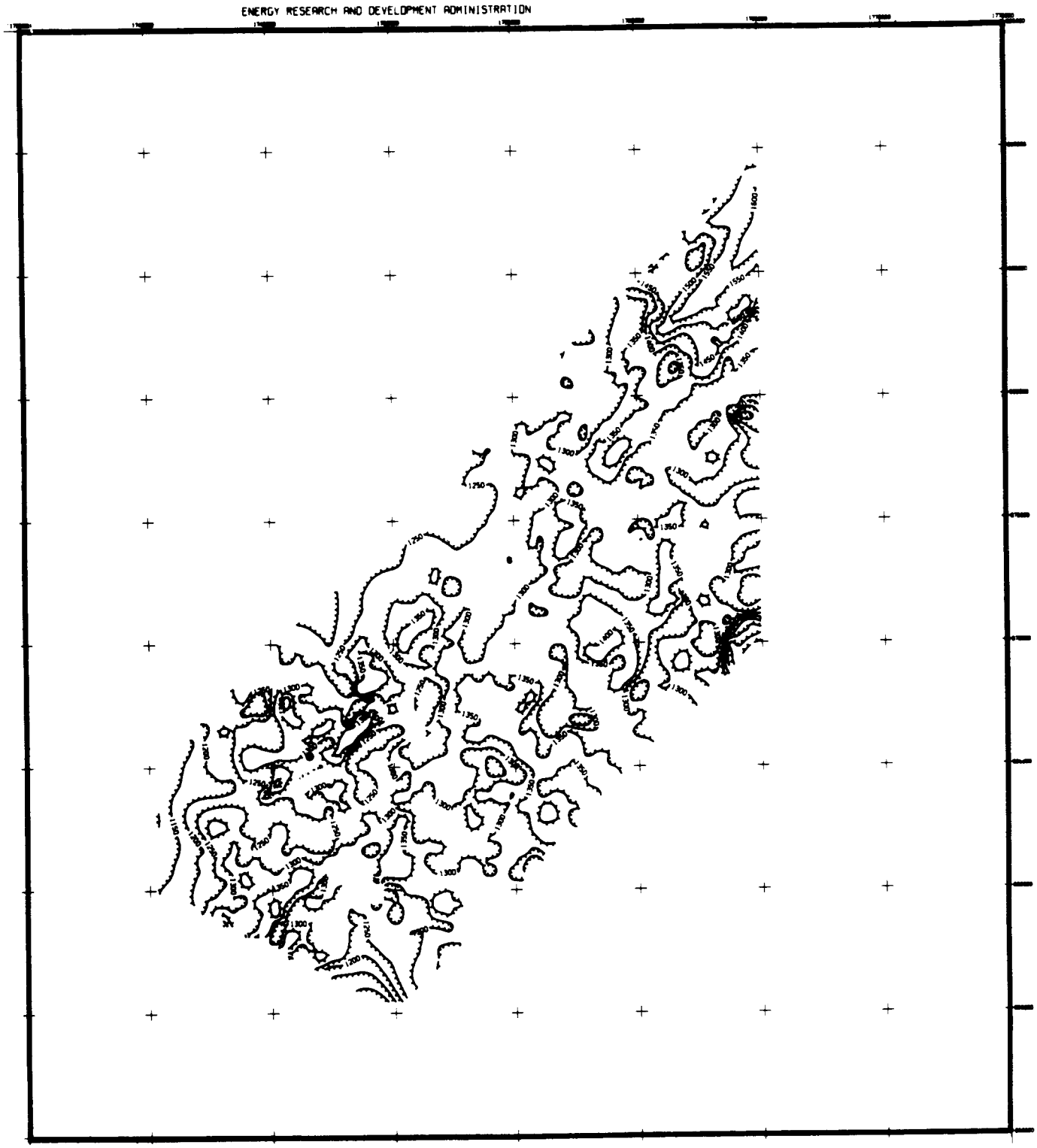

Figure 5.49 (Map 21). Isopach Contour Map, Red-Blue Reflectors

In these equations, Z_n is depth to a reflection and Z_n, V_{in}, and T_n are the thickness, interval velocity, and two-way travel time of layers above the reflector.

Contour depth maps were constructed at 50-foot intervals.

Green Depth Contour Map. The depth contour for the green is the same as shown by the green isopach map (Figure 5.47) described earlier.

Blue Depth Contour Map (Figure 5.50). The blue reflector showed depths from 3171 to 3815 feet and an average depth of 3533 feet. Dip is to the northeast and east; the gradient is steeper in the east direction. The general trend is northeastern. The two major highs are at one-third and two-thirds intervals from the top of the area.

Red Depth Contour Map (Figure 5.51). The red horizon had a depth range of 4452 to 5137 feet. The average depth was 4843 feet. The general trend, as with the blue and green reflectors, is to the east and northeast. The dip to east is greater than to the northeast.

5.4 INTEGRATED INTERPRETATION

5.4.1 FAULT DISTRIBUTION OF THE "PRECAMBRIAN". Figure 5.52 is a composite distribution of the fault pattern interpreted for the reflectors P1, P2, and P3. The general orientation of the faults are NE-SW.

In the discussion of maps (Section 5.3) it was seen how the general trend is NE-SW. Consequently, it is possible that the "Precambrian" faulting system has a major effect on the geological strata above it. Moreover, fracture orientation in Cottage Field is predominately in a NE-SW direction (Martin and Nuckols, 1976) coinciding with the "Precambrian" fault orientation.

The direction of fault propagation is from a lower to a higher level, with dominant movement directed northwest and southwest in the surveyed area.

Figure 5.50 (Map 22). Depth Map, Blue Reflector

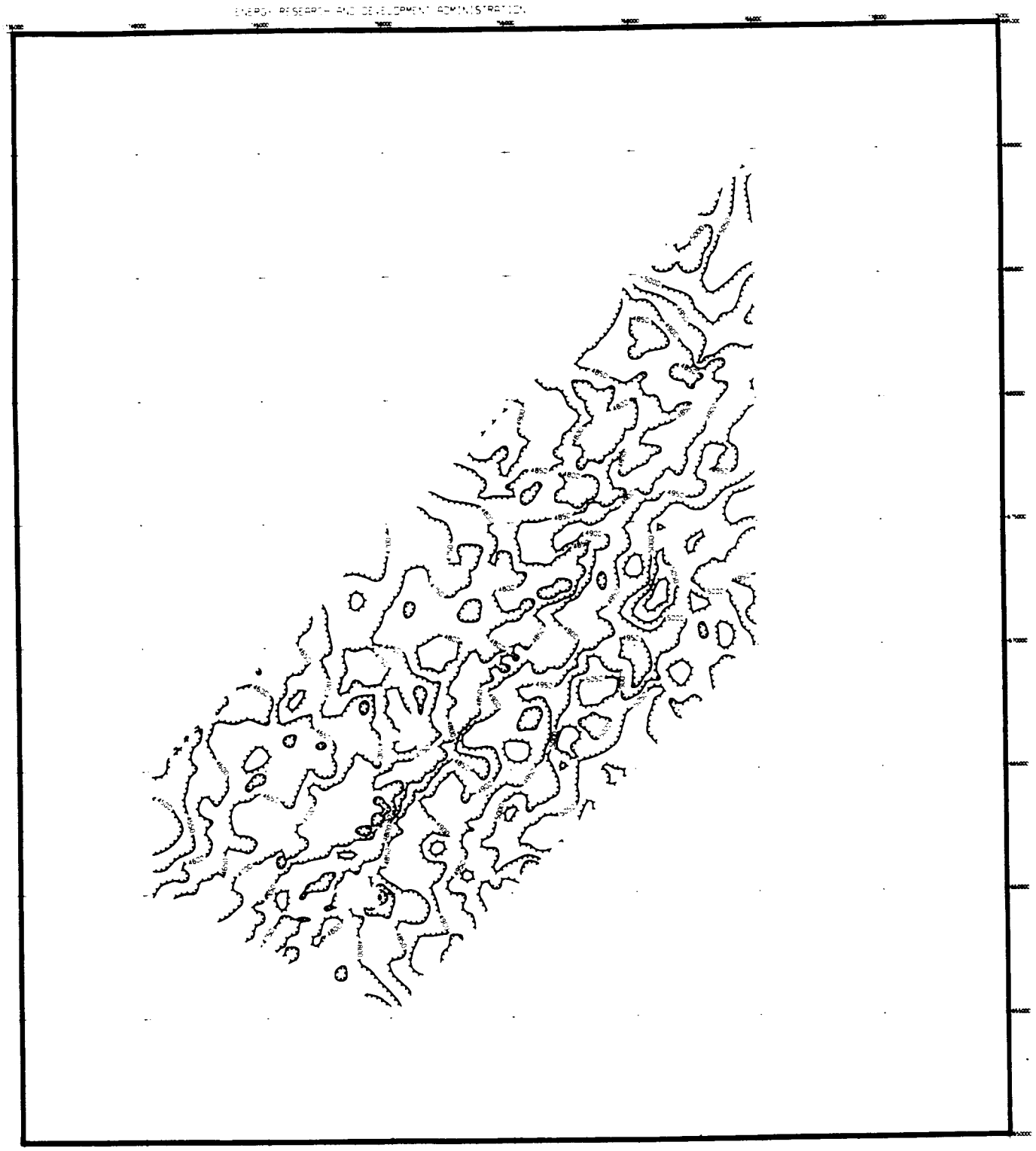

Figure 5.51 (Map 23). Depth Map, Red Reflector

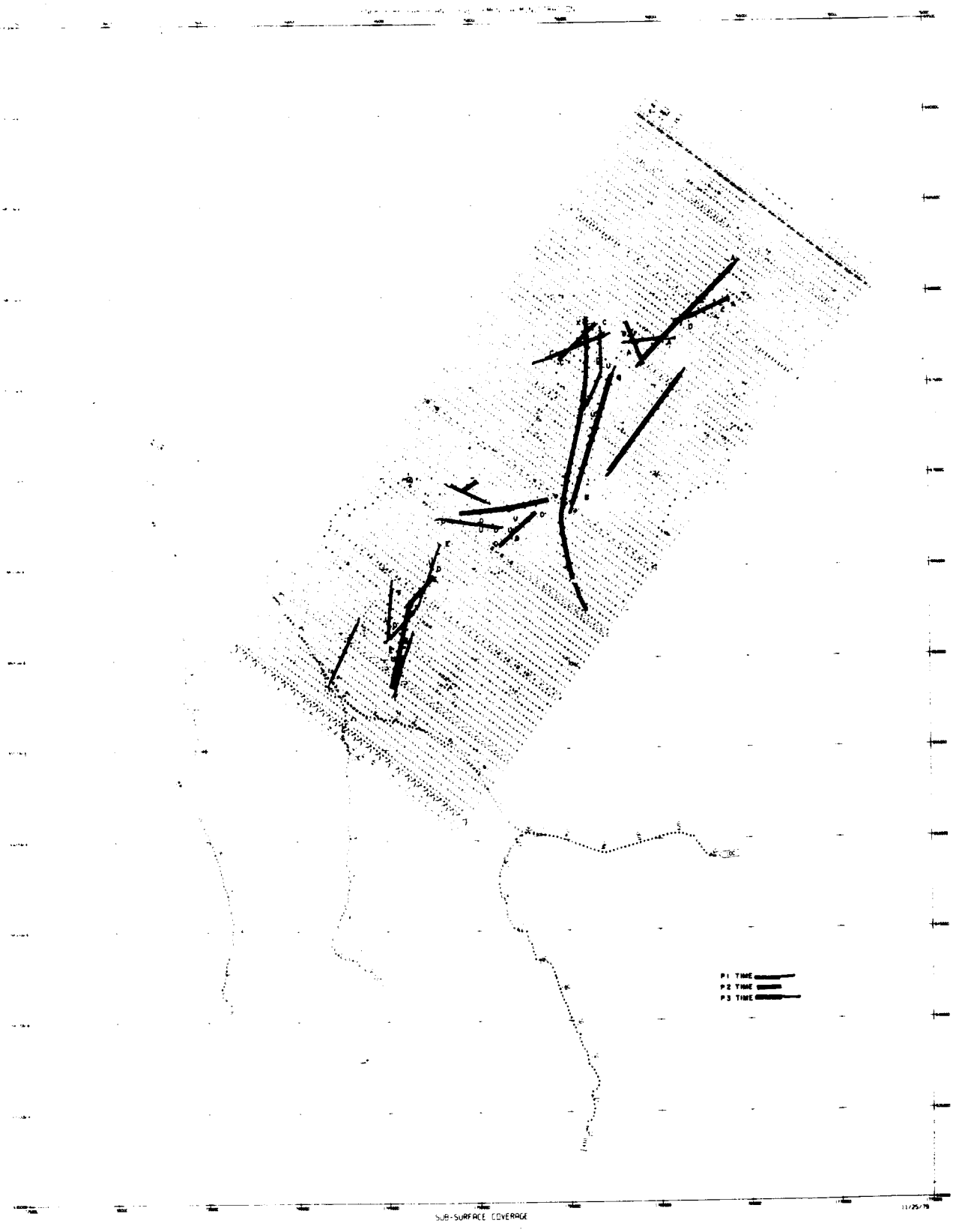

Figure 5.52 (Map 24). Fault Distribution in "Precambrian"

5.4.2 AVERAGE VELOCITY-TO-BASE OF DEVONIAN VS. "PRECAMBRIAN" FAULT SYSTEMS. Figure 5.53 is a composite of "Precambrian" fault systems (Figure 5.52) and the average velocity-to-base of Devonian (Figure 5.46). As noted earlier, the average velocity field could be divided into three zones: two low-velocity zones in northwest and southwest portions of the prospect and a higher-velocity zone in between.

Figure 5.53 reveals that such distribution could be related to the "Precambrian" movements. As indicated in subsection 5.4.1, the upward propagation of the "Precambrian" faulting directly correlates with the low average-velocity anomalies in the northwest and the southwest portions of the surveyed area. The relatively higher velocity in the middle could be related to the "graben block" at the "Precambrian" level.

A mechanism of gas accumulation is postulated: the fault propagations are directed toward the northwest and southwest which causes the fracture of the Devonian shale. Later, gas accumulates in the fractures and consequently the average velocity drops due to the reduction of bulk density in the zone and the higher pore pressure (Backus and Chen 1975, Pennebaker 1968, Reynolds 1970).

5.4.3 INTERVAL VELOCITY OF DEVONIAN VS. "PRECAMBRIAN" FAULT SYSTEMS. Figure 5.54 is a composite of the "Precambrian" fault system (Figure 5.52) and the interval velocity in the Devonian shale (Figure 5.40). The low interval-velocity anomalies are again concentrated in the northwest and southwest portions of the area in addition to the east. Again, the higher-velocity anomalies are in the center of the surveyed area.

The fracturing of shallow layers due to deep-seated faulting, which has been mentioned briefly in the previous section, has been proposed by William K. Overbey, Jr. (1976). Movement of Precambrian fault zones would produce fracturing which probably would have propagated upward into the Devonian shale. This is diagramatically illustrated on Figure 5.54.

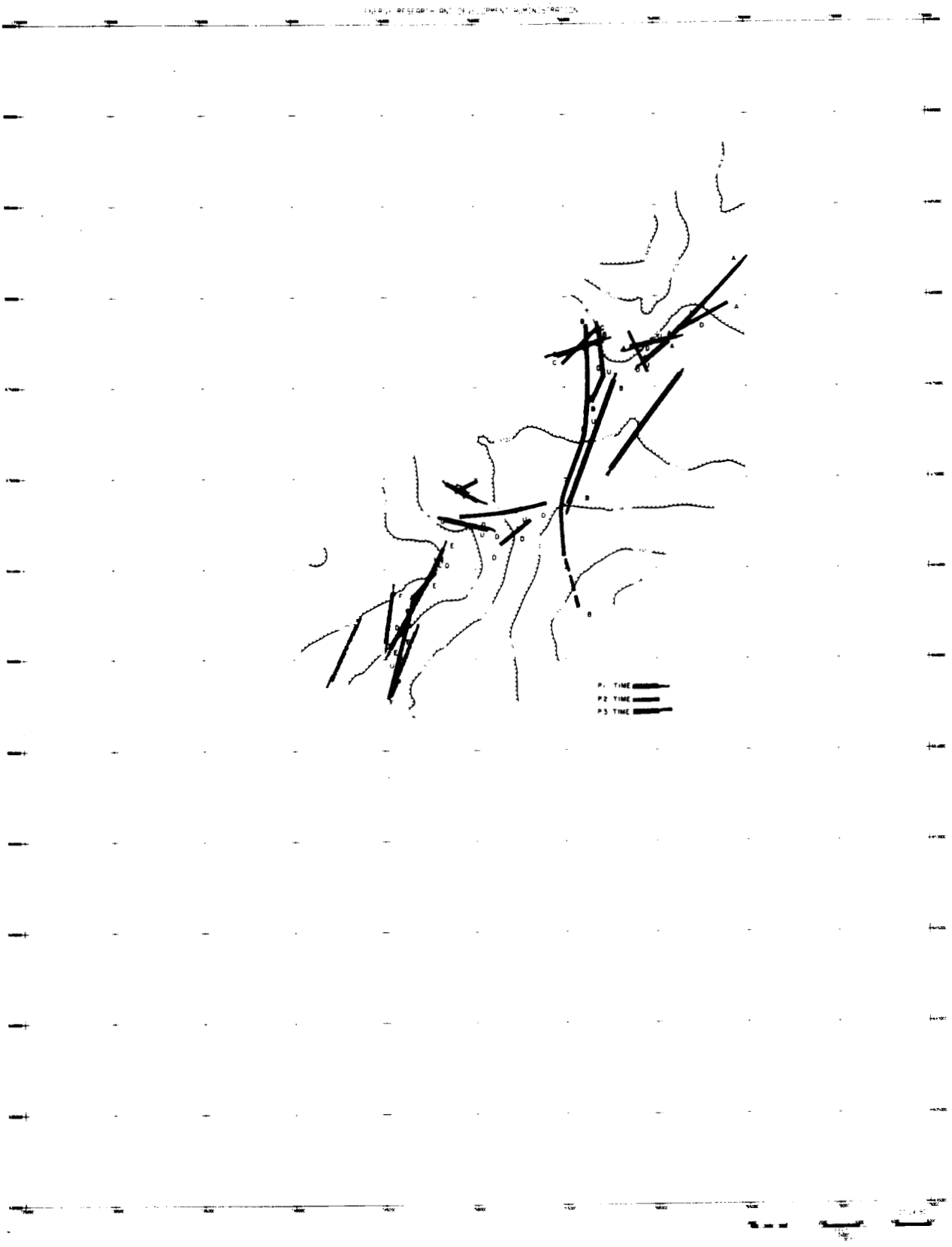

Figure 5.53 (Map 25). Average Velocity-to-Base of Devonian Superimposed on Fault Distribution in Precambrian

GSI-709

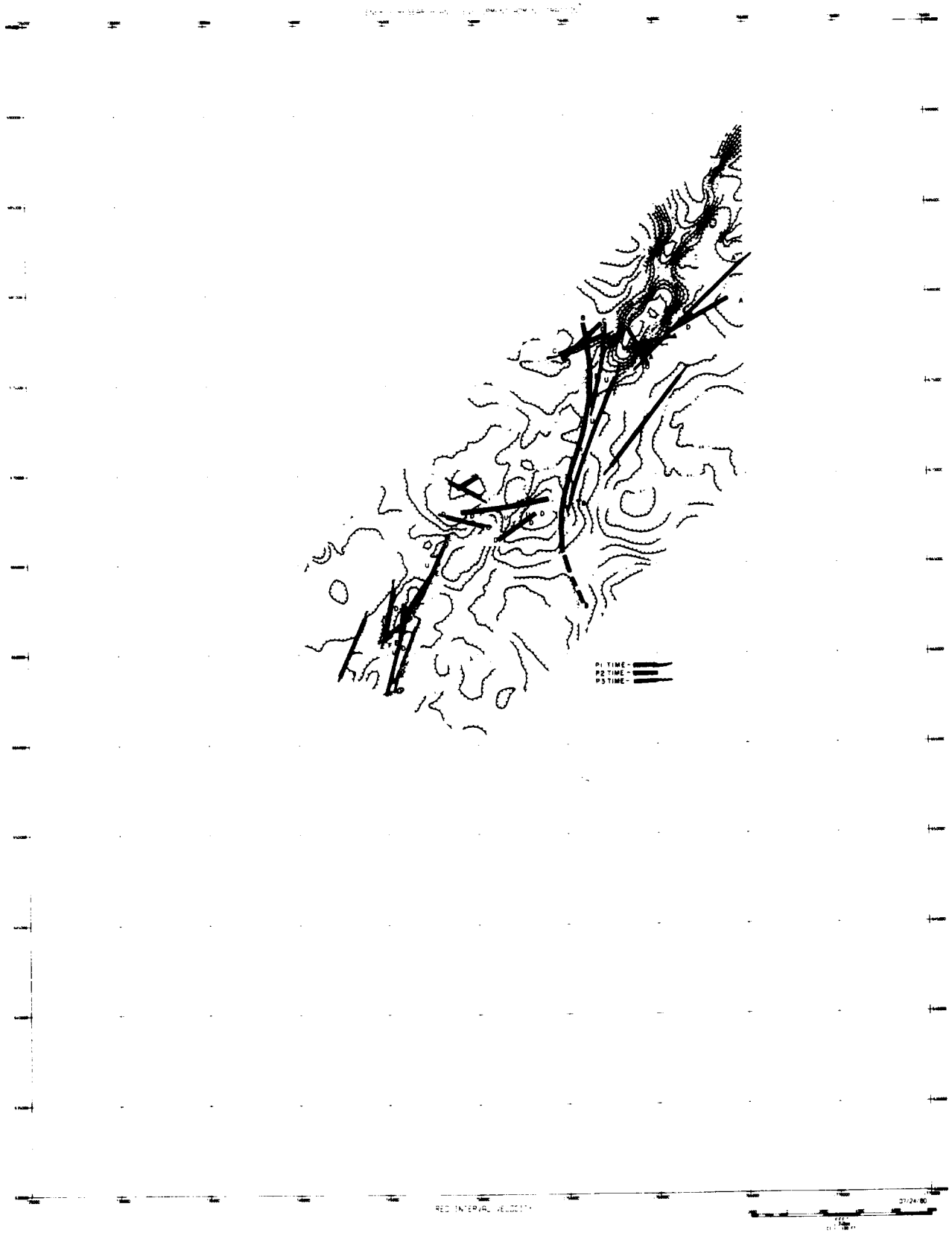

Figure 5.55 (Map 26). Interval Velocity in Devonian Superimposed on Fault Distribution in Precambrian

GSI-709

SECTION VI

CONCLUSIONS

The following is a summary of accomplishments and conclusions from the 3-D seismic survey conducted in Cottage Field in West Virginia.

1. The 3-D seismic method is an effective tool for hydrocarbon exploration. It has the ability to resolve subsurface details due to the dense areal coverage. It utilizes the total reflected and scattered subsurface energy to give an accurate and clear representation of the subsurface reflectors.

2. The SEISCROP maps (horizontal time slices) are effective tools for expeditious construction of structural contour maps for different reflectors.

3. The structural behavior of shallow reflectors are affected by the fault system in the "Precambrian". The trend of the reflectors are in the same direction as the strike of deep faults.

4. Fractures are oriented in approximately the same direction as the faults in the "Precambrian".

5. There is evidence to show that deep fault activities propagate upward and cause fracturing in the Devonian shale. The low velocity in the shale zone is probably controlled by faults in the "Precambrian".

Respectfully submitted,

Nabil A. Morgan
Glenn R. Breed

Approved by:

James H. Funk
Manager, Special Projects
Land 3-D Operations

SECTION VII
REFERENCES CITED

Backus, Milo M. and Roland C. Chen. 1975. Flat spot exploration. Geophys. Pros. 23:533-577.

Bargnal, William D. and William M. Rayan. 1976. The geology, reserve and production characteristics of Devonian shale in S.W. Va. Shumaker, R.C. and W.K. Overbey, Jr., eds. Devonian shale production and potential: seventh Appalachian geology symposium, March 1-4; Morgantown, W.V.: Energy Resource and Development Administration, pp. 82-211.

Consolidated Gas Corporation (No date). Core analysis, Devonian brown shale well 11940, Cottageville, West Virginia. (unpublished).

Fuller, Brent D. 1968. Two dimensional frequency analysis and design of grid operators. SEG Mining Geophysics: Vol. II. pp. 658-708.

Haliburton Services. 1975. Laboratory Report No. F11-T109-75 for Consolidated Gas Supply Corporation. 10 pp.

Martin, P. and E.B. Nuckols III. 1976. Geology and oil and gas occurrence in the Devonian shale - northwestern West Virginia. Shumaker, R.C. and W.K. Overbey, Jr., eds. Devonian shale production and potential: seventh Appalachian geology symposium, March 1-4; Morgantown, W.V.: Energy Resource and Development Administration, pp. 20-40.

Overbey, William K., Jr. 1976. Effect of in situ stress on induced fractures. Shumaker, R.C. and W.K. Overbey, Jr., eds. Devonian shale production and potential: seventh Appalachian geology symposium, March 1-4; Morgantown, W.V.: Energy Resource and Development Administration, pp. 182-211.

Pennebaker, E.S. 1968. An engineering interpretation of seismic data. Presented at Geophysical society of Houston symposium. Houston, Tx. April 10, 1969.

Reynolds, E.B. 1970. Predicting over-pressured zones with seismic data. World Oil. Oct. issue. pp. 78-82.

West Virginia [Topographic]. Dudley H. Cardwell, cartographer. U.S. Geological Survey. 1968. West Virginia Geological and Ecological Survey. 1:250,000; colored.